UNIONE EUROPEA
Fondo Sociale Europeo

Ministero dell'Università e della Ricerca

PON RICERCA E INNOVAZIONE

REACT EU

Università Ca'Foscari Venezia

PhD Programme
in Environmental Sciences
cycle 37

Research Thesis

Exploring innovative formulations for coastal heritage preservation inspired by ancient mortars

SSD: R210

PhD Coordinator
ch. prof. Enrico Bertuzzo

Supervisor
ch. prof. Elisabetta Zendri

PhD Candidate
Marco Destefani
Serial no.858827

La borsa di dottorato è stata cofinanziata con risorse del
Programma Operativo Nazionale Ricerca e Innovazione 2014-2020, risorse FSE REACT-EU
Azione IV.4 "Dottorati e contratti di ricerca su tematiche dell'innovazione"
e Azione IV.5 "Dottorati su tematiche Green"

Table of Contents

Synopsis

The thesis is divided into four chapters,

Chapter 1. Introduction: Gives an overview of the objectives of the research while providing extensive insight into the state of the art regarding lime. Issues such as the history of binders, the chemical and physical properties of materials, the different types and recipes developed over the years, and the different types of additives that have been researched to date to make mortars and plasters more durable and resistant will be examined.

Chapter 2. Materials and Research Methods: This section discusses and illustrates the materials and methodologies that have been used to develop the Doctoral project.

Chapter 3. Results: The analytical results obtained through the course of the experiment are reported and interpreted here. Due to the experimental nature of the research into new mortars and plasters, the chapter has been subdivided into multiple subsections that will respectively deal with: providing a chemical and physical analysis of the starting materials

Chapter 4. Conclusions and Future Prospects: This last chapter summarizes the results obtained in the previous Chapter 3, providing considerations and thoughts based on the previously elaborated data. Furthermore, it is proposed to evaluate possible improvements and future investigations.

1. Introduction

The effects of climate change are visible today all over Europe. The magnitude and speed with which these phenomena are occurring day after day is as alarming as it is dangerous, not only for environmental sustainability but also for the continuity of our cultural heritage. To counter the lack of attention of the masses to these current issues, the 'European Green Deal' was born, a set of political initiatives proposed by the European Commission with the overall goal of achieving climate neutrality in Europe by 2050[1]. Even though Cultural Heritage is constantly being damaged due to environmental change, it was not explicitly mentioned in the Green Deal. At the same time, however, a coordination group composed of experts from the Member States was established following the Work Plan for Culture 2019-2022. The purpose of the group was to examine the contributions of Cultural Heritage to the Green Deal and to identify shortcomings and threats related to heritage in the context of climate change. These investigations resulted in the 'European Cultural Heritage Green Paper', a document demonstrating the relevance of Cultural Heritage in achieving these ambitious objectives of the European Green Deal, developed by Europa Nostra in collaboration with ICOMOS and Climate Heritage Network with the help of the European Heritage Bank Institute[2]. If the European Green Deal combines several general solutions aimed at limiting the global temperature rise, which is fundamental for the preservation of biodiversity and a vast number of cultural places and buildings, also the cultural heritage itself, as expressed in the above-mentioned 'European Cultural Heritage Green Paper', can hide several solutions useful for the achievement of this ambitious goal. In a context such as Europe, characterized by a great interdependence between people and their environment, climate change would lead to drastic changes in people's lifestyles and consequently in their relationship with their Cultural Heritage[1-3]. This sphere and the goods that are part of it are capable not only of providing alternative solutions aimed at shaping a healthier and more environmentally sustainable social and economic reality but also connecting people to the places they inhabit, increasing their sense of inclusion and belonging. The wide variety of cultural assets that features Europe should help to develop a line of thinking where cultural legacies are not only celebrated for the message they carry, but that even production techniques take on the importance they deserve. This should stimulate the development of a more flexible mindset that deviates from today's quick and easy construction solutions and searches for materials and methodologies that can be used to implement the durability of new works and reduce their environmental impact[2-4]. The responsibility for climate change weighs on all societies and the demoscopic

research ‘Sustainable Buildings: the Perception of Italians’ is a clear example of this, showing how the majority of the Italian population today is aware of and sensitive to sustainability issues starting with the built environment. The research, commissioned by GBC Italia, conducted by Eumetra, and presented by Professor Renato Mannheimer last 14 December in Rome during the event ‘The responsibility for change for the wellbeing of people’, observed an acknowledgment of the active role that the building field plays in environmental sustainability, including the intentions of private individuals themselves to make their buildings more efficient[5]. Suffice it to say that a property built on these intentions could be able to reduce CO_2 emissions by up to 40%, construction water consumption, waste produced during construction/demolition, save on total energy consumption and much more. Consequently, as this attention is paid by citizens to private real estate, this should be a fundamental aspect that concerns all building realities, on all possible scales, territory, cities, suburbs, and neighborhoods, to identify a new building culture aimed at sustainability. In this vision, the construction and real estate supply chains play a fundamental role, as their actions substantially influence the achievement of sustainable development goals, and the presence of a growing eco-sustainable market can only be a good omen[5-7]. As of 2023, economic growth in the construction sector in Italy (2023-2024) has slowed down as Italy's GDP grew only +0.7% in 2023, after two years (2021-2022) of strong expansion (+12.3%). Negative factors included high inflation, rising interest rates, geopolitical tensions, and global uncertainty curbed consumption (+1.2% vs. +4.8% in 2022) and investments (+0.9% vs. +11.4% in 2022). Italian exports, though, remained stable abroad, also due to the difficulties of Germany, its main trading partner. The construction sector, in particular, played a leading role between 2021 and 2023, where it recovered most of the losses of the decade-long crisis, thanks to incentives such as the Superbonus and public investments of the PNRR. The demand for housing, although downsized, remains significant, with more than 2 million families intending to change their homes. The construction sector faces a critical phase, with signs of recovery in public investment, but difficulties in the private market and credit. Demographic and economic challenges call for strategic interventions to support businesses and households, promoting urban regeneration and measures to combat inequality. The NRP represents a unique opportunity for the development and modernization of Italy. Its implementation requires effective management of resources, adherence to deadlines, and optimal coordination between entities and businesses[5-6]. This overview demonstrates not only the presence of very good prospects for a revival of the construction economy but also the necessity of aiming for an economic reality in the construction sector aimed at environmental sustainability, a goal that

can be achieved by updating the knowledge gained from cultural heritage research and applying it in the construction sector. It is on this perspective that the project of this thesis is based: to exploit the knowledge of ancient building materials to devise and develop innovative and eco-sustainable materials for the building industry. Traditional, non-cementitious mortars have been the main object of study with the aim of improving their properties and durability and designing them for use in the modern environment[3,8]. Traditional mortars are one of the cornerstones of studies about built Cultural Heritage, an essential feature of ancient masonry in historical architecture, urban and rural European buildings, from antiquity to the present day. Their field of application is quite vast as they can serve as structural elements, protective layers for the masonry, decorative elements, binding agents for mosaic tiles, or, if painted, for frescoes or painted murals[9-12]. The importance of mortars, however, is not always reflected in the attention they deserve in acts of prevention and maintenance, even though they too are an integral part of the built Cultural Heritage. Thanks to academic and research areas of interest, traditional building methods and materials have recently been re-evaluated as valuable alternatives to everyday restoration solutions. Numerous projects have focused on traditional know-how, with the aim of reducing the environmental impact of the interventions, often caused by the excessive use of industrial chemical materials and implementing solutions that are more compatible with ancient masonry. The first noticeable attempt was made in 1981 with the support of ICCROM (International Centre for the Study of the Preservation and Restoration of Cultural Property) to define a strategy for the study of ancient mortars and repair mortars. The same interest has also been expressed in Spain for more than a decade. Various research groups from the CSIC (mainly those working at the Eduardo Torroja Institute), together with other researchers from Spanish universities (Navarra, Seville, etc.), have been working on various noticeable projects[13-18]. The majority of studies on ancient mortars from built heritage and archaeological sites have focused on the characterization and identification of their components from a qualitative perspective, intending to establish a chronology for the construction in question. Additionally, considerable time and effort have been dedicated to the comprehensive examination of mortar deterioration processes and the impact of such alterations on adjacent materials. Presently, research is being conducted into implementing durability, properties and studies on ancient mortars (experience has already been gained with stone materials) and suggesting new mortars to preserve traditional and archaeological masonries. Based on sustainable and durable approaches. It is therefore right to mention the company Mapei S.p.A, with whom this project has been possible. As a

company in the vanguard of building products, it provides many researchers to study the building technologies of the past and then re-propose them in an improved and modern guise.

1.1 Research Objective

The main objective of this doctoral project, in collaboration with Mapei S.p.A., is to design new mortars and plasters to protect traditional masonry and guarantee greater durability, particularly in coastal areas... In terms of durability, structures that have survived for centuries are the most sustainable. It can be reasonably deduced that an increase in knowledge of traditional buildings, their materials, and techniques could result in contributing the innovation throughout the construction industry. The heritage of historical and archaeological sites is inextricably linked to the use of ancient masonry, particularly mortar. This material, frequently disregarded, must be accorded the utmost attention in restoration works, not only to ensure the preservation of the structural and aesthetic values of buildings but also to safeguard historical technological skills and cultural identity. The renovation of existing buildings and the restoration of historical architecture represent an appropriate approach to reducing the impact of buildings from a circular economy perspective. Furthermore, this approach could prove beneficial in promoting the maintenance and life extension of existing buildings. In recent restoration and renovation work, the use of non-compatible and non-durable integration mortars has been demonstrated to present significant challenges, particularly in terms of compatibility with existing masonry structures. It is not uncommon for historic masonry to be treated without the requisite preparation, and pre-packaged industrial mortars are frequently selected on the building materials market without the benefit of appropriate criteria. Although traditional mortars generally show limited durability, multiple studies have shown that many archaeological and traditional materials have proven to be able to withstand the test of time and can therefore be used as models for the tradition-inspired approach to conservation[19-20]. It is therefore imperative that urgent efforts should be made to reduce the environmental impact of existing buildings, both during their use and in their maintenance and repair. This can be achieved by utilizing natural products and waste materials as aggregates and additives, thereby reducing the carbon footprint associated with the production and distribution of these materials. Based on this evidence, the project, aimed at sustainable and practical aspects, studies innovative mortar formulations for durable materials based on natural hydraulic binders[10,21-29].

Lime, a natural material that has been used throughout history as a binder in the production of mortars, interior plasters, foundations, floors, walls, and decorative elements (30; 26; 10), is often regarded as a 'green product' due to its minimal environmental impact and the absence of toxic substances in its composition. Furthermore, lime presents several advantages. It can be produced locally, providing a convenient and sustainable option. It offers breathability to walls, creating an environment conducive to healthy growth. Its antiseptic properties ensure a healthy environment. Its low modulus of elasticity allows for self-healing, preventing the need for frequent maintenance in contrast with the higher levels of resistance shown by Portland cement[31]. Additionally, its low thermal conductivity enhances the thermal capacity of walls, reducing energy consumption. Traditional masonry is a characteristic element of monumental construction, including archaeological areas, and mortars and plasters play a key role in both the stability of the structures and the protection of the surfaces themselves. Mortars and plasters have been used extensively in civil engineering and architectural construction, and their compatibility with ancient mortars has led to their recent reintroduction in restoration work[32]. Architectural heritage is typically exposed to climatic and environmental factors, such as temperature and humidity, which play a key role in its deterioration. Mortars and plasters, being directly linked to the load-bearing structures of a building, represent the interface between physical assets and climate in an open physical system. Since the wide range of deterioration phenomena of natural and anthropic origin to which they are subject, mortars and plasters are often considered "sacrificial materials". In the present research mortars with less environmental impact and greater compatibility with ancient building materials are produced with a focus on durability in coastal environments. The system constituted by the building and its surrounding climate must be considered as a whole. In particular, the coastal environment can be considered extremely harmful to building materials. The presence of soluble salts acts in different ways leading to physical degradation such as micro and macrocracking; loss of cohesion or adhesion; salt accumulation, scaling, disintegration; erosion; and color alteration[23]. Cement-free hydraulic mortars and plasters, widely used in construction throughout history, play a fundamental role both in the stability of structures in dry and humid environments and the protection of surfaces as they constitute an important interface between the built structure and the environment. Mortar formulations have been modified with several additions throughout history to prevent deterioration, not always with noticeable results. To achieve better effectiveness of durability in recent years several studies have focused on the use of additives to improve the water-repellent behavior of mortars, as well as their resistance against degradation by soluble salts[33-37]. The study of mortars is a difficult

task due to the complexity of the mixture, even the smallest changes in individual components or the dosage of mortar can affect the properties of the final product. Mortars are man-made building materials composed of one or more inorganic binders, whose main function is to bind the grains of the inert mass through various chemical transformations, one or more aggregates, which are added to give the mortar mass volumetric stability during the drying stages and to increase the mechanical strength, and water, which is necessary to mix the various components. In addition, other elements, known as additives, are often added to mortars to give the final product-specific characteristics[38-40]. To achieve better effectiveness of durability in recent years several studies have focused on the use of additives to improve the water-repellent behavior of mortars, as well as their resistance against degradation by soluble salts[33,34,36]. Interestingly, there is also evidence of the use of a wide range of natural organic additives (plant fibers and extracts, animal fats, milk, casein, egg yolk, linseed oil, etc.) to improve and optimize the properties and performance of lime-based materials[41-42]. In addition to this evidence for the rediscovery of traditional mortars, we can add the fact that lime-based binders have recently been re-evaluated in the field of heritage conservation, thanks to their many advantages over cement-based mortars: low environmental impact; the possibility of local production; absence of toxic substances; good breathability and thermal capacity; high compatibility when applied to traditional masonry[42]. Based on this vision, which is also more attentive to the aspects of sustainability, the project proposes to study new formulations based on natural air and hydraulic binders, which are considered "green" binders due to their lower environmental impact during production and their high compatibility, also with the addition of pozzolanic, hydraulic materials and also salt modifiers and inhibitors, which can limit the damaging effect that soluble salts have on masonry, particularly in coastal and lagoon environments such as Venice[43-45].

1.2 State of Art – History of Lime

Throughout history, lime products have been a fundamental element in the building industry. The history of lime begins in ancient times, in the Stone Age when traces of burnt lime and several kilns for the production of quicklime were found[10,23,26,46,47]. The first binders derived from calcination processes of natural stones, generically called cementitious, were chalk and air lime. Their discovery was probably coeval and can be imagined to have the same origin as that of terracotta, being also linked to the discovery of fire. Given the fact that chalk was easier to obtain than lime, due to the lower firing temperature, it is likely that it initially found greater application. Indeed, the earliest known example of the systematic use of a cementation reaction in construction is related to the use of gypsum in the support of the decorative frescoes of Cata Huyuk in Asia Minor, dating back to 9000 BC[48-50]. The oldest known artifact made of lime is a concrete used in a pavement found in 1985 in Yiftah in southern Galilee (Israel), dated to 7000 BC. This pavement, which is very compact with a hard, smooth surface, was made of lime and stone and placed on a uniform base of sandy clay. The first traces of the use of lime in construction can be found in the monumental buildings of ancient Egypt. Prof. Sir Flinders Petrie unearthed samples of plaster in the pyramids and temples, some of which are still intact. Three-capped lime putty, 3/4 inch thick, on laths of reed and with a plaster finish from hair was also observed. A plaster of lime plaster was sometimes used in the masonry of the pyramids, to fill joints and level cavities. This was also used over the sculpture to provide a surface for coloring This archaeological discovery superseded the previous discovery, a 25 cm thick fat-lime concrete terrace found in Lepenac Vir, Serbia, dating back to 5600 B.C. Egyptians. A mural, found in Thebes dating back to 1950 BC. Shows an early example of lime-based mortar and conglomerate in Egypt. The discovery of a binder with hydraulic behavior, i.e. capable of setting and hardening even in an underwater environment, goes back to the Phoenicians. As is well known, they had a very advanced civilization and are credited with various inventions such as metal smelting, the first alphabet, etc. The Phoenicians are also credited with the preparation of lime binders. Water cisterns, plastered with hydraulic mortars, have been found in Jerusalem and date back to the reign of Solomon (10th century BC) and the hand of Phoenician workers. The Greeks used lime-based binders extensively; it is therefore worth mentioning the magnificent wall paintings of the Palace of Knossos in Crete, made with a double layer of lime plaster and clay base, dated around 1500 B.C. In Greek temples, it was also not uncommon to find traces of lime putty, in particular, for the outer covering of temples, even if they were built of marble, as

well as colored plaster floors. Pliny himself mentioned a mixture of lime putty with milk and saffron applied in the temple of Elis[10,22,23,26]. The Romans greatly improved the technology of producing air lime by firing good quality limestone and carefully slaking the resulting quicklime, which was then mixed with clean sand. In Rome, examples of plastering could often be found, being the most common external finish of private houses, which was, however, mostly destroyed in Nero's fire in 64 A.D and subsequent reconstruction. Pliny the Younger himself quoted 'no builder should employ lime that has not been worked for three years'. Vitruvius[46,51,52]. They only knew of aerial lime, i.e. lime capable of setting in contact with air, while natural hydraulic lime, which is also capable of setting under water, was unknown. The Romans were, however, able to make hydraulic mortars by adding pozzolana to the mix. Like the Greeks and Phoenicians before them, they were not unaware that certain volcanic deposits, when ground and mixed with sand and aerial lime, provide a mortar that not only has mechanical strength higher than those obtained with lime alone but also the property of resisting the action of both fresh and seawater. To formulate hydraulic mortars, the Romans mainly used red or purple volcanic tuffs, found in various places (around the Bay of Naples, on the island of Santos, or the dark-colored volcanic earth from the island of Thera, and, later, deposits of Rhine trass, a volcanic tuff from southern Germany). It follows that the main binder of the Roman period was in fact "calcestruzzo", concrete, a mortar made from slaked lime, sands, cocciopesto, pozzolanic sands, fired brick fragments, in its different variants. This practice probably predates the use of volcanic materials: there is evidence from the Minoan civilization of Crete (circa 1700 BC) of the use of adding crushed pottery residues to lime mortars to improve their mechanical strength, impermeability, and durability. The popularization of Roman technology was facilitated by the publication around 13 B.C. of 'De architecture' by the architect and engineer Marcus Vitruvius Pollonius. This work constitutes an extremely detailed source of information regarding Roman construction methods and is considered *de facto* the world's first example of industrial standards[47,52,53].

Following the fall of the Roman Empire, like the rest of the arts and learning, the art of building underwent a great impoverishment, and the knowledge of mortars was lost for the most part, such as hydraulic mortars: in the medieval period, castles and cathedrals were erected with simple traditional lime mortar, which survived the test of time not so much because of the properties of the mortar itself, but rather because of the large size of the buildings and the shrewdness of the builder himself. During the Middle Ages, many of the kiln-building caveats were neglected and there was a return almost everywhere to the upright type of country kiln, without a brick lining, generating much '*vincotto*', i.e. uncalcined stone, sunk into the ground

in areas suitable for using two loading levels, that of the stone above and that of the wood and lime discharge below, or again to the sloping kiln. The consequence of the rudimentary nature of many of these kilns was a general decline in lime quality. It was only later, in the 14th century, with the adoption of still intermittent but brick and wood-fired kilns, and in the 18th century, grate-fired with charcoal, that the quality successes of Roman times were restored[48,50,51,54].

The phenomenon of the revival of the arts and interest in classical literature during the Italian Renaissance led to a revaluation and intense study of the ancient arts of plaster and stucco. In the hands of Raphael and other eminent representatives, stucco work quickly caught on in Italy. Further improvements took place in the following centuries, and especially between the 17th and 19th, with the various innovations introduced in lime manufacturing technology, with the replacement of wood with coal for firing and the discovery of new sources of materials with pozzolanic behavior for making hydraulic mortars. In any case, during these centuries the general level of quality remained very variable, and the standards achieved in Roman times were, as a rule, no longer achieved. Cement remained the undisputed construction binder for much of the 20th century. The oil crisis of the 1970s underlines, perhaps for the first time, the fragility of Portland, at least from an energy point of view, due to the enormous number of resources needed for its production. Then from 2000, words like 'Environmental Sustainability' 'Ecological Architecture,' and 'Conservation of Cultural Heritage' became central themes in the economic and political agendas of the most developed countries: lime reappeared as one of the possible solutions to these problems[48,50,54].

Today, lime, by virtue of the lower demand for energy in production, the healthiness imparted to buildings and the compatibility with the historical building, is proposed to us as the building binder of the third millennium, with that 'freshness' and 'capacity to amaze' that only an extraordinary material can boast, after centuries of hard and tireless work[10,26,29,46,47,53,55].

1.3 Lime: characteristics, production and processing

The raw material for the manufacture of aerial lime is limestone with a calcium carbonate ($CaCO_3$) content of more than 95%. The main quality of the lime rock is its purity and high calcium carbonate content; it is well known that aerial lime is all the better the whiter the limestone for calcination[26,46,47,53]. The rock must be bright white, homogenous, without earthy veins, alterations or patinas with a fine-grained and tightly packed structure that can be saccharoidal or microcrystalline. The impurities that can be found derive from the presence of magnesium carbonate and siliceous or clayey fractions associated with limestone. These lead to a decrease in the technical qualities of the binder and therefore must not normally exceed 10% of the total volume. If the ferruginous impurities give the lime a yellowish or pinkish tint, a certain content of clay minerals produces a limited hydraulicity with greyish coloring to more or less deep blue or hazelnut shades, green tones if the natural rock is rich in chlorites. A particular type of limestone extraction derives from the exploitation of coarse debris deposits found within riverbeds at the exit of the watercourse from hills and mountains. The cultivation of river gravel is characteristic of many Apennine and Alpine streams; in the area of the Brenta and Piave (Veneto region) are extracted pebbles composed of pure limestone and sizes ranging between 5 and 30 cm in diameter that give a lime of excellent quality. The extraction in bed allows to use a material already crushed and of adequate size to the cooking techniques, avoiding long operations of splitting and selection from possible earths levels already eliminated by the running waters[10,29,47,56-61].

1.3.1 Lime production

The first operation in the lime production cycle, limestone is calcined in suitable molds at a temperature between 900 and 950°C. This causes the endothermic decomposition of calcium carbonate[10,26,46] (1):

$$(1)\ CaCO_3 + 42{,}52\ \text{Kcal/mol} \rightarrow CaO + CO_2$$

During this phase calcium oxide or lime (CaO) is formed with a weight loss of about 44%, which corresponds to a decrease in volume in the calcareous mass of about 20%. The characteristics of the final product depend on several factors; among these, the most important is the compactness of the rock, which can limit the decomposition reaction that proceeds progressively from the outside to the inside of the rock fragments. The temperature in the furnaces reaches about 1100 °C to allow complete calcination even of the inner parts of large rock fragments. The temperature should not exceed the indicated values, only with a constant and "sweet" cooking the calcium oxide crystals remain small and therefore have a high active

surface area necessary to carry out the subsequent hydration operations correctly and completely. Above the optimum temperature values, a large crystal structure of quicklime is gradually created with reduced reactivity; in these cases, hydration is completed with difficulty and lime can cause blooms or detachments in the mortars even after taking[47,56,58-61,62-65].

1.3.2 Quenching

The quicklime, to be used, must undergo a quenching process, from which is obtained a plastic and workable product that in the presence of air tends to harden[12,26,46,47,57,66-68] (2) :

$$(2)\ CaO + H_2O \rightarrow Ca(OH)_2 + 15{,}6\ \text{kcal/mol}$$

The quenching reaction is therefore exothermic, whose product consists of calcium hydrate, also known as slaked lime or hydrated lime. The products coming out of the traditional ovens are never perfectly homogeneous and therefore the well-cooked quicklime blocks must be separated from the unbaked or overbaked fractions. The clods of good quality are recognized because light and white or whitish with a fairly compact consistency, although of a mealy appearance; are free of hard, uncooked nodules or heat-reduced parts such as heavy and very dense clods resulting from excessive temperature. When the slaking of selected parts is carried out with ordinary systems, this can also be done on-site, the lump lime is placed inside containers called baths, where it is mixed with water to obtain hydrated or slaked lime. When slaking quicklime, different products can be obtained depending on the amount of water that is added during the slaking process and the purity of the lime itself. When slaking is undertaken with an excess of water (approximately 3/4 times the amount used for quicklime), a dense, oily paste known as slaked lime is obtained (Conversely, when an even higher quantity of water is used, limewater, a diluted aqueous suspension of calcium hydrate, is obtained)[46,47,57,60,61,66-68].

The *slaked lime yield* of an aerial lime is expressed as the volume of fresh slaked lime obtained by slaking a given mass of quicklime and is expressed in m^3/ton. The different types of lime that can be distinguished are as follows:

- **Fat lime**, where the yield is greater than 2.5m^3/ton;
- **Lean Lime**, where the yield ranges between 1.5 and 2.5 m^3/ton.

1.3.2.1 Fat Lime

Fat lime can be obtained if quicklime that does not contain magnesium or carbonate filler due to poor baking is slaked. Fat limes are derived from the purest limestones, exhibit high plasticity (ease of workability in construction applications), longer setting time (especially when thicker applications) and good water solubility (it dissolves when exposed to moisture). A "fat lime" is designated as such due to its propensity to undergo a substantial volume increase upon contact with water, reaching a two- to three-fold increase in size. Notably, the hardening of this substance occurs exclusively in the presence of carbon dioxide present in the ambient atmosphere. The best fat limes have a calcium hydrate ($Ca(OH)_2$) content greater than 90%, which is also the reason behind their white hue. The closer said content is to 100%, the purer (and fatter) the lime is. On the contrary, lean lime can be obtained if quicklime that does contain magnesium or carbonate filler due to poor baking is slaked. Lean lime is derived from impure limestones (i.e. with a CaO content of less than 94%) or poorly fired limestones (where there is the presence of uncooked parts or overcooked parts). MgO is one of the most frequent impurities in lime and its presence contributes to the thinness of the lime; moreover, MgO is formed earlier than CaO (the decomposition temperature of magnesium carbonate is lower than that of calcium carbonate) at the end of the lime firing process, MgO will be overcooked and will therefore hydrate more slowly than CaO. Fat limes are mainly used to produce lime mortars for plastering, as a base for distemper and matrix in concrete, used for white washing plastered surfaces and other industrial applications[29,47,53,57,61,66,68].

1.3.2.2 Lean (Poor) Lime

On the contrary, a lean lime can be obtained if quicklime that does contain impurities due to poor baking such as carbonate filler, clay impurities and MgO is slaked. Lean lime is derived from impure limestones (where the CaO content is less than 94%) or poorly fired limestones (where there is the presence of uncooked or overcooked parts). The reduced content of calcium oxide (CaO) along with the presence of MgO, silica, alumina and iron oxide contribute to the poor performance of the final product. Magnesium oxide (MgO) is one of the most prevalent impurities in lime, and its presence contributes to the thinness of the final product. In fact, MgO is formed earlier than CaO during the process of lime firing due to the lower decomposition temperature of magnesium carbonate (350 °C) in confront to that of calcium carbonate (>825 °C). Consequently, MgO gets overcooked and shows a lower rate of hydration compared to CaO. Lean limes are defined by grayish/yellowish shades and require a longer slaking time due to the

impurities which also affect the setting and hardening, making it unsuitable for structural applications but rather for temporary structures[29,47,53,57,61,66,68].

1.3.2.3 Hydraulic Lime

Hydraulic lime is a mixture of silica, alumina and iron oxide combined together with calcium oxide. This composition enables it to set and harden without the presence of carbon dioxide (CO_2), producing a lime suitable for use in underwater or damp environments. Hydraulic limes are capable of setting and hardening both underwater and in low-oxygen conditions. When mixed with water, it forms a thin paste; however, precise water management is required to prevent hardening prior to use. The classification of hydraulic lime is based on its clay content, which influences its hydraulic (water-setting) properties.

- **Feebly hydraulic limes**: show a clay content less than 5-10% and their setting time is the longest among the others (taking about 21 days to fully set) they are suitable for applications in damp locations and less critical construction work;
- **Moderately hydraulic lime**: they exhibit a clay content between 10-20%, capable of setting in just 7 days are often applied in moderately damp areas and for more substantial structures;
- **Eminently hydraulic lime**: They have the highest content of clay (20-30%) which makes them suitable for wet areas and significant construction work.

The versatility of hydraulic lime in conditions where traditional lime is inadequate is a significant advantage, rendering it valuable for foundation work, underwater applications and structures exposed to high levels of moisture. Hydraulic lime is available in three different grades; NHL 2, NHL 3.5 and NHL 5. The NHL stands for Natural Hydraulic Lime. The number relates to compressive strength in MPa (Megapascals) or N/mm^2 at 28 days. These grades were historically associated with the terms feebly hydraulic, moderately hydraulic and eminently hydraulic respectively. These terms refer to each grade's degree of hydraulicity, that is their ability to set under water without exposure to air[40,67-73].

1.3.2.4 Magnesian lime

During the project, in addition to carbonate-based limes, other types of limes, i.e. magnesian limes, were studied and used for specimen preparation. Limes known as "magnesian" or "dolomitic" are named after dolomitic limestones. Dolomite is a compound of magnesium and calcium carbonates ($CaMg(CO_3)_2$) that is formed by the substitution of Mg atoms in the alternating layers of Ca in the normal calcium carbonate structure ($Ca(CO_3)$) and this is coupled to a change of bond strength and a displacement of atoms. As a result of this, dolomite is harder and denser than normal calcite, although the substitution process often remains incomplete, so not all dolomitic limestones contain the same amount of ($CaMg(CO_3)_2$) [74-76]. In natural environments, the presence of carbon oxides can make minerals that contain MgO or CaO undergo carbonation reaction:

(3) $CaO + CO2 \rightarrow CaCO_3 + 179$ kJ/mole;

(4) $MgO + CO2 \rightarrow MgCO_3 + 118$ kJ/mole.

In nature it is difficult to find pure oxide minerals, most commonly these are found as a chemical combination of calcium and magnesium oxides with other oxides forming a silicate matrix. Magnesium and calcium are the only common elements capable of forming stable carbonate minerals and it's usually a process occurring on geologic time scales[78]. Similarly, normal limestones may contain small percentages of calcium and magnesium carbonates, this time separated into their respective forms $Ca(CO_3)$) and magnesite ($MgCO_3$). Depending on the proportion of magnesite, different types of magnesian limestones can be identified:

- High calcium limestone-0-5 $MgCO_3$ content%);
- (Magnesium limestone-5-35 $MgCO_3$ content%);
- (Dolomitic limestone-35-46 $MgCO_3$ content%) (American Society for Testing and Materials, 1976)

In contrast to traditional lime production, magnesian limestones must be calcined between a temperature of 510°C and 750°C, a considerably lower range than calcitic limestones, and may follow only one or two steps:

(5) $CaMg(CO_3)_2 + heat = Cao*MgO + CO_2$

(6) $CaMg(CO_3)_2 + heat = CaCO_3*MgO + CO_2$

(7) $CaCO_3$*MgO + CO_2 + *heat* = Cao*MgO + CO_2

If the process follows reaction Eq.3, the dolomite will be fully calcinated at 750°C, while if it follows the two steps described in Eq.4 and 5, the first will occur at about 510°C and the second at 900°C[74-78]. Since each limestone has its composition, it will require specific firing temperatures that will have to be determined by testing to avoid the formation of overburnt material that could cause problems during quenching. Extinguishing also exhibits two different behaviors depending on the type of lime, magnesia (MgO) combines with water in a more time-consuming manner than CaO, and the presence of impurities or overburnt parts contributes to the increase of the extinguishing time[74,76,79]. A further distinction can be observed in the extent of carbonation of the hydroxide, which in the case of magnesium lime does not exceed 60% (in contrast to 95% in calcium hydroxide). This reaction does not strictly depend on the concentration of carbon dioxide (CO_2) but also on the ambient temperature. Despite this, magnesian limes can develop good binding power and good mechanical strength even before its carbonation, thanks to its characteristic fibrous and microcrystalline structure. The presence of overburnt parts may lead to delayed extinguishing compared to the majority of the mortar matrix, causing expansion fractures. To ensure complete hydration, magnesium lime is usually quenched in an autoclave at pressures between 1.7-7atm with a temperature ranging between 115-165°C[74,77,80].

1.3.3 Mortar production

In construction, lime is used to form mortars, a fundamental backbone of building industry whose origins go back a long way in history[26,48,50]. A mortar is a mixture of lime and sand made plastic by the addition of water and one or more other substances to give the blend specific properties. When hydrated lime or slaked lime is mixed with sand and water, for the application enlisted earlier, they undergo a specific exothermic reaction (8):

(8) $Ca(OH)_2 + CO_2 \rightarrow CaCO_3 + H_2O$

This type of mixture at the same time as the above-mentioned reaction (6) takes place, in which carbon dioxide (CO_2) reacts with lime dissolved in water, undergoes a contraction where it assumes a certain consistency while some of the water evaporates[60,81]. The traditional classification of binders is based on their

property to harden the mortar mixture in air or in contact with water; from this comes the subdivision into air-bound, class that includes gypsum and air lime, and hydraulic binders, including cement and its derivatives. For certain intrinsic characteristics, hydraulic lime may assume an intermediate position, where some types demonstrate properties similar to those of aerial binders while others have better hydraulic properties. Mixtures of binders with water are defined as pastes (fluxes if particularly fluid) while those containing granules of different stone-origin measurements are defined mortars (if made of binder, water and granules such as sand) or concrete (if they are made up of larger stone granules like gravel or stones)[10,12,26,29,46,67].

1.3.3.1 Magnesian Mortars and Hydromagnesite

As with lime mortars based on calcium oxide (CaO), the same process of carbonation of hydrated lime, obtained from limestones with varying amounts of magnesium carbonate, such as dolomite, can produce mixtures defined as 'magnesian mortars' ($CaMg(CO_3)_2$)[74-77]. In this kind of mixtures, the bond that develops within the matrix during the curing phase, i.e. in the presence of MgO, $Mg(OH)_2$ and moisture, gives rise to a new phase called hydromagnesite ($Mg_5(CO_3(OH)_2 \cdot 4H_2O$). From the calcination of dolomitic limestones, the main products obtained are calcium and magnesium oxide and hydroxide, as exposed earlier, and multiple studies have already researched about both the process of carbonation of MgO and the sorption of CO_2 by MgO and $Mg(OH)_2$ at high temperatures in order to explain the formation of hydromagnesite[77,78,82,83]. An earlier study[84], has demonstrated that the carbonation process of the phase occurring during curing made by: Magnesium Oxide (MgO) + Carbon Dioxide (CO_2) + Water (H_2O), is highly dependent on the CO_2 concentration and environmental temperature. This knowledge has been deepened by another research made by Dheilly[83] which used $Mg(OH)_2$ directly to assess the development of both microstructure and strength in cured lime paste mortars at ordinary temperatures. The study was able to demonstrate, regardless of temperature that in moist air atmosphere MgO converted into hydromagnesite (9):

$$(9)\ MgO \rightarrow Mg(OH)_2 \rightarrow Mg_5(CO_3)_4(OH)_2 \cdot 4H_2O + Mg_5(CO_3)_4(OH)_2 \cdot 5H_2O$$

From the results, it could be observed that the presence of $Mg(OH)_2$ in lime mortars helped enhancing the mortar strength and this was supported by SEM investigations which shown that empty spaces between sand grains are more easily filled when the lime is a pure $Mg(OH)_2$ paste. The presence of hydromagnesite

was found to be capable of enhancing the development of binder between sand grains, providing the reason behind the improved mortar cohesion and the cause behind the increase in strength[74,78,83].

1.3.3.2 Porcelain Mortars

There is another type of mortar on which this research has focused, the so-called porcelain mortar. This type of mortar is often referred to in the jargon of the old Ligurian masters as "porcelain" or "purselana" in the context of building materials. The first traces found date back to the second half of the 16th century and were characterized by an exceptional consistency and whiteness, despite constant contact with seawater. These mortars are the subject of much debate, both as regards their origin and the methods used to produce them, except for the presence of potassium alum, a compound widely used at the time to dye fabrics for tanning leather. This alum was extracted from the Tolfa Mountains in the second half of the 15th century, along with kaolin, another main ingredient in porcelain mortars. There is no scientific evidence that the combination of calcinated kaolin and potassium alum contributed to the toughness of the mortar although the famous French builders and architect Loriot and Rondelet experimented with these properties[85-88].

1.4 Inert materials (aggregates)

The term 'aggregate' is defined as a component of mortar and can be further subdivided into the following categories: sand aggregate (coastal and river sand), crushed stone, natural and artificial materials with pozzolanic behavior, and hardened mortar fragments. Aggregates can be divided into two macro-categories: those that do not react chemically when in contact with lime (i.e. aggregates) and those that interact in the carbonation reaction of lime (i.e. reactants). Sand is one of the most utilized materials in the production of plaster. It is derived from clastic sedimentary rocks, obtained through the erosion of rocks, including sandstone, a sedimentary rock. It typically consists of granules between 2 and 0.063 mm in size and is composed of materials such as calcite, feldspars, quartz (characteristic of light sands) magnetite, and hematite (present in dark sands). This specific material is only mechanically integrated into the mortar matrix and does not engage in any chemical interactions with the other components. The function of these materials is to form a skeleton for the mortar, which undergoes a reduction in volume during the setting and hardening process due to the formation of a new crystalline arrangement as the water evaporates from

the mixture. The distribution of this shrinkage over the surface of the individual granules serves to prevent the formation of cracks or detachments between the crystals, as any stresses would otherwise be accommodated by the surrounding material. Sand, a product derived from the disintegration of compact rock through the action of waves, currents and weathering, plays an essential role in the production of mortars. Riverside sands are the optimal choice, whereas those originating from marine sources are less suitable due to their NaCl content. Mortars are best composed of sands with compact, non-friable grains. Silica sands with a high quartz content are highly recommended, as the greater the angularity and coarseness of the grains, the more effective the binding between the materials in the mixture. Crushed stone is composed of sharp-edged stone chips and fragments, obtained from hard rock through the process of crushing. The most suitable rocks are those that are more compact and resistant, including limestones, granitic or siliceous rocks. Natural pozzolan is a volcanic rock that is found in various locations throughout Italy, including Lazio, Campania, and Sicily. Pozzolan is composed as follows: aluminum oxide, silicon dioxide and a small percentage of other oxides such as iron oxide. In particular, the metastable glassy structure allows pozzolana to react with hydrated lime, forming rapidly, even at room temperature, a product that is both hydraulically soluble and insoluble, similar to those characteristic of hydraulic binders[89-90]. Similarly, they are capable of hardening in both air and in moist environments, or in submerged conditions. A substantial body of research has demonstrated that pozzolan has recently been employed extensively as a substitute for Portland cement due to its superior attributes, including cost-effectiveness, reduced heat emission, reduced permeability, and enhanced chemical resistance[91-93]. Another recent addition to the field of aggregates which caught our attention were the hollow glass microspheres, namely (HGMS). These nearly perfect engineered spherical bubbles of thin glass shells range approximately around 50 microns in size, exhibiting a really low density (0,1 up to 0,4 g/cm^3) and are typically used as a functional filler in anti-humidity paints thanks to their light weight and strength. Being a rather newborn material, its properties made us select it as a suitable filler for the mortar specimens, with the hope of achieving light but still hard structures capable of handling high humidity environments[94-97].

1.4.1 Additives

As was said previously, additives are additional materials that are mixed along with binders and inerts in order to achieve specific properties both in the fresh mortar and in the hardened one. Among the most common additives in mortars, pozzolana is certainly the best known, its properties make it possible to take and harden mortars in an underwater environment[90,91,98,99]. Its limited availability in North-East Europe has made it necessary to search for alternative elements that can be inserted into the mortar composition. In order to increase the hydraulic properties of mortars, Smeaton introduced iron and calcined mortar into the mortar mixture, his research was later verified by Faujas de St. Fond and Daudin in 1797 and 1808 respectively[100]. During this period of experimentation and development of various theories, researchers chose to keep the ideas established by Vitruvius and Pliny. While the Romans worked mainly with pozzolana, it is known that they also used some artificial materials: brick powder, tile powder or ceramic powder produced a less permeable mortar. Belidor, a staunch follower of Vitruvius, recommended flakes and flakes of stone from a blacksmith's forge and Raffineau de Lille suggested and preferred crushed bricks. Vicat later improved this by recommending the use of burnt clay or crushed bricks, supported by John[100]. In 1830-38, Charles W. Pasley conducted many experiments on countless artificial additives for hydraulic mortar, such as crushed gypsum, crushed flint, pure alumina, iron flakes from a goldsmith, and various metal oxides and carbonates. While the popular and common additives, such as iron filings, were tested in a laboratory, organic vernacular additives, natural ingredients found locally and used instead of lime due to prohibitive costs and scarcity, were proving equally adequate[100-102]. A model of the popularity and continued use of organic materials has emerged over the centuries. Blood has been the 'organic' one that has been used continuously for almost 2000 years. Eggs, egg whites and milk were almost equally popular, only experiencing brief periods of disuse. The treaties which mentioned organic additives were less technical in nature and lacked laboratory testing programs. However, the long-standing use of these organic additives has demonstrated the properties they impart. The key works ranged from those of Hugh Plat in 1594 to those of Joseph Moxon and Richard Neve in 1703 and 1726, respectively, to those of George Burnell in 1850. Accelerated setting time was achieved through fig juice, molasses increased hardness, and cheese served as a thickener, to name some elements of the pantry[28,33,103-106].

As in the past times, nowadays different types of materials are being tested as supplementary additives for the production of mortars, to modify and improve certain characteristics to make them more useful in the

application field. While many studies are still researching about past mortars composition (both lime-based and cement-based) others are focusing their efforts into developing new products to enhance mortars properties such as the mechanical strength, resistance to degrading agents, breathability and much more. One of the latest, most popular theme of research is the study of new solutions to limit the effect of soluble salts on building materials. Being the city of Venice, a backbone of Italian Cultural Heritage, and many other built entities, located in lagoon or coastal environments, the actuality of the issue of soluble salt decay becomes rather clear, as enlisted in numerous studies[44,45,107-112]. As some of the previous enlisted studies, one of the latest solutions against the presence of soluble salts in buildings is the use of salt crystallization inhibitors. Other fields also make use of inhibitors, such as oil extraction, to limit carbonates and sulphates deposits, in water desalination plants to reduce saline accumulation (Chernozhukov et al., 1969; Thabet et al., 2023). These additives can work in different ways depending on their nature: they can either inhibit the growth of the salt crystal during nucleation or solubilize the early formed crystals preventing the crystallization at the beginning stage[113,114]. Another kind of inhibitor acts instead on the pressure between the growing crystal and the inner pore surface of the building material. It creates a thin polymeric layer that takes the place of the saturated solution, making contact between the pore and the crystal core and deleting the amount of pressure exerted by the salt. It is therefore mandatory to introduce Chitosan, a product widely used for agricultural and biomedical purposes as antibacterial and antioxidant[115-117]. Among the qualities of Chitosan such as: non-hydrophobicity, environmentally friendly and biodegradability it participates, together with $CaCO_3$ in the formation of durable and hard mollusk shells in nature[116] and its functional groups makes it able to react with salts of different nature. These were the reasons it was chosen to be tested as a potential additive for this thesis. Thanks to recent research, it has been discovered that some inhibitors, such as Sodium Ferrocyanide, are able to modify the morphology of the salt crystal, affecting both nucleation and growth by anchoring themselves on the active crystal growth points, and limiting their growth[118]. Thus, Sodium Ferrocyanide was selected as a suitable candidate for experimentation. Multiple studies have tested these kinds of inhibitors on previous research with more or less good results. A study by Lubelli et al. from 2007, tested two different inhibitors on salted Spanish limestone, Czech sandstone and Dutch brick, namely Sodium Ferrocyanide and DTPMP (Diethylenetriamine Penta or methylene phosphonic acid). These two inhibitors gave different results as the first was highly effective on sodium chloride (NaCl) while the second was influenced by the nature of the substrate but still rather effective, making DTPMP the third inhibitor chosen for testing.

A problem was highlighted during the research: the limit of the spray application of both products on the specimens which may have limited the action against soluble salts[114]. Another study was carried out on the basis of this issue, a work about the effectiveness of crystallization inhibitors and consolidation of plaster in marine environments made by Renso M. in 2020[119]. The solution proposed was the application of said products by brush, to allow a longer reaction time and a deeper penetration in the matrix of the specimens but still some limitations could be found. Therefore, this work proposes to mix the inhibitors inside the mixture of the fresh mortar as a standard additive to enable a more homogeneous distribution of the latter on the cured mortar.

1.4.1.1 Metakaolin

The development of building materials that offer technical and environmental benefits represents a significant challenge for the new millennium. Supplementary cement materials (SCM) are finely ground solid materials that are used to replace part of the clinker in a concrete or cement in a concrete mixture. Thermally activated clays, in particular kaolinic clays, have recently been re-evaluated as a source of additional cement materials to reduce CO_2 emissions and energy consumption from cement production[120-122]. These materials include metakaolin (MK), a pozzolanic addition, classified as a new generation of additional cement material. Most metakaolin is commonly used in the Portland cement industries as an additive to improve the compressive strength of cement. The use of metakaolin in cement-based systems offers, in addition to technical advantages, significant environmental benefits. According to Smiley et al (1998)[124], replacing 8.1% cement with metakaolin and adding a little more water, the compressive strength of modified portland cement is the same as that of unmodified after seven days, and higher than that of unmodified cement after 28 days (73.3 MPa to 64.4 MPa)[123]. Metakaolin is distinctive in that it is not a by-product of an industrial process and is not wholly natural; it is derived from a naturally occurring mineral and is manufactured expressly for cementation applications. The production of metakaolin typically involves heat treatment, specifically the calcination of kaolin clay within a specified temperature range. Metakaolin is an additive that is employed to enhance the physical characteristics of Portland cement, which is obtained through the calcination of kaolin[125-127].

2. Research strategy and Materials

This PhD project lasted three years, during which periods of research and experimentation alternated with the purpose of deepening the knowledge about suitable solutions for the main objective. This process was oriented towards the development of new mortar formulations that have a number of characteristics, such as durability, resistance to weathering agents and, in particular, resistance to the crystallization of soluble salts and freeze-thaw. One of the most important aspects, in addition to those already mentioned, was to study those aspects of mortars that are often overlooked, such as the workability of the mix, specific weight, thixotropy and spreading. These aspects, observed during the experience at Mapei S.p.A., led us to consider a vision that focuses on the application aspects, as well as the physical-mechanical aspects of mortars. Understanding the properties of fresh mortars makes it possible to identify which application contexts are most suitable for which formulation. Freshly mixed mortars were analyzed according to these terms, during the first hour after mixing, determining specific weight variation (EN-1015/6[128]) and consistency variation (EN-1015/3[129]) together with the thixotropy test. Once the necessary analyses had been carried out, the fresh dough was poured into special moulds, whose dimensions varied from cubic shapes to parallelepipeds depending on the requirements required by the standards for tests on hardened mortars. The maturity times were then chosen systematically for each series, up to 28 days for Series 1 and 2 and 90 days total for successive series, a choice motivated by the search for a product based on traditional kicks and therefore requiring longer maturation times than others. An exceptional case was series 3, which was analyzed by XRD analysis during the maturation phase, to verify the formation of characteristic elements in the formulations and to evaluate their carbonation. The tests that were carried out following the maturation of the samples could be divided into two main groups: analyses concerning the behavior towards water (Water capillary absorption (EN-15801[130]); Water vapor permeability (UNI-EN 1015/19[131]) and those concerning the resistance of mortar to degradation agents or mechanical force (Resistance to Soluble Salts UNI EN 12370[132]; Resistance to Freeze/Thaw UNI EN 12371[133]; Flessive/Compressive strength resistance EN-1015-11[134]). For this purpose, the project featured a variety of formulations, different both in the main components and additives selected. In order to simplify the whole process, a block diagram is granted in order to have a more complete view of the entire PhD and the choices that determined the sample series (Fig.1).

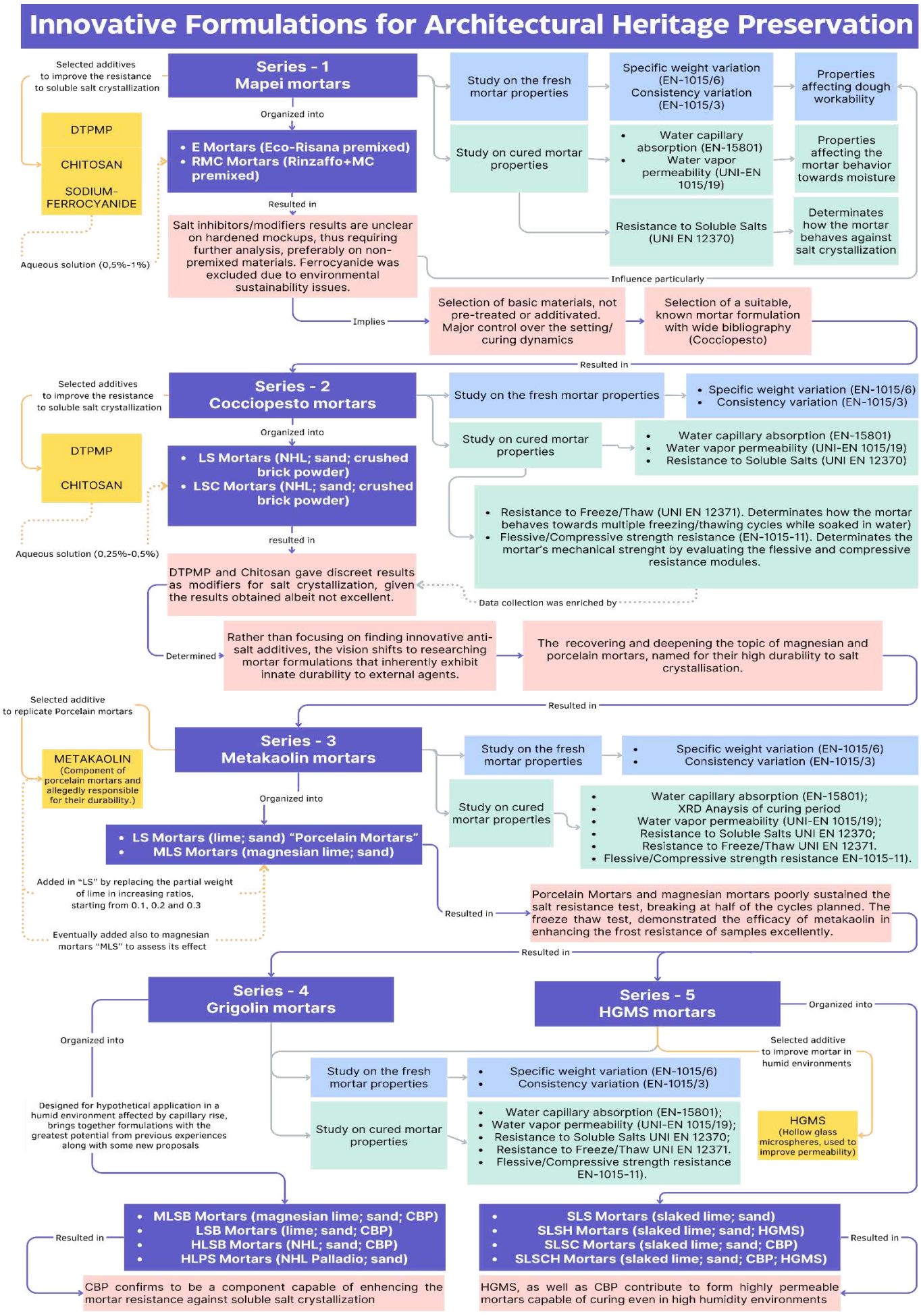

Figure 1 Block Diagram for the whole research project

2.1 Binders

During the course of studies, different types of binders were studied to evaluate the best alternatives for the development of new mortars and plasters, with particular attention on the resistance against freeze-thawing and soluble salt crystallization. After the first experiments with premixed products by Mapei S.p.A, as exposed before, the need for more natural materials was found, therefore, the following experimentations of the research featured non-premixed mortars but more natural starting materials (Tab.1):

Table 1 listing of binder materials used during the project

Binder type	Name/Producer	Characteristics
Premixed	Mape Antique Eco Risana, Mapei S.p.A	A premixed mortar powder for macroporous dehumidifying plasters, free from cement, composed of natural hydraulic lime (NHL 3.5 and NHL 5), natural sands, special additives and microfibers. It is a mortar designed for indoor/outdoor plastering, used on wet masonry walls containing water soluble salts[135].
Premixed	Mape Antique Rinzaffo, Mapei S.p.A	Mape-Antique Rinzaffo is a premixed cement-free rinzaffo composed of lime and Eco-Pozzolana, natural sands, special additives and microfibers, which needs to be combined with Mape-Antique MC[136].
Premixed	Mape Antique MC, Mapei S.p.A	MC is a premixed mortar powder for macroporous dehumidifying plasters, also free from cement, composed of lime and Eco-Pozzolana, natural sands, special additives and microfibers, with very low emission of volatile organic substances[137].
Natural Hydraulic Lime	White lime Lafarge	NHL 3,5; ($Ca(OH)_2$:15-65%; Ca_2O_4Si: 10-45%; $CaCO_3$: 10-40%[138].
	NHL Palladio Grigolin	Hazelnut-coloured lime suitable for interior and exterior decorative plasters, for use in the restoration sector as a binder and for dehumidifying applications[139].
Natural Lime	Hydrated Lime CL 80 Grigolin	Hydrated lime super ventilated by Grigolin S.p.A ($CaCO_3$> 98 %). (CaO + MgO ≥ 80%; average particles diameter 0.1μm)[140].

Magnesian Lime	Hydrated Magnesian Lime Grigolin	Magnesia hydrated lime by Grigolin S.p.A, ($CaCO_3$+$MgCO_3$ > 98%) (CaO + MgO ≥ 85%, MgO ≥ 30%; average particles diameter 0.1μm)[141].
Slaked Lime	Slaked lime Fassa Bortolo S.r.l	Hydrated lime paste by Fassa Bortolo S.r.l. Specific weight: ca. 1.300kg/m^3; average particle diameter inferior to 0,1mm (CaCo3 < 4%)[142].

2.2 Aggregates/inert

For the production of different mortar formulations, different types of aggregates were chosen. The choice of each was driven by the search for materials that were as little processed and or treated as possible, so as not to influence the processes taking place during the setting and curing phases of the mock-ups.

2.2.1 Sand Ticino Vaga

The sand is part of the VAGA WET SANDS, siliceous aggregates washed, calibrated and dedusted for use in mortars, concrete and bituminous conglomerates. Siliceous sand with Particle size from 0,1 mm to 0,9 mm (Category 0/1 mm according to EN 12620 "Concrete aggregates"; Category 0/1 mm according to EN 13139 "Mortar aggregates")[143]. Ideal for on-site preparation of finishing mortars and fine plaster; also used in floriculture and nurseries and for all applications requiring extra-fine natural sand (Fig.2).

Figure 2 Package of Ticino VAGA siliceous sand[143].

2.2.2 Crushed brick powder "CBP"

The cocciopesto San Marco Terreal used as an inert aggregate in the production of samples was produced starting from the grinding of terracotta bricks brand San Marco Terreal. The powder obtained has a particle size of 0,1-0.2μm.

2.3 Additives

In the experimental phase, three chemical saline growth inhibitors/modifiers were selected for testing: Chitosan, DTPMP and Sodium-Ferrocyanide, whose characteristics are enlisted below (Tab.2).

Table 2 Product specifics for salt inhibitors/modifiers

<table>
<tr><th colspan="3">Chitosan</th></tr>
<tr><td rowspan="4"> 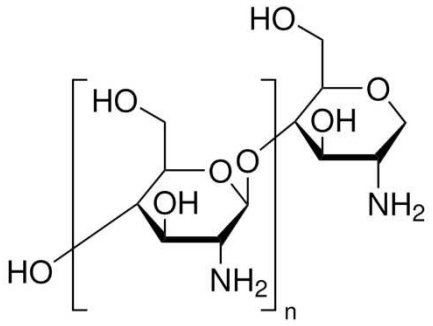
144</td><td>Substance</td><td>Poly(D-glucosamine)
Deacetylated chitin</td></tr>
<tr><td>Producer</td><td>Sigma-Aldrich</td></tr>
<tr><td>Formula</td><td>C12H24N2O9</td></tr>
<tr><td>N. CAS</td><td>9012-76-4</td></tr>
<tr><td colspan="3">Molecular weight:573.20; Off white to beige and faint brown to light brown appearance (powder/chips); Deacetylation: ≥ 75.0 % (Kjeldahl method); Viscosity: 200 - 800 cps[144].</td></tr>
<tr><th colspan="3">DTPMP - Dietylenetriaminepentakis</th></tr>
<tr><td rowspan="4"> 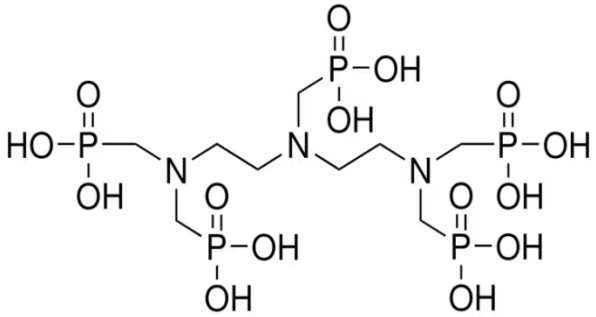
145</td><td>Substance</td><td>Dietylenetriaminepentakis</td></tr>
<tr><td>Producer</td><td>Sigma-Aldrich</td></tr>
<tr><td>Formula</td><td>C9H28N3O15P5</td></tr>
<tr><td>N. CAS</td><td>15827-60-8</td></tr>
<tr><td colspan="3">Molecular weight:573.20; Yellow to very dark yellow to very dark brown appearance (liquid/viscous liquid); Titration: ~ 50 % (Kjeldahl method); Refractive index N20/D: 1.468-1.478; Water content: ~ 35 %; Phosphorus 31 NMR Spectrum structure confirmed[145].</td></tr>
</table>

Sodium-Ferrocyanide		
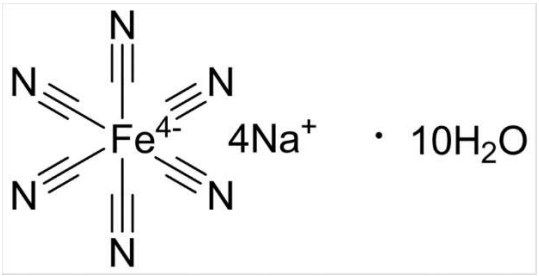 146	Substance	Sodium Ferrocyanide decahydrate ≥98.0%
	Producer	Sigma-Aldrich
	Formula	C6FeN6Na4 · 10H2O
	N. CAS	14434-22-1
Molecular weight: 484.06; Faint yellow to yellow appearance (powder/crystals); Redox Titration: ≥ 98.0 % (Permanganate titration method); Chloride (Cl) ≤ 0.20 %; Sulphate (SO_4^{2-}) ≤ 0.20 %[147].		

2.3.1 Metakaolin

Kaolin powder with a high degree of purity (98%) produced by Al.Fe Natura (Fig.3), was selected for the production of metakaolin in a laboratory setting through the application of heat treatment, which involves the calcination of kaolin clays within a specified temperature range. The thermal transformation of kaolinite, which has been the subject of a substantial body of research, demonstrated that the heating and cooling parameters, including temperature, heating and cooling rates, and environmental conditions, exert a considerable influence on the dehydroxylation process. A review of the literature on metakaolin reveals that the peak area of amorphous phase bands in the FTIR spectrum of kaolin calcined at 700 °C or 650 °C for 30–60 minutes is greater than that obtained at 800 °C. Given that elevated temperatures result in the formation of inert material, the decision was taken during this project to calcinate the kaolin in a muffle at a temperature of 650°C for a total of 60 minutes.

Figure 3 Package for kaolin powder used for calcination

2.4 Mock-ups Production

To ensure maximum reproducibility of the mock-ups, the mixtures have been mixed with a 120-mm triple helix-whip, threaded shM14, mortar mixer paddle. The mixing of the components was carried out following the scheme suggested by Mapei S.p.A to allow a homogeneous distribution of different components, consisting of:

30 seconds mixing at slow speed » 30 seconds pause » 1 minute slow speed

This was chosen as it refers to an optimal methodology to ensure, thanks to the pause time, that every small fraction of the powder is going to be well hydrated, establishing therefore, the optimal conditions for producing good mortars. The second crucial moment in the production of mortars is the one following the casting of the dough into the molds, the hardening phase of the mortar itself, which is distinguished in two main moments: *setting* and *curing* time. The *setting* time is the most delicate stage as the mortar, still liquid, is undergoing carbonation. During this phase, the mortar develops most of its compressive strength, at the end of which it can be removed from the moulds and handled, without risk of damage, to be placed in a controlled space where it can spend the necessary *curing* time. It is therefore necessary to maintain a controlled environment that presents the optimal conditions for the maturation of the dough. Below are

enlisted the setting and curing time chosen for each batch of mock-ups, determined by multiple factors such as the nature of the binder and the components used in the formulation (Tab.3).

Table 3 Series mock-up number, setting and curing time

Series ID	Mock-up number	Setting time (days+T°+RH%)	Curing Time (days+T°+RH%)
Series 1	270	2 days (T:20°C; RH:95%)	28 days (T:20°C; RH:50%)
Series 2	350	2 days (T:20°C; RH:70%)	28 days (T:20°C; RH:50%)
Series 3	360	2 days (T:20°C; RH:70%)	90 days (T:20°C; RH:50%)
Series 4	120	2 days (T:20°C; RH:70%)	90 days (T:20°C; RH:50%)
Series 5	60	2 days (T:20°C; RH:70%)	90 days (T:20°C; RH:50%)

Both phases were monitored using an Omega OM-EL-USB-2-LCD data logger to signal considerable fluctuations in temperature and humidity that could alter the two phases. Firstly, the choice to limit the maturation phase to only 28 days for Series 1 and Series 2, was dictated by the characteristics of the binders used, which take approximately 28 days to reach full maturity, and the need to combine the demand for results, the quantity of samples to be produced and the time required for sequential analyses. Hydraulic limes, as well as the products by Mapei, reach an acceptable degree of hardness in a relatively short time and then continue to harden progressively over a much longer period. According to the general regulations for cement mortar and concrete mixtures (ASTM International, 2025), 28 days of maturation are sufficient to allow the mixture to develop 90% of its potential hardness. This ensures sufficient mechanical strength and the development of optimal physicochemical properties for use in construction. The different formulations proposed during the studies are outlined below:

2.4.1 1st Set: "Mapei"

The first set of samples was produced from materials supplied by Mapei S.p.A. to which additives were added, selected based on in-depth research of the most recent architectural studies. Therefore Chitosan [$(C_6H_{11}O_4N)n$], Diethylenetriamine-Penta/DTPMP [$C_9H_{28}N_3O_{15}P_5$] and Sodium Ferrocyanide [$Na_4Fe(CN)_6$] were selected on the basis of their ability to inhibit the attack of soluble salts on building materials, or more specifically to reduce the adverse effects of the crystallization action of soluble salts from seawater and marine aerosol within a porous material. Models of Mape Antique Eco-Risana (Natural Hydraulic Lime) and Mape Antique Rinzaffo (both made with natural lime and pozzolan) mortars were developed to verify their chemical and physical properties (Tab.4). They were produced in molds without support to evaluate their properties in mass and with support to test their applicability on masonry. The samples were then named ECO (for the Eco Risana models) and MC (for the combination of Rinzaffo and MC models). Additives were included in the mortar recipe by replacing the amount of water expected for the mixture with an aqueous solution in three different concentrations (0%, 0.5% and 1% by weight). As for the rinzaffo/plaster combination (MC samples), the additive addition was performed only in the plaster section. To improve their resistance to salt crystallization, DTPMP, Chitosan and Sodium Ferrocyanide were used at different concentrations. In order to ensure an even distribution of the components, primarily the anti-salting agents, the latter were added to the water used to mix the dry components. Two types of aqueous solutions were then created, one at 0.5% and the other at 1% solubilized anti-salt product. In particular, where DTPMP and sodium ferrocyanide had no problems dissolving, chitosan showed low solubility. The problem was solved by adding 1 ml acetic acid and heating the aqueous solution to 30°C. The solution was then allowed to cool before continuing with the mixing.

Tab 4. Composition for 1st Set mock-ups: "Mapei"

Mortar Code	Mortar Composition (*wt*)
E_1/2/3	Mape antique Eco-Risana
E_CL05_1/2/3	Mape antique Eco-Risana + Chitosan (liquid) 0. 5%
E_CL1_1/2/3	Mape antique Eco-Risana + Chitosan (liquid) 1%
E_CS05_1/2/3	Mape antique Eco-Risana + Chitosan (solid) 0.5%

E_CS1_1/2/3	Mape antique Eco-Risana + Chitosan (solid) 1%
E_D05_1/2/3	Mape antique Eco-Risana + DTPMP 0.5%
E_D1_1/2/3	Mape antique Eco-Risana + DTPMP 1%
E_NFCN05_1/2/3	Mape antique Eco-Risana + Sodium Ferrocyanide 0,5%
E_NFCN1_1/2/3	Mape antique Eco-Risana + Sodium Ferrocyanide 1%
RMC_1/2/3	Mape antique Rinzaffo + MC
RMC_CL05_1/2/3	Mape antique Rinzaffo + MC + Chitosan (liquid) 0.5%
RMC_CL1_1/2/3	Mape antique Rinzaffo + MC + Chitosan (liquid) 1%
RMC_CS05_1/2/3	Mape antique Rinzaffo + MC + Chitosan (solid) 0.5%
RMC_CS1_1/2/3	Mape antique Rinzaffo + MC + Chitosan (solid) 1%
RMC_D05_1/2/3	Mape antique Rinzaffo + MC + DTPMP 0.5%
RMC_D1_1/2/3	Mape antique Rinzaffo + MC + DTPMP 1%
RMC_NFCN05_1/2/3	Mape antique Rinzaffo + MC + Sodium Ferrocyanide 0,5%
RMC_NFCN1_1/2/3	Mape antique Rinzaffo + MC + Sodium Ferrocyanide 1%

2.4.2 2nd Set: "Cocciopesto"

Natural hydraulic lime was the foundation of the second set, featuring lime and sand mortars (MS) added eventually with brick powder (MSC) with the inclusion of chitosan and DTPMP. Chitosan [$C_6H_{11}O_4N$)n] and DTPMP [$C_9H_{28}N_3O_{15}P_5$] were selected as salt inhibitors, included inside the matrix in order to study which properties would have been influenced and how. The addition of the two admixtures was performed by replacing the mixing water with a 0.5%–0.25% aqueous solution of chitosan or DTPMP. Furthermore, mixtures with chitosan in powder form at 0.5 and 0.25% admixture/binder were prepared. Sodium Ferrocyanide [$Na_4Fe(CN)_6$] has not been re-proposed due to its incompatibility with the eco-sustainability requirements. Following the results obtained during past studies, particular attention was given the

different ratio between binder and aggregate, discovered to strongly influence both physical and mechanical properties of mortars: a binding:aggregate ratio of 1:1 will result in a greater pozzolanic reactivity of the mortar while a ratio of 1:3 will develop faster carbonation and faster setting times (Casadio et al., 2005; Cazalla et al., 2000; Gameiro et al., 2014; Lawrence, 2006). The lime mortars were prepared by mixing NHL and sand with a mass ratio of 1:2 meanwhile the cocciopesto mortars were prepared at a mass ratio of 1:1.7:0.3 NHL/sand/CBP where the crushed brick powder worked as a substitute of the sand. A total of 350 mock-ups were produced, with 25 replicas for each formulation. Tab.5 reports the names and composition of the different formulations.

Tab 5. Composition for 2nd Set mock-ups: "Cocciopesto"

Mortar Code	**Mortar Composition (*wt*)**
LS_1/2/3	NHL + Sand (1:2)
LS_CL025_1/2/3	NHL + Sand (1:2) + Chitosan (liquid) 0.25%
LS_CL05_1/2/3	NHL + Sand (1:2) + Chitosan (liquid) 0.5%
LS_CS025_1/2/3	NHL + Sand (1:2) + Chitosan (powder) 0.25%
LS_CS05_1/2/3	NHL + Sand (1:2) + Chitosan (powder) 0.5%
LS_D025_1/2/3	NHL + Sand (1:2) + DTPMP 0.25%
LS_D05_1/2/3	NHL + Sand (1: 2) + DTPMP 0.5%
LSC_1/2/3	NHL + Sand + Brick powder (1:1.7: 0.3)
LSC_CL025_1/2/3	NHL + Sand + Brick powder (1:1.7:0.3) + Chitosan (liquid) 0.25%
LSC_CL05_1/2/3	NHL + Sand + Brick powder (1:1.7:0.3) + Chitosan (liquid) 0.5%
LSC_CS025_1/2/3	NHL + Sand + Brick powder (1:1.7:0.3) + Chitosan (powder) 0.25%
LSC_CS05_1/2/3	NHL+ Sand + Brick powder (1:1.7:0.3) + Chitosan (powder) 0.5%
LSC_D025_1/2/3	NHL + Sand + Brick powder (1:1.7:0.3) + DTPMP 0.25%
LSC_D05_1/2/3	NHL + Sand + Brick powder (1:1.7:0.3) + DTPMP 0.5%

2.4.3 3rd Set: "Metakaolin"

Given that a binding:aggregate ratio of 1:1 will result in a greater pozzolanic reactivity of the mortar while a ratio of 1:3 will develop faster carbonation and faster setting times, this time the mock-up products will feature different binding:aggregate ratio to determine which is the most suitable in terms of durability and performance. The focus of this set was to characterize and study the performance of some past formulations known as "Porcelain" mortars and "Magnesian" mortars. The literature on these subjects is poorly detailed, leaving only small quotations about their composition or the field applications that distinguished them. Both were, however, primarily known for their high resilience in high humidity environments such as spas or port areas. Accordingly, it was decided to formulate on the basis of the collected notions "Porcelain" mortars (based on lime, sand and metakaolin) and "Magnesian" mortars (based on magnesian lime and sand) on the various lime/sand ratios mentioned above and illustrated below (Tab.6). Regarding metakaolin powder, it was decided to produce the latter directly in the laboratory by altering the available kaolin powder. The addition of the metakaolin was then performed by replacing the partial weight of lime in increasing ratios, starting from 0.1, 0.2 and 0.3.

Tab 6. Composition for 3rd Set mock-ups: "Metakaolin"

Mortar Code	Mortar Composition
L1S1_1/2/3	Natural lime + Sand (1:1)
L09S1M01_1/2/3	Natural lime + Sand + Metakaolin (0.9:1:0.1)
L08S1M02_1/2/3	Natural lime + Sand + Metakaolin (0.8:1:0.2)
L07S1M03_1/2/3	Natural lime + Sand + Metakaolin (0.7:1:0.3)
L1S2_1/2/3	Natural lime + Sand (1:2)
L09S2M01_1/2/3	Natural lime + Sand + Metakaolin (0.9:2:0.1)
L08S2M02_1/2/3	Natural lime + Sand + Metakaolin (0.8:2:0.2)
L07S2M03_1/2/3	Natural lime + Sand + Metakaolin (0.7:2:0.3)
L1S3_1/2/3	Natural lime + Sand (1:3)

L09S3M01_1/2/3	Natural lime + Sand + Metakaolin (0.9:3:0.1)
L08S3M02_1/2/3	Natural lime + Sand + Metakaolin (0.8:3:0.2)
L07S3M03_1/2/3	Natural lime + Sand + Metakaolin (0.7:3:0.3)
ML1S1_1/2/3	Magnesian lime + Sand (1:1)
ML09S1M01_1/2/3	Magnesian lime + Sand + Metakaolin (0.9:1:0.1)
ML08S1M02_1/2/3	Magnesian lime + Sand + Metakaolin (0.8:1:0.2)
ML07S1M03_1/2/3	Magnesian lime + Sand + Metakaolin (0.7:1:0.3)
ML1S2_1/2/3	Magnesian lime + Sand (1:2)
ML09S2M01_1/2/3	Magnesian lime + Sand + Metakaolin (0.9:2:0.1)
ML08S2M02_1/2/3	Magnesian lime + Sand + Metakaolin (0.8:2:0.2)
ML07S2M03_1/2/3	Magnesian lime + Sand + Metakaolin (0.7:2:0.3)
ML1S3_1/2/3	Magnesian lime + Sand (1:3)
ML09S3M01_1/2/3	Magnesian lime + Sand + Metakaolin (0.9:3:0.1)
ML08S3M02_1/2/3	Magnesian lime + Sand + Metakaolin (0.8:3:0.2)
ML07S3M03_1/2/3	Magnesian lime + Sand + Metakaolin (0.7:3:0.3)

2.4.4 4th Set: "Grigolin"

The fourth set of mock-ups concerns the evaluation of possible mortar solutions contextualized in an environment with high humidity and heavy capillary rise. The chosen formulations this time cover different types of limes, starting from traditional, magnesian and natural hydraulic limes that have been combined with sand and additionally brick powder to enhance their pozzolan properties. All samples have been left setting and cured for a total of 90 days in a controlled environment (Tab.7). This part of the project focuses on the formulation and subsequent analysis of mortars that have as their main purpose a good yield and mechanical resistance in a humid environment as well as good resistance against soluble salts.

The main conditions that have influenced the formulation regard the workability of the dough, as it must demonstrate excellent grip and hardening skills without being affected by the presence of a high relative humidity index (HR) and capillary rise. Secondly, the mortar matrix is expected to mature over time, and demonstrate high resistance against efflorescences and sub-efflorescences, even if exposed to conditions that are not entirely favorable, such as the constant presence of humidity both in the environment and in the wall support. These formulations include past formulations and new propositions to be investigated. The selection fell on different materials such as Palladio NHL by Grigolin S.p.A, a natural hydraulic mortar which is indicated for humid environments which was also not treated with additional products, and a proposition in terms of inert components: the hollow glass microspheres. These, in particular was inspired by its use in the construction field, where the addition of hollowed microspheres provides excellent breathability to paints or finishing plasters, thereby counteracting the growth of mould or efflorescence due to the presence of soluble salts (Tab.7).

Tab 7. Composition for 4th Set mock-ups: "Grigolin"

Mortar Code	Mortar Composition (binder+inhert+additive)
L1S1.7C0.3_1/2/3	Lime\Sand\Brick Powder (1:1.7:0.3)
ML1S1.7C0.3_1/2/3	Magnesian Lime\Sand\Brick Powder (1:1.7:0.3)
L1S0.7C0.3_1/2/3	Lime\Sand\Brick Powder (1:0.7:0.3)
NHL1S0.7C0.3_1/2/3	NHL (Lafarge)\Sand\Brick Powder (1:0.7:0.3)
PL1S3_1/2/3	NHL (Grigolin)\Sand (1:3)
NHL1S3HGMS_1/2/3	NHL (Lafarge)\Sand\HGMS (1:3:0.07)
NHL1S3HGMSD_1/2/3	NHL (Lafarge)/Sand/HGMS (1:3:0.07) +40ml DTPMP
NHL1S3HGMSCL_1/2/3	NHL (Lafarge)/Sand/HGMS (1:3:0.07) +20ml Chitosan (liquid)

2.4.5 5th Set: "HGMS"

The fifth and last set features NHL and Slaked lime-based mortars combined with different types of additional inert materials. Crushed brick powder (CBP), along with the newly introduced hollow glass microspheres (HGMS) were the two inert additions chosen for this batch of mock-ups. In specific, Although the pozzolanic properties given by brick dust are now common knowledge, the same cannot be said for HGMS, spherical bubbles of thin-walled amorphous glass, that are approximately 50 microns in size, with a really low-density value. This last phase of the study therefore aims to study and compare the properties of the two aggregates added, verifying, as before, their durability and resistance against moisture and soluble salts (Tab.8).

Tab 8. Composition for Set n°5 "HGMS" mock-ups

Mortar Code	Mortar Composition
SLS_1/2/3	Slaked Lime/Sand (1:3)
SLSH_1/2/3	Slaked Lime/Sand/HGMS (1:3:0.07)
SLSC_1/2/3	Slaked Lime/Sand/CBP (1:2.7:0.3)
SLSCH_1/2/3	Slaked Lime/Sand/CBP/HGMS (1:2.7:0.3:0.07)

2.5 Analytic Techniques and Methodologies

2.5.1 Fresh Mortar Evaluation

Fresh evaluation is a critical aspect of mortar testing, due to the importance of the characteristics of the dough once it has been mixed. There are multiple characteristics that need to be mentioned and the workability is probably one of the most important as it determines how easy it is to work.

2.5.1.1 Consistency Variation

The mortar's consistency was determined by using a Tecnotest manual flow table to study the fresh mixtures according to EN 1015-3 (Fig.4). The variation in consistency over time was observed by performing three repetitions at t = 0, t = 30, and t = 60 min. The purpose of these examinations on fresh products is to spot any potential issues with the workability and other physical properties of every formulation.

The flow value is determined by measuring the mean diameter of a test sample. The bulk sample of fresh mortar is reduced to a minimum sample size of 1.5 liters. Where the flow of dry mortars is being measured, these should be mixed with water in accordance with BS EN 1015-2[129,148]. The test procedure involves placing the mould (60mm in height, internal diameter : base 100mm - top 70mm) in the center of the flow table and filling it in two layers, each layer being tamped ten times with the tamper. The mould must be held firmly in place. Excess mortar is removed from the top of the mould with a palette knife and the area around the base cleaned with a cloth. Approximately 15 seconds is allowed to elapse, and the mould is then removed and the table is jolted 15 times at a rate of one jolt per second. The diameter of the spread mortar is measured in two directions at right angles to each other using calipers, with both results being reported[129,148].

Figure 4 Shock table used for the test

2.5.1.2 Specific weight Variation

The EN-1015-6[128] specifies a method for determining the bulk density of fresh mortars including those containing mineral binders and both dense and lightweight aggregates. The bulk density of mortar is determined by calculating the mass of dough contained in a measuring vessel, a pycnometer. There are different standard methods given for filling and compacting the mortar within the calibrated container. The method used depends upon the consistency of the fresh mortar as determined by the flow table test:

1. **Flow value less than 140mm (stiff mortar) - Vibration method**

   The calibrated container is filled to overflowing with mortar using a scoop, then placed on a vibrating table and vibrated until no further settlement of material is seen. Extra material can be added if necessary. The container is then weighed to an accuracy of 1 gram.

2. **Flow value between 140mm and 200mm (plastic mortar) - Shock method**

   The calibrated container is filled with mortar to approximately half its height using a scoop. It is then tilted about 30mm on alternate sides and allowed to fall ten times onto a solid base. Where the mortar contains an air entraining admixture the number of shocks is reduced to five. The container is then filled to overflowing and the shock compaction repeated. The container is then weighed to an accuracy of 1 gram.

3. **Flow value greater than 200mm (soft mortar)**

   The calibrated container is filled with mortar using a scoop until it is overflowing. The container edges are wiped clean with a damp cloth and the container weighed to an accuracy of 1 gram. The bulk density ρm in kg/m3 is calculated by use of the formula[148]:

$$\rho m = \frac{m_2 - m_1}{V_v}$$

m_1 = mass of empty container

m_2 = mass of container plus mortar

V_v = volume of container

2.5.2 Hardened Mortar Evaluation

Meanwhile the fresh mortar evaluation focuses on characteristics which mainly affect the application of the product, the hardened ones are meant instead to describe the behavior of the mortar once the setting and curing time have passed. Properties such as the capillary water absorption, the water vapor permeability and freeze-thaw test in particular focus on the behavior of the mock-ups towards water, which is one of the most critical agents of decay when it comes to building materials. Other properties, such as flessive and compressive strength are related to the mechanical performance of the hardened mortar and finally the soluble salt resistance, one of the main focus of the project, regarding the resistance of the samples against the action of salt[130-134].

2.5.2.1 Capillary water absorption

The normative provided for the analysis of capillary water absorption on mortar specimens in UNI EN-15801 (2010)[130]. This evaluation measures the water absorbed by a porous building material when put in contact with a supplier of deionised water for surface and time unit. The dry specimens, with a prismatic shape in the range of (3/5/5 cm), are placed on top of absorbent paper blocks one centimetre high. The weight measurements were made at predetermined intervals, buffering the excess water from the bottom

of the sample with a cloth. The water absorption is then calculated through the next formula expressed in mg/cm^2:

$$Qi = \frac{(m1 - m0)}{A} \times 1000$$

Where mi= specimen mass (mg) at time ti (√s); m0 = mass of the dry specimen (mg); A= surface area of the wet side. The capillary absorption coefficient, defined as the coefficient of the absorption curve in the first linear part, is calculated by linear interpolation of the experimental data. The average of three specimens was considered[130].

Figure 5 Mock-ups undergoing capillary absorption test

2.5.2.2 Water vapor Permeability

The UNI-EN-1015/19[131] measures the quantity of water vapor that flows, in unit of time, for a surface unity in standard environmental conditions, through a sample whose sizes are known. The procedure for this test method involves the production of specimens that are exposed to water vapor pressure, with the rate of moisture transfer determined by the change in mass. Test specimens consisting in a square layer of mortar (10-30mm thick and slightly larger in diameter than the cups) are placed, after curing, in the test cups and the edges sealed with an impermeable sealant, which remains constant in mass under the test conditions (Fig.6). The cups are manufactured so that the test specimen is held on a ledge below which the chemical solution is placed as there must be an air gap of 10mm + 5mm between the test specimen and the chemical solution. The test cups are then placed in the curing chamber at a temperature of 20°C ± 2°C and at a relative humidity of 50% + 5%. The cups are weighed at intervals and a graph drawn plotting time against mass. If three points can be placed on a straight line, the quantity of water vapor passing through the test specimen is taken to be constant[131].

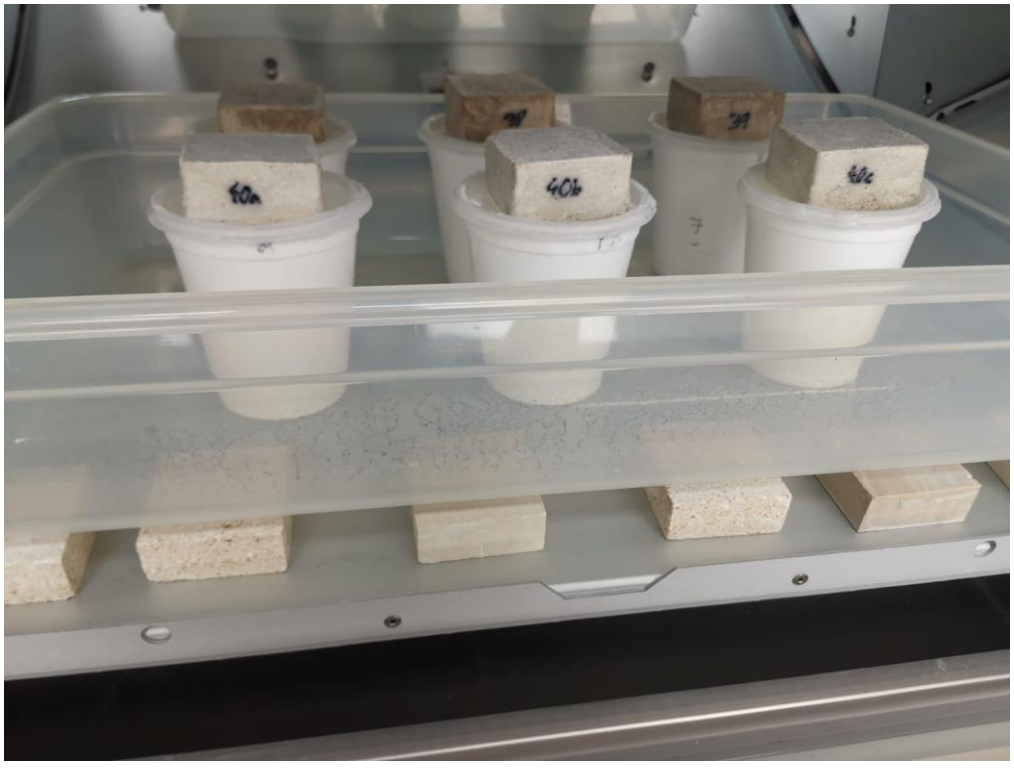

Figure 6 Mock-ups inside the climate chamber for ensuring the controlled environment

2.5.2.3 Freeze/Thaw Resistance

Freeze and Thaw resistance is meant to evaluate the capacity of the mortar formulation to sustain damage caused by the inner crystallization of water molecules inside the matrix. This test is run by alternating multiple cycles of freezing and thawing in water mock-ups and recording their weight and appearance variation[133]. Each cycle is characterized by a six hours long thawing period, undergone in air and a thawing period where the mock-ups are immersed in water (Fig.7). Cycles must be repeated until mock-ups are manually removed or the chosen number of cycles is reached. At the end of each cycle it is necessary to evaluate the mock-ups through an identification test and a weight variation test. While the second is meant to show the weight variation along the multiple cycles the first is mainly related to the visual evaluation of the single mock-up on a scale from 1 to 5:

0. Mock-up is intact.
1. Minor damages (smoothing of the edges and angles that do not compromise the integrity of the mock-up).
2. One or more minor cracks (<0,1mm wide) or the detachment of small fragments (<0,1mm^2 for each).
3. One or more cracks, holes ad detachment of bigger fragments than point n°2 or alteration on the mock-up's veining.
4. Mock-up is broken in one or more big cracks.
5. Mock-ups is in pieces or disintegrated.

Figure 7 Mock-ups undergoing freeze/thaw cycles

2.5.2.4 Soluble Salt Resistance

This test (EN 12370:2010[132]) is representative of a context in which the masonry is subject to capillary rise, thus leading to the inflow of saline solutions within the same. After drying to a constant mass, the test pieces are immersed in a 14% sodium sulphate solution and then dried in a ventilated oven (105±5) °C and finally cooled. This sequence describes a test cycle which is repeated 15 times, measuring the percentage change in mass.

$$\Delta M = \frac{M_f - M_{dl}}{M_d} \times 100$$

M_d the mass of the dried sample (g).

M_{d1} the mass of the dried sample with label before the first cycle (g).

M_1 is the mass of the dried sample with label after 15 cycles (g).

ΔM is the relative difference in mass before and after the test as a percentage.

The failure or fracture of the test piece during the test shall be repaired together with the number of completed test cycles, all shall be complete with photographic documentation of the initial and final conditions[132] (Fig.8).

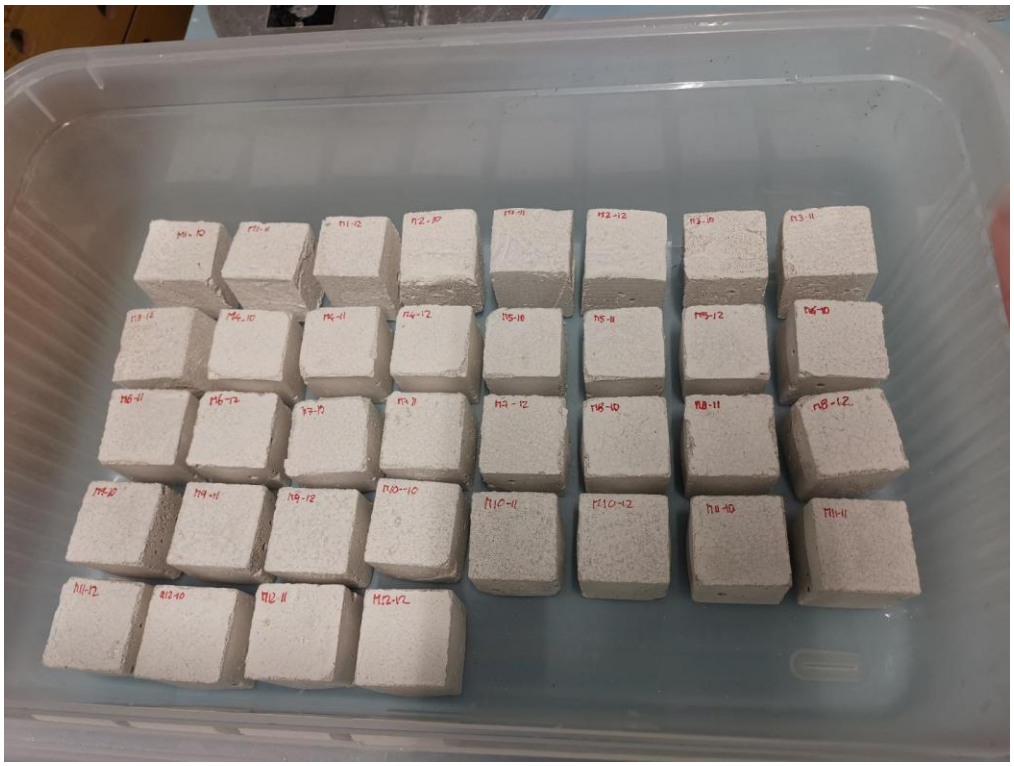

Figure 8 Cured cubic mock-ups used for the resistance to soluble salts test

2.5.2.5 Flessive/Compressive Strength

In order to assess mortars from a purely mechanical point of view, specific tests must be carried out. This type of evaluation involves subjecting the specimens to mechanical stresses that stress certain properties of the mortar, which will then determine the type of field application (i.e. the characteristics that distinguish a mortar for decorative or structural use)[134]. For these tests, prism mock-ups shall be produced, with dimensions of 160mm x 40mm x 40mm. Prior to use, molds are wet with a thin layer of lubricating oil. After setting, the prims are removed from the molds and cured for the specified time (28 days for premixed mortars, 90 days for non-premixed mortars). A testing machine is then used for this evaluation, with supports depending on the type of test. For the determination of Flessive module, the machine shall have two steel supports of 25mm x 50mm x 50mm, spaced 100mm ± 0,5mm apart and a third steel support of the same dimensions as the others, inserted in the descending arm of the mechanical press, located centrally between the other two supports. The three vertical planes through the axes of the three supports shall be

parallel and remain parallel, equidistant and normal to the direction of the prism under test. The flexural strength of a hardened mortar is therefore determined by three-point loading of the prism specimen. On the specimen's failure and breakage, recorded as maximum MPa sustained before breakage, the compressive strength can be determined on each half of the prism. By replacing the previous press supports with two same sized circular supports, one lower and one upper, the prism pieces are therefore crushed and the compressive force module evaluation will correspond to the maximum pressure value (MPa) sustained by the sample before failure. In both cases, the instrumentation will produce a MPa/sec graph showing the development of the material's structural resistance over time under constant mechanical pressure[134,148] (Fig.9).

Figure 9 Mock-up undergoing compressive strength resistance evaluation with additional (side) probe for monitoring its integrity

Chapter 3. Results

As described in the Synopsis section of this thesis, Chapter 3 will report the analysis and evaluation of the cumulative analytical results of the three years of mortar experimentation. A more in-depth discussion of the aforementioned can be found in Chapter 4.

As illustrated above, this thesis reports the research on different types of limes, from which various formulations of mortars were devised with the objective of high durability and resistance to degradation agents, in particular the action of soluble salts, frequently found in maritime or marshy environments. Specifically, each formulation, as shown in the block diagram (Fig.1) will be analyzed from a physical and application point of view with a distinction between the fresh mortar and hardened mortar phases.

3.1 Fresh mortar evaluation

As illustrated in Section 2, the samples produced were mixed with different types and quantities of additives to modify their physical and mechanical properties. This section is concerned with illustrating the results regarding the characteristics of the mixes from the time of their production until they are poured in the molds. During this time, three main properties were studied: the adhesion on a sloping support, the variation of the specific weight, and the consistency of the dough. These are the main characteristics useful to characterize a freshly mixed mortar from an application point of view. They originate from the rheology of the mix itself and are directly related to the nature and quantity of the additives incorporated during the mixing phase. Since we are orienting these mixtures towards a reality such as the conservation of architectural heritage, it goes without saying that a solid prerogative of each formula is to result in a mixture that is easy to spread, demonstrates optimal adhesion even on vertical or sloping walls, and is self-sufficient in the setting phase, i.e., that does not require particular attention to environmental conditions during application.

In the first phase of the study, the Chitosan (dissolved or dispersed), DTPMP, and $Na_4Fe(CN)_6$ (0.5%-1%) were the first to be mixed with Mapei S.p.A. pre-mixed mortars. Concerning the spreading property of fresh mortars (Ch.2.5.1), the solutions of in water dissolved Chitosan, DTPMP, and sodium ferrocyanide had fairly evident effects on the rheology of the formulations (Tab.9). Chitosan and sodium ferrocyanide share the ability to make the mixes denser and often difficult to spread effectively at high concentrations, except for the dry chitosan, as demonstrated by the consistency variation section of the table below (Tab.9).

About Chitosan in aqueous solution, as reported in Chapter 2, it was dissolved in an acidic environment with acetic acid, and this produced a weakly acidic and viscous solution (pH 6.5), in direct proportion to the concentration of the additive itself. When these solutions come in contact with the basic binders in water are neutralized. This causes the formation of a hydrogel-like precipitate, first reported by Chenite et al., 2001[149], which is why the re-basification of the environment due to the presence of calcium hydroxide ($Ca(OH)_2$) and the viscous nature of the aqueous solution itself was held responsible for the thickening effect of the additive on the fresh dough. The presence of Chitosan in the liquid or dissolved phase and ferrocyanide do not appear to have influenced the evaluation of the density and their respective changes over time (Tab.9). The formulations containing DTPMP, on the other hand, made the dough more liquid and less compact even at low concentrations. DTPMP is a phosphonic acid, used among other applications, in the construction industry, and it can act as a retardant, as it can form complexes with various Ca^{++}, Na^{+}, K^{+}, etc. cations, and consequently, is able to delay the setting time of the mortar compared to normal, making the mix more workable and fluid[150]. The high concentrations of DTPMP used in the aqueous solution, with particular reference to the first series of samples (0.5%-1%), resulted in excessive fluidization of the dough, making it difficult to handle at times due to its consistency but proved to be lighter than normal doughs, as evidenced by the 'Specific weight' section of the table (Tab.9). Sodium ferrocyanide had no other effects on the freshly mixed doughs except a slight increase in the consistency of the fresh dough. However, given the aim of making the mortars more environmentally sustainable, it was decided not to investigate it further during the project, even considering the sodium ferrocyanide's low toxicity, since ferrocyanides tend not to release free cyanide[147,151-153]. Although it is not a mutagenic substance, it may generate irritation through indigestion, inhalation, or skin contact. Thus, leading to its exclusion from further applications during the project.

The moderate use of the solution of Chitosan, Chitosan flakes and DTPMP in half the previous concentration, took place in the second series samples, based on natural hydraulic lime. As proof of the aforementioned results, even when combined with non-premixed mortars and in lower concentrations (0.25%-0.5%), a water solution of chitosan can concretely reduce the fluidity of the mortar. Chitosan left in flakes does not affect the variation of the mortar's consistency, producing spreading measures similar to mortar without additives, although slightly increasing its specific weight like the dough mixed with the solution of dissolved chitosan. DTPMP itself, albeit in smaller quantities, increased the fluidity of the mixes, making them more workable, easier to spread and compact in the molds. Aware of the properties of

Chitosan and DTPMP solutions, their concentration was decreased and maintained at minimal amounts in subsequent compositions, not to alter the fresh mixtures' workability. This is the case of the latest series, Series 5, which featured an additional product to the mixture of lime (NHL) and sand: the hollow glass microspheres (NHL1S3HGMSD_1/2/3). As proof of the results obtained previously, the presence of DTPMP in the series 4 composition resulted in a moderately viscous dough, which was initially slightly fluid and then became more compact one hour after mixing. Chitosan added to series 4, on the other hand, produced a dough with a quicker hardening even when added in small quantities, as demonstrated by the reduced mortar spread during slump test (NHL1S3HGMSCL_1/2/3) (Tab.9).

Table 9 Mock-up composition, consistency variation (slump diameter) and apparent density evaluation;

Mock-up Mixture ID - Code (number of specimens replicates)	***Mock-up Composition***	**Consistency Δ Slump diameter (cm)**	**Δ Specific weight**	**Thixotropic test (cm)**
Series 1				
E_1/2/3	EcoRisana(Mapei)	160/160/120 Δ:146,66 var:-25,00%	1,32±0,06	3
E_CL05_1/2/3	EcoRisana(Mapei)_LiquidChitosan(0,5%)	130/120/100 Δ:116,66 var:-23,07%	1,33±0,06	3
E_CL1_1/2/3	EcoRisana(Mapei)_LiquidChitosan(1%)	120/110/110 Δ:113,33 var:-8,33%	1,33±0,07	3
E_CS05_1/2/3	EcoRisana(Mapei)_SolidChitosan(0,5%)	140/135/125 Δ:133,33 var:-10,71%	1,29±0,07	3
E_CS1_1/2/3	EcoRisana(Mapei)_SolidChitosan(1%)	135/135/120 Δ:130,00 var:-11,11%	1,3±0,07	3

E_D05_1/2/3	EcoRisana(Mapei)_DTPMP(0,5%)	140/160/150 Δ:150,00 var:7,14%	1,16±0,03	2
E_D1_1/2/3	EcoRisana(Mapei)_DTPMP(1%)	150/150/140 Δ:146,66 var:-6,66%	1,22±0,02	2
E_NFCN05_1/2/3	EcoRisana(Mapei)_Na4Fe(CN)6·H2O(0,5%)	120/115/110 Δ:115,00 var:-8,33%	1,33±0,09	3
E_NFCN1_1/2/3	EcoRisana(Mapei)_Na4Fe(CN)6·H2O(1%)	120/120/100 Δ:113,33 var:-16,66%	1,35±0,10	3
RMC_1/2/3	RinzaffoMC(Mapei)	130/120/115 Δ:121,66 var:-11,53%	1,91±0,07	4,5
RMC_CL05_1/2/3	RinzaffoMC(Mapei)_LiquidChitosan(0,5%)	115/115/100 Δ:110,00 var:-13,04%	1,98±0,07	5
RMC_CL1_1/2/3	RinzaffoMC(Mapei)_LiquidChitosan(1%)	110/110/100 Δ:106,66 var:-9,09%	2,05±0,09	6
RMC_CS05_1/2/3	RinzaffoMC(Mapei)_SolidChitosan(0,5%)	130/125/120 Δ:125,00 var:-7,69%	1,98±0,06	5
RMC_CS1_1/2/3	RinzaffoMC(Mapei)_SolidChitosan(1%)	130/120/115 Δ:121,66 var:-11,53%	1,98±0,06	6
RMC_D05_1/2/3	RinzaffoMC(Mapei)_DTPMP(0,5%)	155/150/145 Δ:150,00 var:-6,45%	1,39±0,01	2
RMC_D1_1/2/3	RinzaffoMC(Mapei)_DTPMP(1%)	160/160/150 Δ:156,66 var:-6,25%	1,6±0,06	2

RMC_NFCN05_1/2/3	RinzaffoMC(Mapei)_Na4Fe(CN)6·H2O(0,5%)	130/125/120 Δ:125,00 var:-7,69%	1,91±0,07	5
RMC_NFCN1_1/2/3	RinzaffoMC(Mapei)_Na4Fe(CN)6·H2O(1%)	130/130/115 Δ:125,00 var:-11,53%	1,93±0,07	5
Series 2				
LS_1/2/3	Lime1Sand2	190/190/180 Δ:186,66 var:-5,26%	1,95±0,08	5
LS_CL025_1/2/3	Lime1Sand2_LiquidChitosan(0,25%)	160/160/150 Δ:156,66 var:-6,25%	1,99±0,09	5
LS_CL05_1/2/3	Lime1Sand2_LiquidChitosan(0,5%)	160/150/145 Δ:151,66 var:-9,37%	2,02±0,07	4,5
LS_CS025_1/2/3	Lime1Sand2_SolidChitosan(0,25%)	190/190/180 Δ:186,66 var:-5,26%	1,98±0,07	5
LS_CS05_1/2/3	Lime1Sand2_SolidChitosan(0,5%)	190/190/180 Δ:186,66 var:-5,26%	2,00±0,08	4,5
LS_D025_1/2/3	Lime1Sand2_DTPMP(0,25%)	250/250/240 Δ:246,66 var:-4,00%	1,75±0,02	4
LS_D05_1/2/3	Lime1Sand2_DTPMP(0,5%)	270/270/260 Δ:266,66 var:-3,70%	1,43±0,02	4
LSC_1/2/3	Lime1Sand2_CrushedBrickPowder	200/200/190 Δ:196,66 var:-5,00%	2,07±0,08	5,5

LSC_CL025_1/2/3	Lime1Sand2_CrushedBrickPowder_LiquidChitosan(0,25%)	160/160/150 Δ:156,66 var:-6,25%	2,11±0,09	5
LSC_CL05_1/2/3	Lime1Sand2_CrushedBrickPowder_LiquidChitosan(0,5%)	160/150/145 Δ:151,66 var:-9,37%	2,14±0,07	5
LSC_CS025_1/2/3	Lime1Sand2_CrushedBrickPowder_SolidChitosan(0,25%)	190/190/180 Δ:186,66 var:-5,26%	2,13±0,08	5
LSC_CS05_1/2/3	Lime1Sand2_CrushedBrickPowder_SolidChitosan(0,5%)	190/190/180 Δ:186,66 var:-5,26%	2,13±0,09	5
LSC_D025_1/2/3	Lime1Sand2_CrushedBrickPowder_DTPMP(0,25%)	250/250/240 Δ:246,66 var:-4,00%	1,87±0,02	4,5
LSC_D05_1/2/3	Lime1Sand2_CrushedBrickPowder_DTPMP(0,5%)	270/270/260 Δ:266,66 var:-3,70%	1,55±0,02	4,5
Series 4				
NHL1S3HGMS_1/2/3	NHL1Sand3Microspheres50g	135/132,5/120 Δ:129,16 var:-11,11%	1,70±0,02	5
NHL1S3HGMSD_1/2/3	NHL1Sand3Microspheres50gDTPMP40g	200/185/150 Δ:178,33 var:-25,00%	1,68±0,01	6,5
NHL1S3HGMSCL_1/2/3	NHL1Sand3Microspheres50gChitosan20g	127/130/120 Δ:125,66 var:-5,51%	1,73±0,03	5

Crushed brick powder (CBP), also known as brick waste in most studies, is a remarkable additive to the building and research sector as it is capable of enhancing the mechanical resistance and hydraulic properties of the traditional lime mortars[9,44,154-161]. In the application of fresh mixture, as studied in this project, CBP is also able to enhance the workability of the mixture, demonstrating slightly higher spreading values than mortars without it[162-165] (Tab.10). The presence of other additives, too, influenced the dough workability, except for the chitosan flakes who didn't show any considerable effect. As seen previously in Tab.9 chitosan in liquid solution tends to thicken the dough making it less easy to spread, while DTPMP on the other hand, is able to produce very smooth mixtures, which makes casting in molds and removing residual air bubbles much easier (Tab.10).

Table 10 Mock-up composition, consistency variation and apparent density evaluation related to "cocciopesto "mortars;

Series 2				
Mock-up Mixture ID - Code (number of specimens replicates)	***Mock-up Composition***	**Consistency Δ Slump diameter (cm)**	**Δ Specific weight**	**Thixotropic test (cm)**
LS_1/2/3	Lime1Sand2	190/190/180 Δ:186,66 var:-5,26%	1,95±0,08	5
LS_CL025_1/2/3	Lime1Sand2_LiquidChitosan(0,25%)	160/160/150 Δ:156,66 var:-6,25%	1,99±0,09	5
LS_CL05_1/2/3	Lime1Sand2_LiquidChitosan(0,5%)	160/150/145 Δ:151,66 var:-9,37%	2,02±0,07	4,5
LS_CS025_1/2/3	Lime1Sand2_SolidChitosan(0,25%)	190/190/180 Δ:186,66 var:-5,26%	1,98±0,07	5
LS_CS05_1/2/3	Lime1Sand2_SolidChitosan(0,5%)	190/190/180 Δ:186,66 var:-5,26%	2,00±0,08	4,5
LS_D025_1/2/3	Lime1Sand2_DTPMP(0,25%)	250/250/240 Δ:246,66 var:-4,00%	1,75±0,02	4

LS_D05_1/2/3	Lime1Sand2_DTPMP(0,5%)	270/270/260 Δ:266,66 var:-3,70%	1,43±0,02	4
LSC_1/2/3	Lime1Sand2_CrushedBrickPowder	200/200/190 Δ:196,66 var:-5,00%	2,07±0,08	5,5
LSC_CL025_1/2/3	Lime1Sand2_CrushedBrickPowder_LiquidChitosan(0,25%)	160/160/150 Δ:156,66 var:-6,25%	2,11±0,09	5
LSC_CL05_1/2/3	Lime1Sand2_CrushedBrickPowder_LiquidChitosan(0,5%)	160/150/145 Δ:151,66 var:-9,37%	2,14±0,07	5
LSC_CS025_1/2/3	Lime1Sand2_CrushedBrickPowder_SolidChitosan(0,25%)	190/190/180 Δ:186,66 var:-5,26%	2,13±0,08	5
LSC_CS05_1/2/3	Lime1Sand2_CrushedBrickPowder_SolidChitosan(0,5%)	190/190/180 Δ:186,66 var:-5,26%	2,13±0,09	5
LSC_D025_1/2/3	Lime1Sand2_CrushedBrickPowder_DTPMP(0,25%)	250/250/240 Δ:246,66 var:-4,00%	1,87±0,02	4,5
LSC_D05_1/2/3	Lime1Sand2_CrushedBrickPowder_DTPMP(0,5%)	270/270/260 Δ:266,66 var:-3,70%	1,55±0,02	4,5

The following results concern instead mortars based on carbonate and magnesium lime combined with different percentages of metakaolin (Tab.11). Prior to the 90 days of curing, instead of the 28 days of previous series, the samples were evaluated as usual on fresh mortar properties in order to determine the metakaolin influence on the dough consistency and sp.weight. The presence of metakaolin produced easily spreadable dough whose fluidity appeared proportional to the amount of metakaolin substituted to the lime. For samples based on traditional lime (LxSx_series, Tab.11), the specific weight shows a slight increase when in presence of metakaolin in combination with the increasing lime:sand ratio, but increasing the amount of metakaolin per se does not produce changes. The same could not be said for magnesian lime based mortars where, neither the changes in additive amount nor the variation of binder:aggregate seems to produce a distinguishable trend. The exceptions though, are represented by ML09S3M01_1/2/3, ML08S3M02_1/2/3, ML07S3M03_1/2/3 where the specific weight shows lower values than the expected, probably due to an measuring error (Tab.11).

Table 11 Mock-up composition, consistency variation, and apparent density evaluation related to Metakaolin mortars;

Series 3				
Mock-up Mixture ID - Code (number of specimens replicates)	***Mock-up Composition***	**Consistency Δ Slump diameter (cm)**	**Δ Specific weight**	**Thixotropic test (cm)**
L1S1_1/2/3	Lime1Sand1	160/145/130 Δ:145,00 var:-18,75%	1,66±0,01	7
L09S1M01_1/2/3	Lime09Sand1_Metakaolin01 (0.9:1:0.1 wt.)	147/140/137 Δ:141,33 var:-6,80%	1,72±0,02	6
L08S1M02_1/2/3	Lime08Sand1_Metakaolin02 (0.8:1:0.2 wt.)	155/147/140 Δ:147,33 var:-9,68%	1,74±0,00	6
L07S1M03_1/2/3	Lime07Sand1_Metakaolin03 (0.7:1:0.3 wt.)	147/140/137 Δ:141,33 var:-6,80%	1,73±0,02	6
L1S2_1/2/3	Lime1Sand2	160/145/130 Δ:145,00 var:-18,75%	1,82±0,01	5
L09S2M01_1/2/3	Lime09Sand2_Metakaolin01 (0.9:2:0.1 wt.)	147/140/137 Δ:141,33 var:-6,80%	1,84±0,02	5
L08S2M02_1/2/3	Lime08Sand2_Metakaolin02 (0.8:2:0.2 wt.)	155/147/140 Δ:147,33 var:-9,68%	1,86±0,02	5
L07S2M03_1/2/3	Lime07Sand2_Metakaolin03 (0.7:2:0.3 wt.)	166/150/147 Δ:154,33 var:-11,44%	1,85±0,02	5
L1S3_1/2/3	Lime1Sand3	160/145/130 Δ:145,00 var:-18,75%	1,91±0,03	5
L09S3M01_1/2/3	Lime09Sand3_Metakaolin01 (0.9:3:0.1 wt.)	166/150/147 Δ:154,33 var:-11,44%	1,94±0,02	5,5
L08S3M02_1/2/3	Lime08Sand3_Metakaolin02 (0.8:3:0.2 wt.)	155/147/140 Δ:147,33 var:-9,67%	1,91±0,03	5,5
L07S3M03_1/2/3	Lime07Sand3_Metakaolin03 (0.7:3:0.3 wt.)	166/150/147 Δ:154,33 var:-11,44%	1,95±0,01	5

ML1S1_1/2/3	MagnesianLime1Sand1	132/142/130 Δ:134,66 var:-1,52%	2,29±0,02	7
ML09S1M01_1/2/3	MagnesianLime09Sand1_Metakaolin01 (0.9:1:0.1 wt.)	150/142/137 Δ:143,00 var:-8,67%	2,27±0,03	5
ML08S1M02_1/2/3	MagnesianLime08Sand1_Metakaolin02 (0.8:1:0.2 wt.)	145/135/150 Δ:143,33 var:+3,45%	2,30±0,02	5
ML07S1M03_1/2/3	MagnesianLime07Sand1_Metakaolin03 (0.7:1:0.3 wt.)	150/147/142 Δ:146,33 var:-5,33%	2,34±0,01	5
ML1S2_1/2/3	MagnesianLime1Sand2	147/137/145 Δ:143,00 var:-1,36%	2,45±0,03	6
ML09S2M01_1/2/3	MagnesianLime09Sand2_Metakaolin01 (0.9:2:0.1 wt.)	137/130/127 Δ:131,33 var:-7,30%	2,46±0,01	6
ML08S2M02_1/2/3	MagnesianLime08Sand2_Metakaolin02 (0.8:2:0.2 wt.)	142/140/137 Δ:139,66 var:-3,52%	2,47±0,02	6,5
ML07S2M03_1/2/3	MagnesianLime07Sand2_Metakaolin03 (0.7:2:0.3 wt.)	152/150/148 Δ:150,00 var:-2,63%	2,44±0,04	6,5
ML1S3_1/2/3	MagnesianLime1Sand3	142/140/138 Δ:140,00 var:-2,82%	2,49±0,01	5,5
ML09S3M01_1/2/3	MagnesianLime09Sand3_Metakaolin01 (0.9:3:0.1 wt.)	175/160/155 Δ:163,33 var:-11,42%	1,74±0,01	5,5
ML08S3M02_1/2/3	MagnesianLime08Sand3_Metakaolin02 (0.8:3:0.2 wt.)	165/160/155 Δ:160,00 var:-6,06%	1,75±0,02	5
ML07S3M03_1/2/3	MagnesianLime07Sand3_Metakaolin03 (0.7:3:0.3 wt.)	165/160/155 Δ:160,00 var:-6,06%	1,75±0,01	5,5

The latest series featured a more varied range of formulations, focusing more on variety than redundancy of formulations as in previous series with the purpose of developing mortars for specific application in high-humidity environments. In order to compare several formulations together to identify which one would be most useful in protecting a masonry in a wet environment, where capillary rise phenomena of salty water

are diffused, some past formulations were selected. Some of the mortars that gave the best results have been reintroduced in this last phase. Among the samples in Tab.12, it's possible to find mortars from series 2 and 3 like L1S1, L1S1.7C0.3 and ML1S1.7C0.3 (the last two of which were added with CBP to furtherly increase their physical and mechanical properties). As a further addition to the research, a new element was introduced to the study in order to understand its influence on mortars, hollow glass microspheres (HGMS). The presence of hollow glass microspheres HGMS was observed to increase the workability of the dough, making it full-bodied, uniform, and easily stretchable, as in the case of SLSH and SLSCH samples, but also reduce its average specific weight, resulting in a lighter dough.

Table 12 Mock-up composition, consistency variation and apparent density evaluation related to 4th and 5th series mortars;

Series 4+5				
Mock-up Mixture ID - Code (number of specimens replicates)	***Mock-up Composition***	**Consistency Δ Slump diameter (cm)**	**Δ Specific weight**	**Thixotropic test (cm)**
L1S1.7C0.3_1/2/3	Lime1Sand1.7_CrushedBrickPowder0.3	120/117,5/115 Δ:117,50 var:-4,17%	1,75±0,01	5
ML1S1.7C0.3_1/2/3	MagnesianLime1Sand1.7_CrushedBrick Powder0.3	130/127/117 Δ:124,66 var:-10,00%	1,74±0,01	5,5
L1S0.7C0.3_1/2/3	Lime1Sand0.7_CrushedBrickPowder0.3	130/110/115 Δ:118,33 var:-11,53%	1,63±0,01	5,5
NHL1S0.7C0.3_1/2/3	NHLime1Sand0.7_CrushedBrickPowder 0.3	140/135/130 Δ:135,00 var:-7,14%	1,74±0,01	5,5
PL1S3_1/2/3	PalladioNHLime1Sand3	140/132,5/142,5 Δ:138,33 var:+1,79%	1,86±0,01	6
NHL1S3HGMS_1/2/3	NHL1Sand3Microspheres50g	135/132,5/120 Δ:129,16 var:-11,11%	1,7±0,02	5
NHL1S3HGMSD_1/2/3	NHL1Sand3Microspheres50gDTPMP40g	200/185/150 Δ:178,33 var:-25,00%	1,68±0,01	6,5

NHL1S3HGMSCL_1/2/3	NHL1Sand3Microspheres50gChitosan20g	127/130/120 Δ:125,66 var:-5,51%	1,73±0,03	5
SLS_1/2/3	SlakedLimeSand	120/115/111 Δ:115,33 var:-7,50%	1,77±0,02	5,5
SLSH_1/2/3	SlakedLimeSand_HGMS	145/135/125 Δ:135,00 var:-13,79%	1,65±0,04	6
SLSC_1/2/3	SlakedLimeSand_CruchedBrickPowder	125/120/115 Δ:120,00 var:-8,00%	1,77±0,05	6
SLSCH_1/2/3	SlakedLimeSand_CruchedBrickPowder_HGMS	145/140/125 Δ:136,66 var:-13,79%	1,65±0,02	6,5

3.2 Hardened mortar evaluation

This section deals with illustrating the results inherent to the physical-mechanical analysis of the hardened state of mortars, i.e. once the solid matrix has matured enough, estimated in 28 days for the first two series (i.e. the days indicated in the mixing instructions for the Mapei mortars of series 1 and the total days chosen for the second series, consisting of traditional mortars, a minimum time interval required by traditional mortars to develop a minimum of mechanical resistance, albeit not complete) (Tab.9,10) and 90 days for the natural hydraulic limes and magnesian lime mixtures[40,67-73]. As illustrated previously in the block diagram (Fig.1), this section's purpose is to illustrate the behavior of the proposed formulations in order to assess their durability in a hypothetical field application. The evaluation of permeability and capillary absorption coefficient makes it possible to identify the susceptibility of the mature mortar to water absorption and retention. These values, combined with freeze/thaw, mechanical and soluble salt resistances, are able to identify which mortars make the best use of their constituent components according to their sustainability and durability goals.

3.2.1 Capillary Absorption and Water Vapor Permeability

The behavior of a porous building material towards water can be assessed through the analysis of capillary absorption, which simulates the water uptake that a certain material could undergo due to rain or flooding. The porous structure of the material determines the absorption of water due to the vertical and horizontal capillary effect, dragging with it possible pollutants and elements harmful to the building such as soluble salts. By comparing the data obtained from the mortars without and with additives, it was possible to determine their effects on the water absorption. The first series of mock-ups, based on premixed mortar powders mainly composed of natural hydraulic lime, eco pozzolan, natural sands, special additives and microfibers (Tab.1), showed absorption curves different from the generally observed trend, as can be seen from Fig.9 and 10. The trends of the first period of Eco-Risana Mapei (E^{s1}) and Rinzaffo and Mc Mapei (RMC^{s1}) based samples did not show a linear trend when subjected to the absorption. It is possible to observe that all the samples, less those with dry Chitosan additives, maintained lower absorption levels till 3 hours since the beginning of the test. This difference is more noticeable in the E-series samples than in the RMCs (Tab.13).

Table 13 Hydric behavior, data regarding water vapor permeability and capillary water absorption are listed: WDD= density of moisture flow rate; μ= moisture resistance factor; sd = water vapor diffusion equivalent air thickness; CA = coefficient of water absorption by capillarity; TOP = total open porosity as determined by the volume of water absorbed by capillary absorption.

Mock-up ID	**Average TOP**	**WDD**	**μ**	**sd**	**CA**
	%	**g/(m²•s)**		**m**	**g/cm²•s$^{-1/2}$**
E_1/2/3	24,54±2,67	127,5±50,75	6,39±2,54	0,14±0,05	0,28±0,01
E_CL05_1/2/3	17,59±2,03	70,83±36,8	15,84±12,79	0,34±0,27	0,28±0,01
E_CL1_1/2/3	20,61±0,71	69±33,47	15,42±11,33	0,33±0,24	0,28±0,01
E_CS05_1/2/3	19,48±1,4	71,78±16,04	11,69±2,98	0,25±0,06	0,32±0,03
E_CS1_1/2/3	19,74±1,53	61,32±42,2	17,95±10,13	0,39±0,22	0,36±0,04
E_D05_1/2/3	19,77±1,16	85,94±46,8	12,56±9,69	0,27±0,21	0,28±0,01
E_D1_1/2/3	21,12±0,75	84,16±54,38	15,44±14,75	0,33±0,32	0,28±0,28
E_NFCN05_1/2/3	23,07±1,21	71,39±50,74	23,33±26,47	0,50±0,57	0,29±0,01

E_NFCN1_1/2/3	20,37±1,62	77,63±54,35	20,57±22,94	0,44±0,49	0,28±0,01
RMC_1/2/3	12,35±1,96	95,3±29,15	8,70±2,87	0,19±0,06	0,28±0,01
RMC_CL05_1/2/3	13,92±1,36	101,79±65,81	12,89±12,97	0,28±0,28	0,28±0,01
RMC_CL1_1/2/3	16,16±1,06	86,44±56,3	17,8±20,04	0,38±0,43	0,27±0,01
RMC_CS05_1/2/3	13,75±3,52	85,44±31,57	10,13±3,69	0,22±0,08	0,28±0,15
RMC_CS1_1/2/3	17,72±1,28	87,33±49,62	11,09±5,63	0,24±0,12	0,36±0,07
RMC_D05_1/2/3	12,31±0,59	83,11±54,66	19±21,63	0,41±0,46	0,28±0,01
RMC_D1_1/2/3	15,94±1,01	85,54±56,61	18,71±21,53	0,40±0,46	0,28±0,01
RMC_NFCN05_1/2/3	18,38±2,11	83,39±50,72	16,16±16,46	0,35±0,35	0,28±0,01
RMC_NFCN1_1/2/3	15,91±0,69	84,09±49,78	15,33±15,05	0,33±0,32	0,28±0,01

Despite the best expectations, as can be seen, the samples did not reach sufficient stability within eight days of the start of the test. Therefore, the graphs have been split in order to better evaluate their behavior when mixed with anti-salt additives and when not. Fig.9, Fig.10 shows in detail the first 6 hours of capillary absorption in order to better understand the different behaviors, meanwhile Fig.11 and Fig.12 show the whole test duration, which is set at 8 days (831,38 $s^{1/2}$)[130].

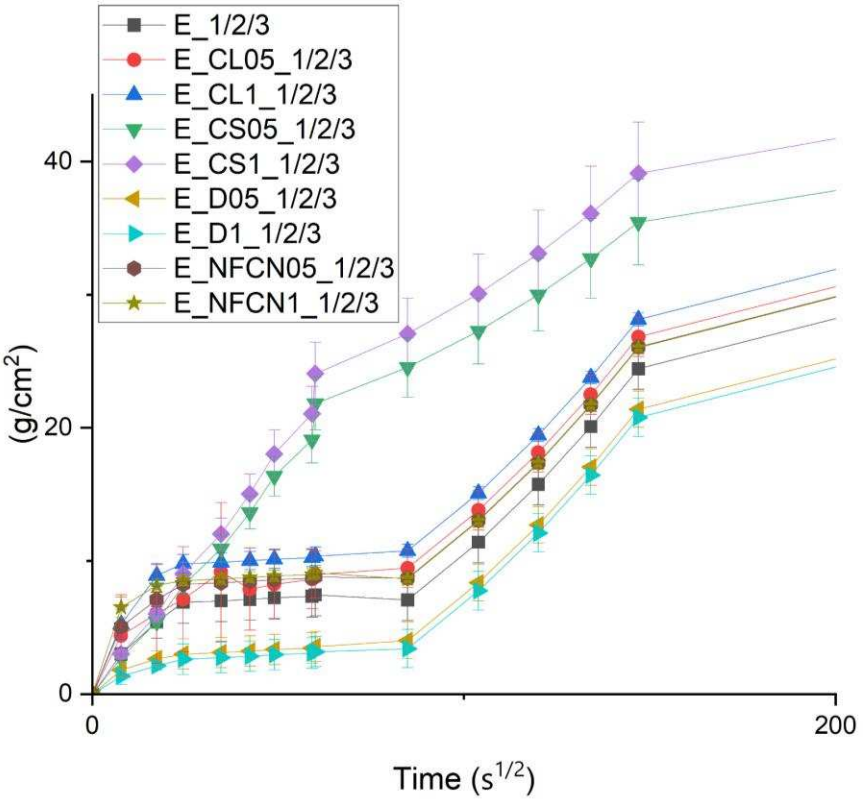

Figure 9 Capillary absorption curve for E samples, expressed as the quantity of water absorbed per surface unit (g/cm^2) over time (s½) in the first 6 hours.

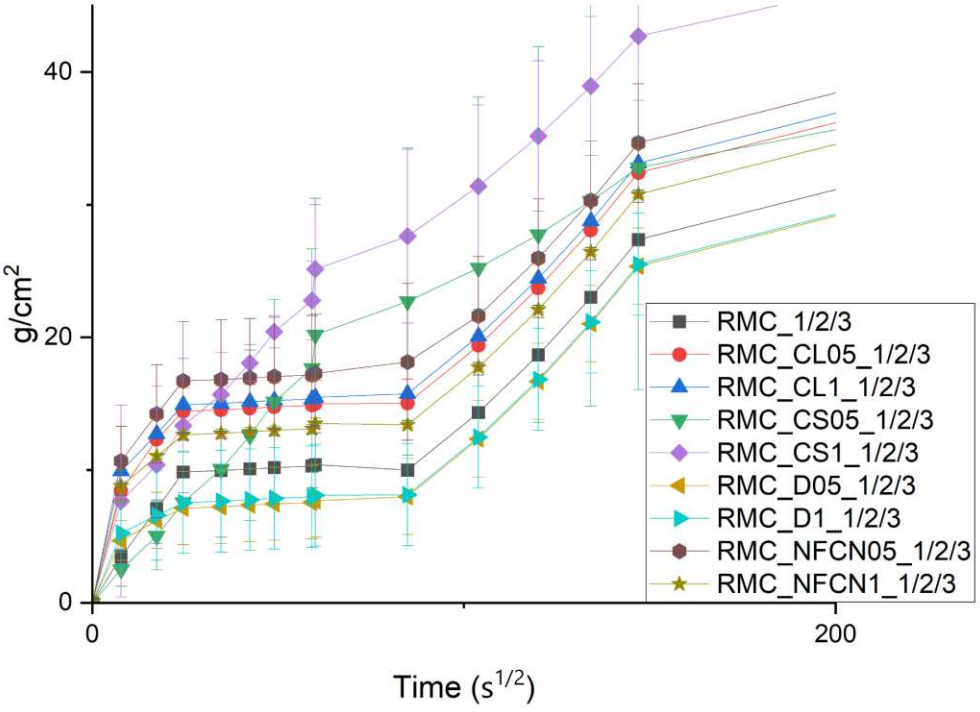

Figure 10 Capillary absorption curve for RMC samples during the first 6 hours.

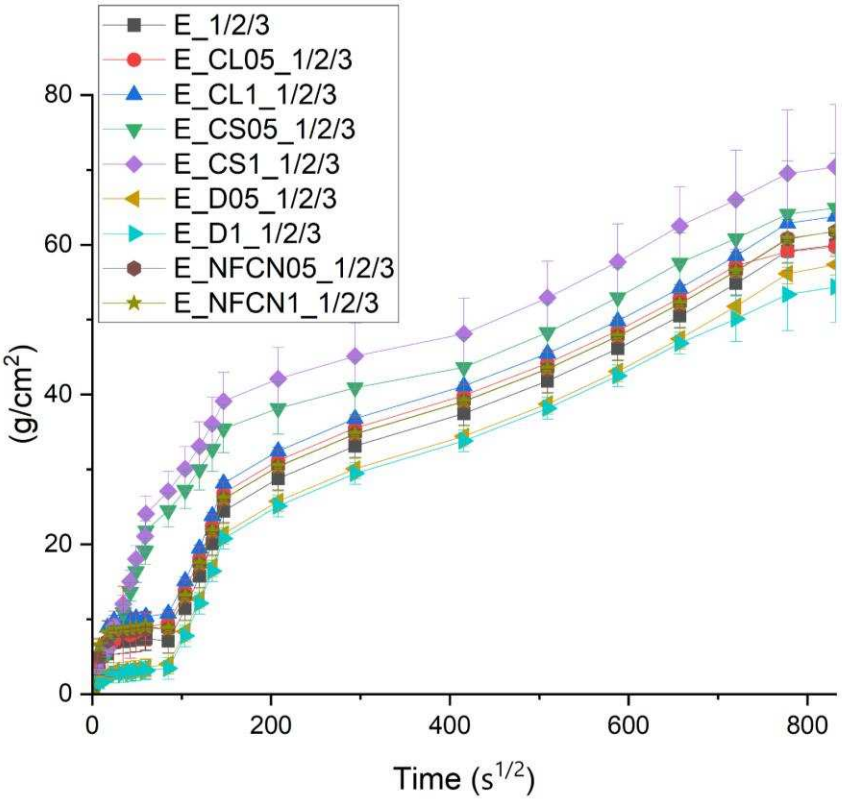

Figure 11 Capillary absorption curve for E samples, showing the measurement until day 8.

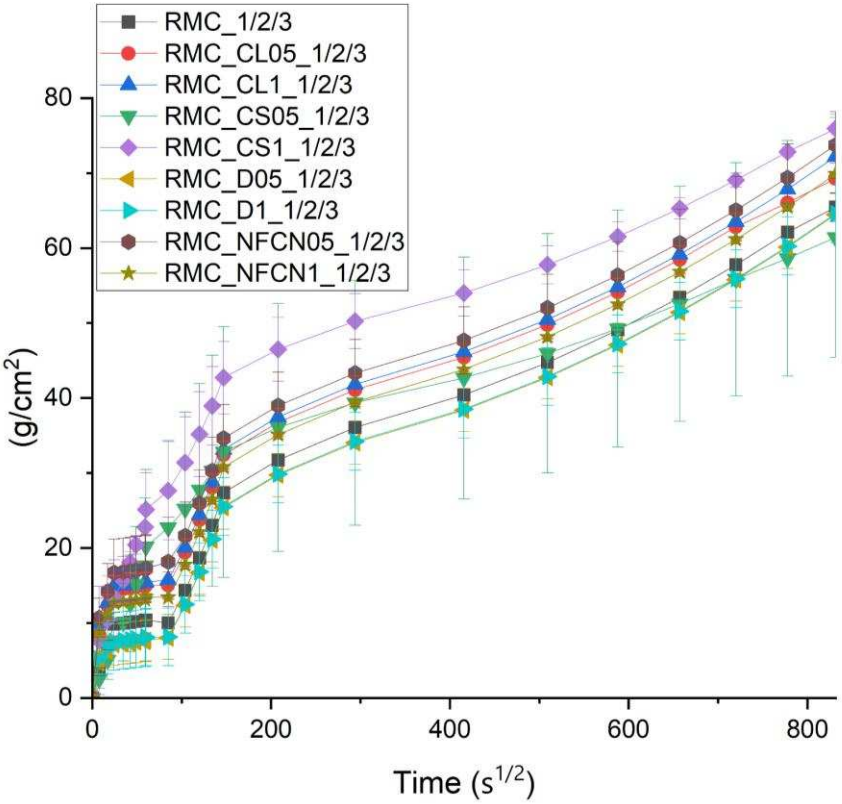

Figure 12 Capillary absorption curve for RMC samples, showing the measurement until day 8.

As can be seen from the graphs above, the premixed samples of series 1 did not finish the test by reaching a stable weight variation, as a consequence the test was stopped, according to regulations on day eight[130]. Focusing on Fig.11,12, concerning the whole test period, the weight variance of the samples continues to increase, meaning that water is still being absorbed via capillary action almost as if the samples were not fully matured despite the 28-day maturation period which was indicated in the instructions of the products, as well as being the average regulated curing period required before testing[36,130,166-172]. This behaviour is shown not only by the E^{s1} and RMC^{s1} samples mixed with anti-salt products but also by the pure ones, thus proving that the dubious continuous absorption is probably due to the nature of mortar and not to the presence of additives. It is interesting to note that, regardless of the type of base formulation, the absorption curve seems to stop within the first six hours (Fig.9,10) and then resume absorption, almost as if the samples were composed of several layers. Although this theory is applicable to the case of the RMC samples, where the base is made up of a layer of Rinzaffo about 5mm thick followed by the MC layer, it cannot justify the behaviour of the Eco-Risana-based samples.

The effect of the anti-salt products is highlighted also in Fig.9,10, where the timeline stops at 12 h since the beginning. Following the above described behaviour, it seems that the presence of additives does not interfere with it except for chitosan flakes. In both formulations (E^{s1}, RMC^{s1})the presence of chitosan flakes seems to increase the water absorption rate, much more than when solubilized in the mixing water. Chitosan, as a polycationic polymer, has a positive charge that can interact with negatively charged molecules, among which we can consider the dipole moment of H_2O molecules as an explanation for the increased absorption of water. An increase in water absorption is also recorded in the samples mixed with ferrocyanide, while in the case of DTPMP a slight reduction compared to the untreated sample.

In the following graphs, the values of total open porosity (TOP) with those of the capillary absorption coefficient (CA) and permeability (μ) were plotted (Fig.13-16). This allowed for the evaluation of any hidden relationships between the properties of the samples and the definition, where possible, of trends that explain the data in Tab.13. Focusing attention on the graph in Figure 13, relating to the samples of Eco-Risana, we can take as reference the values of permeability (μ) and total open porosity (TOP) of the untreated sample (E). As can be seen, the presence of additives in the compound leads to higher permeability values than normal, with higher values represented by samples treated with ferrocyanide

(inversely proportional to the concentration of the solution). This implies that the presence of an extraneous element like our products will combine with the permeable structure of the Eco-Risana, making it less permeable (higher μ and lower TOP values). The permeability depends mainly on the distribution and size of the pores present in the mortar matrix, therefore, for greater TOP value, the resistance to water vapor should be small. In this case we observe that the μ value increases, TOP decreases, therefore it can be said that the presence of additives, regardless of their nature, acts as a condensing agent, thus reducing the number of total open pores and increasing the bulk resistance to water vapor (Fig.13).

If we look at the samples based on Rinzaffo+MC we can see how the permeability is proportional to the increase in total open porosity by considering as reference point the untreated standard sample (RMC) (Fig.14). In this case an abnormal behaviour is observed, since normally the more the vapour resistance (μ) increases the lower the number of open pores (TOP). The addition of the additives produced mortars with a high resistance index to the passage of water vapour while increasing in most cases (excluding RMC_D05 which shows the same values as TOP) the number of open pores, thus demonstrating a sealing effect, hypothetically due to a structure consisting of large pores and constrictions that cause condensation, thus slowing the passage of vapor (Fig.14).

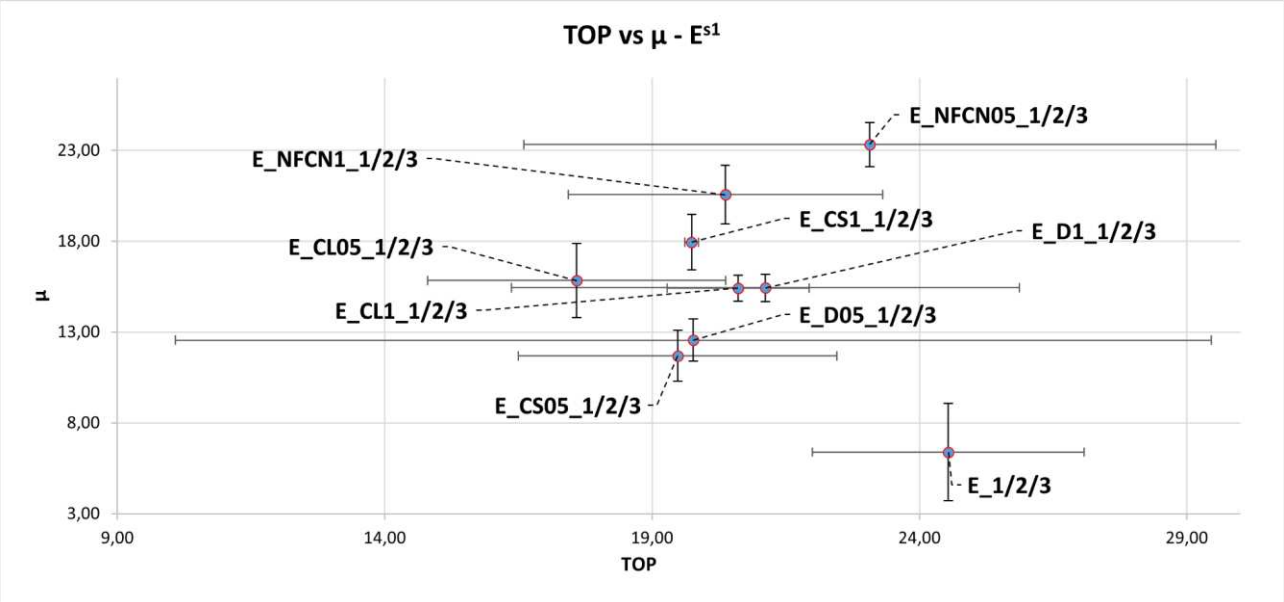

Figure 13 Plotting of TOP vs μ of samples from series 1st: Eco Risana samples.

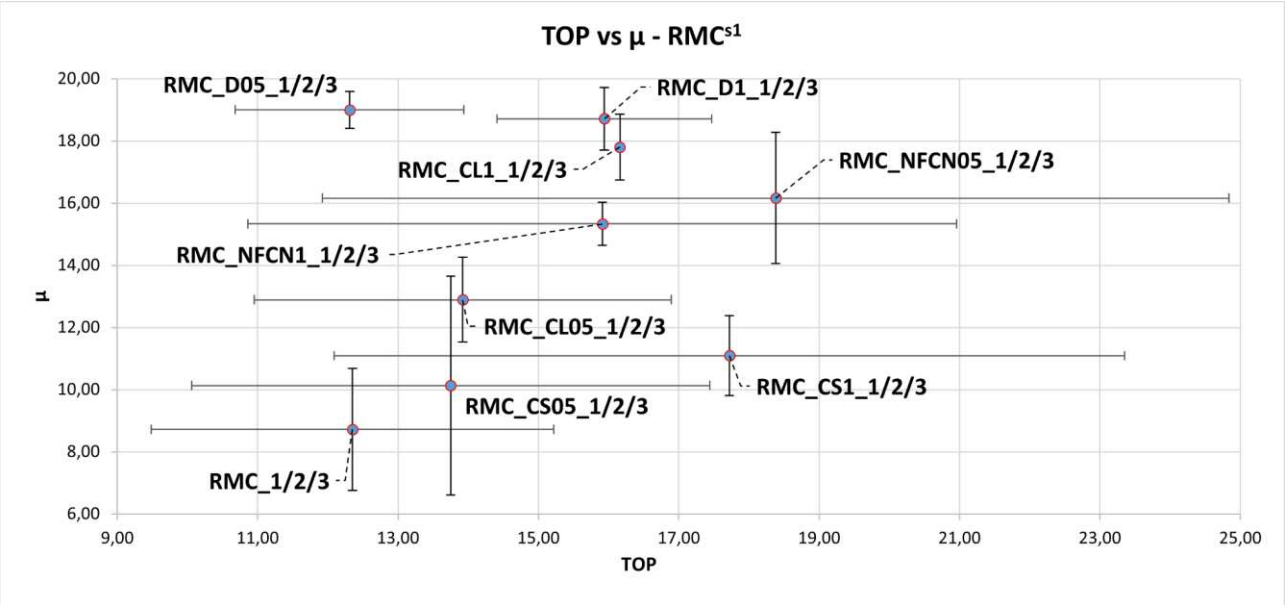

Figure 14 Plotting of TOP vs µ of samples from series 1st: Rinzaffo+MC samples.

It is known that open porosity (TOP) and capillary absorption coefficient (CA) are positively related so through this knowledge it will be possible to interpret the effectiveness of additives on the samples produced[173-174]. As can be seen in Fig.15, concerning the samples based on Eco-Risana, the majority of additives used have resulted in formulations whose structure has undergone a reduction in open porosity, while maintaining almost intact CA values. The nature of the additives, also referring to the previous graph (Fig.13) favours steam condensation inside the samples probably due to a contrast between the anti salt products we introduced and the special additives indicated in the product description (Tab.1). Concerning samples based on RMC (Fig.16) a different pattern can be observed, if not contrary to that seen previously (Fig.15). Here the addition resulted in an increased number of total open pores, probably due to the creation of more numerous and evenly distributed pores in the sample, made by an interference at the chemical level of the additive molecules which prevented the MC product from over compacting during the setting phase, creating a porous and uniform network (Fig.16).

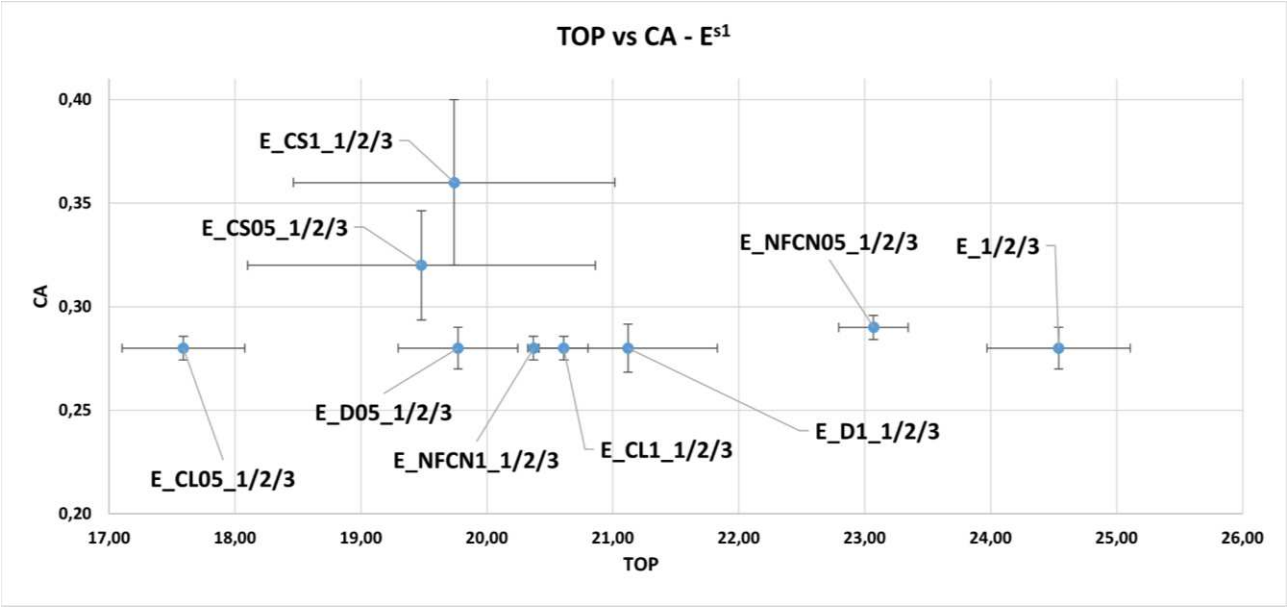

Figure 15 Plotting of TOP vs CA of samples from series 1st: Eco Risana samples.

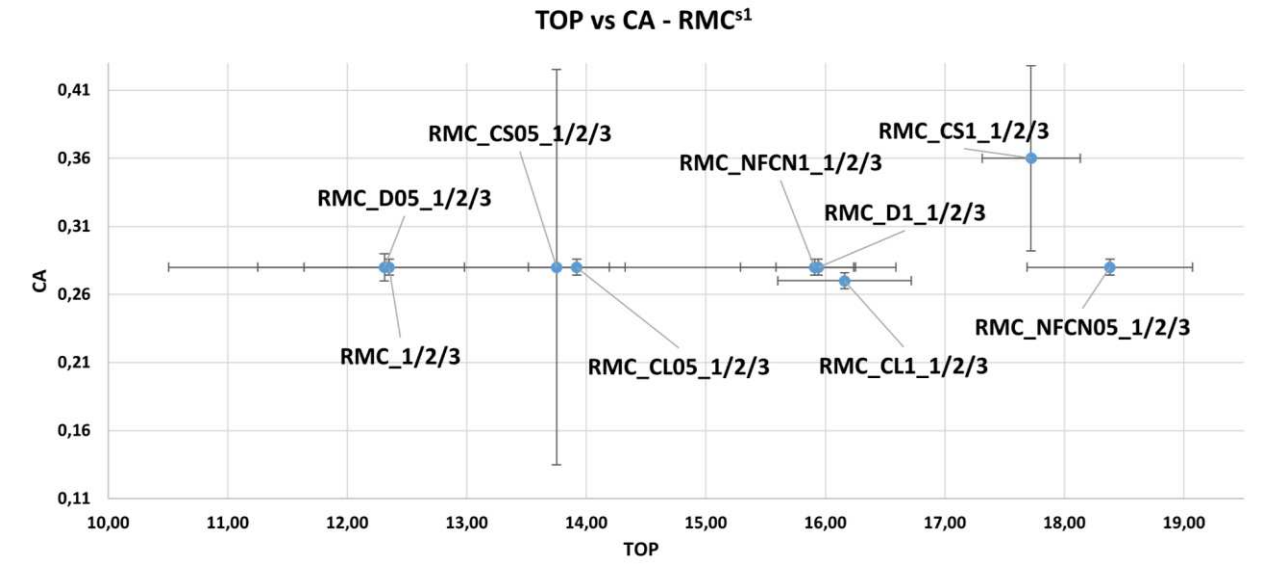

Figure 16 Plotting of TOP vs CA of samples from series 1st: Rinzaffo+MC samples.

By observing the behavior of Fig.17,18 regarding the second series capillary absorptions, the performance of the LS^{s2} and LSC^{s2} samples was more linear and normal than their predecessors (Tab.14). As can be seen, the addition of CBP (Crushed brick powder) raised the level of water absorption, causing an increase in the total amount of water absorbed, which can also be seen in the TOP values shown in the table. For the values concerning the moisture flow rate, unfortunately a trend was not found. Apparently, the variation of CA in the three replicates is greater than that between one mixture and the other, implying that the variability is such that looking for a relationship in this type of sample is difficult. To be considered is that the

hydration of the mortar is reactivated during the water absorption phase, then forming gel phases that reduce the CA coefficient (Fig.17,18). Understanding the nature and distribution of pores helps to interpret behaviours such as capillary absorption. The variable size and dimensions of the pore network determine the extent of the phenomenon which is regulated by adhesion, cohesion and surface tension forces and the relative sizes of the pores. The capillary absorption effect (which is increased in pores of smaller diameters) therefore also characterizes porous building materials such as mortars studied in this project. Considering Tab.14 it's possible to notice that total open porosity (TOP) and permeability (μ) are not perfectly correlated between the samples; these differences are probably due to a specific pore size distribution, indicating the presence of a possible network with a high amount of closed pores or it is also possible that this difference depends on lower water absorption in the presence of certain additives (Tab.14). Dry chitosan at a concentration of 0.5% and DTPMP were able to isolate, at least partially, the lime and sand (LS) samples from capillary rising action. In the RMC samples, the influences of the additives are more difficult to distinguish, given the proximity of the respective results. It is nevertheless notable that DTPMP helped to reduce water intake. As it can be seen from the Average TOP, the samples added with the phosphonic acid developed a reduced porosity while it did not seem to affect the LS samples.

Table 14 Hydric behavior, data regarding water vapor permeability and capillary water absorption are listed: WDD= density of moisture flow rate; μ = moisture resistance factor; sd = water vapor diffusion equivalent air thickness; CA = coefficient of water absorption by capillarity; TOP = total open porosity as determined by the volume of water absorbed by capillary absorption.

Mock-up ID	**Average TOP**	**WDD**	**μ**	**sd**	**CA**
	%	**g/(m²•s)**		**m**	**g/cm²•s⁻¹**
LS_1/2/3	18,48±0,46	58,16±3,24	14,23±0,87	0,30±0,01	2,50±0,10
LS_CL025_1/2/3	16,70±0,12	58,51±0,37	14,11±0,10	0,30±0,00	2,20±0,17
LS_CL05_1/2/3	21,11±0,26	53,23±1,87	15,69±0,61	0,34±0,01	2,67±0,12
LS_CS025_1/2/3	15,86±0,48	74,43±3,45	10,81±0,55	0,23±0,01	1,91±0,01
LS_CS05_1/2/3	11,02±1,54	54,10±3,42	15,42±1,03	0,33±0,02	1,47±0,15
LS_D025_1/2/3	15,86±0,99	57,16±1,86	14,48±0,53	0,31±0,01	1,83±0,06
LS_D05_1/2/3	12,97±1,32	59,64±0,55	13,81±0,14	0,30±0,00	1,63±1,63
LSC_1/2/3	27,29±0,72	52,29±0,7	15,96±0,23	0,34±0,00	1,63±0,15

LSC_CL025_1/2/3	27,12±1,08	77,48±13,43	10,49±2,06	0,23±0,00	1,59±0,17
LSC_CL05_1/2/3	27,37±0,79	61,35±16,55	13,95±4,14	0,30±0,10	1,70±0,10
LSC_CS025_1/2/3	22,68±0,12	40,58±3,5	21,05±1,94	0,45±0,04	2,07±0,06
LSC_CS05_1/2/3	22,88±0,31	48,34±0,65	17,37±0,25	0,38±0,01	1,87±0,11
LSC_D025_1/2/3	20,72±0,83	72,60±8,18	11,18±1,42	0,24±0,03	1,70±0,10
LSC_D05_1/2/3	20,67±0,62	59,08±25,55	15,55±7,33	0,33±0,16	1,77±0,11

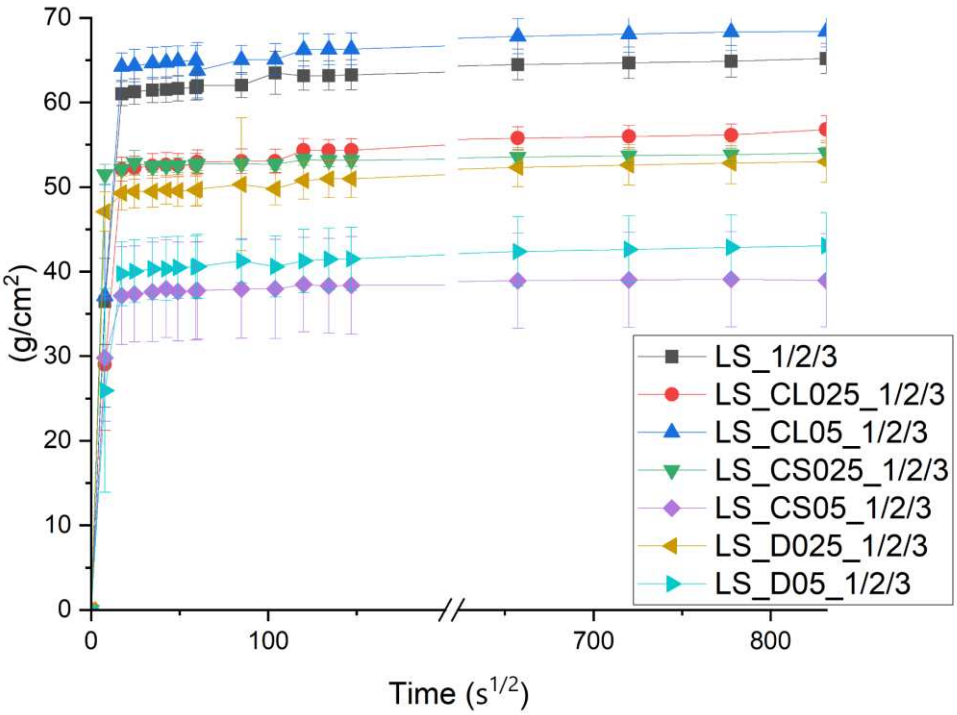

Figure 17 Capillary absorption curve for LS samples, showing the measurement until day 8.

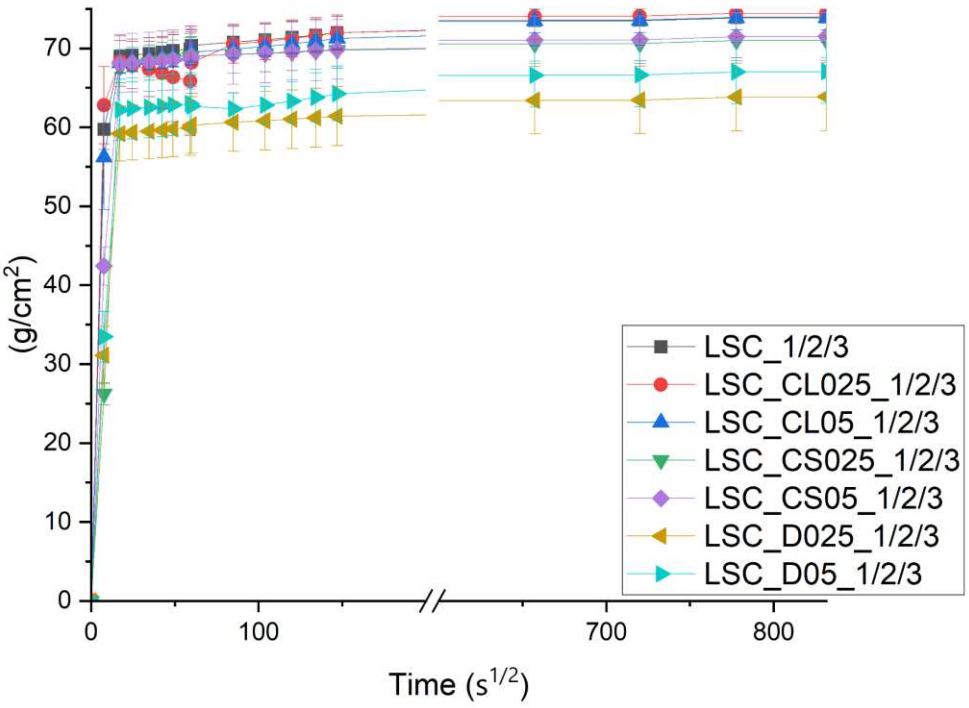

Figure 18 Capillary absorption curve for LSC samples, showing the measurement until day 8.

Fig.19 and Fig.20 show the plotted data of total open porosity (TOP) and permeability (μ), such a comparison is necessary in order to be able to interpret the influence of additives on the analysed samples at the same time. As it can be seen, the addition of chitosan solution 05% has reproduced the effects already seen on RMC illustrated in Fig.14,16, with an increase in porosity while increasing at the same time the resistance to water vapour. In the case of LS_CS05 and LS_D025, the presence of chitosan flakes produced a sealing effect on the sample, probably due to the presence of flakes which occluded the pore network of the sample concerned. The cases represented by LS_D05, LS_CS025 and LS_CL025 showed abnormal behaviour, since lower TOP values would have given higher permeability resistance values whereas here less porous, more breathable mortars were obtained (Fig.20).

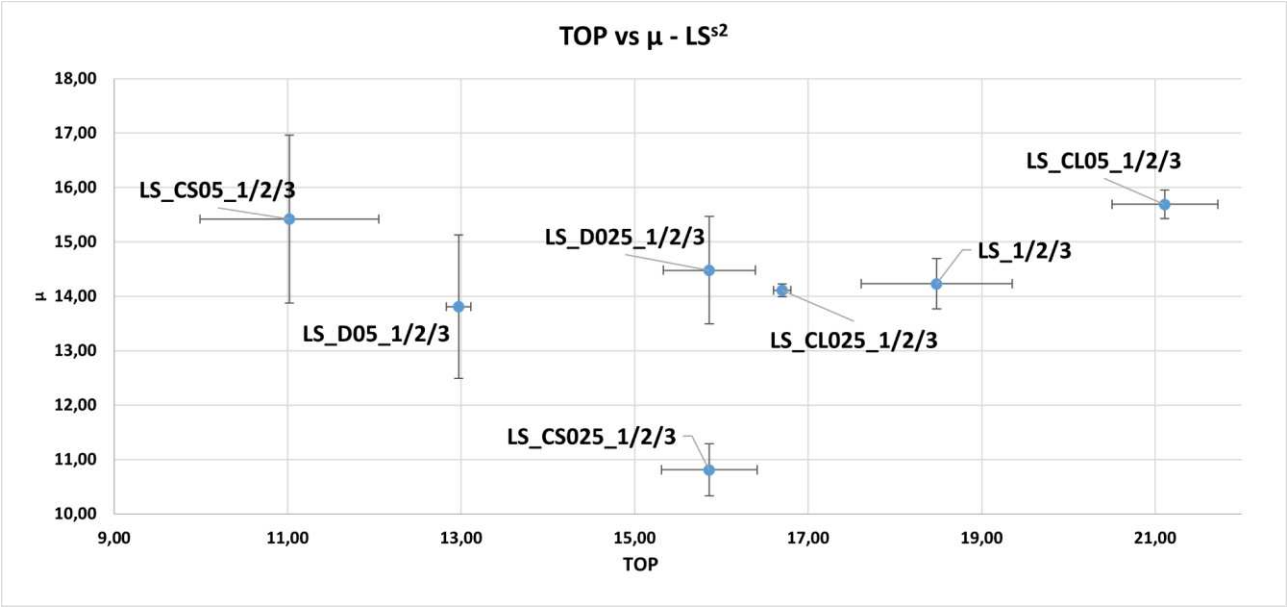

Figure 19 Plotting of TOP vs μ of samples from series 2nd: LS samples.

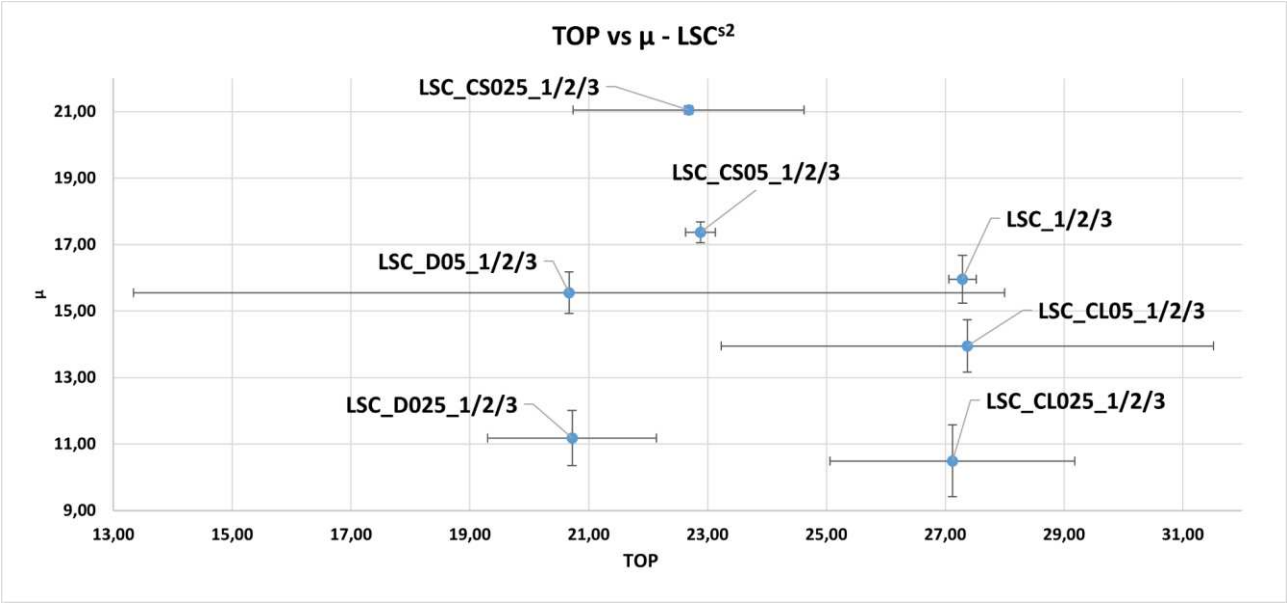

Figure 20 Plotting of TOP vs μ of samples from series 2nd: LSC samples.

If we look at the graph comparing the total open porosity (TOP) values with the capillary absorption coefficient (CA) (Fig.21,22), we find some correspondence with the above data (Tab.14; Fig.19,20). Since permeability is inversely related to porosity and the same one is positively related to capillary absorption coefficient, it is possible to find a match for sample LS_CL05, which demonstrates that chitosan in liquid form and higher concentration is able to make the mortar less permeable, but at the same time increasing the number of open pores and consequently, the ability to absorb water by the capillary. About the other samples on LS basis, we also note here the above waterproofing effect, where the reduction of TOP is accompanied by a lower CA value. About samples on a LSC basis however, it is possible to note that the

presence of additives has affected the water absorption performance of the samples, reducing both their CA and TOP values, except for LSC_CL05 and LSC_CL025 (Fig.22). This abnormal behavior would result in increased capillary absorption values, albeit slightly higher than the LSC sample, although having a sealed effect that reduces aerosol passage during permeability tests (Tab.14).

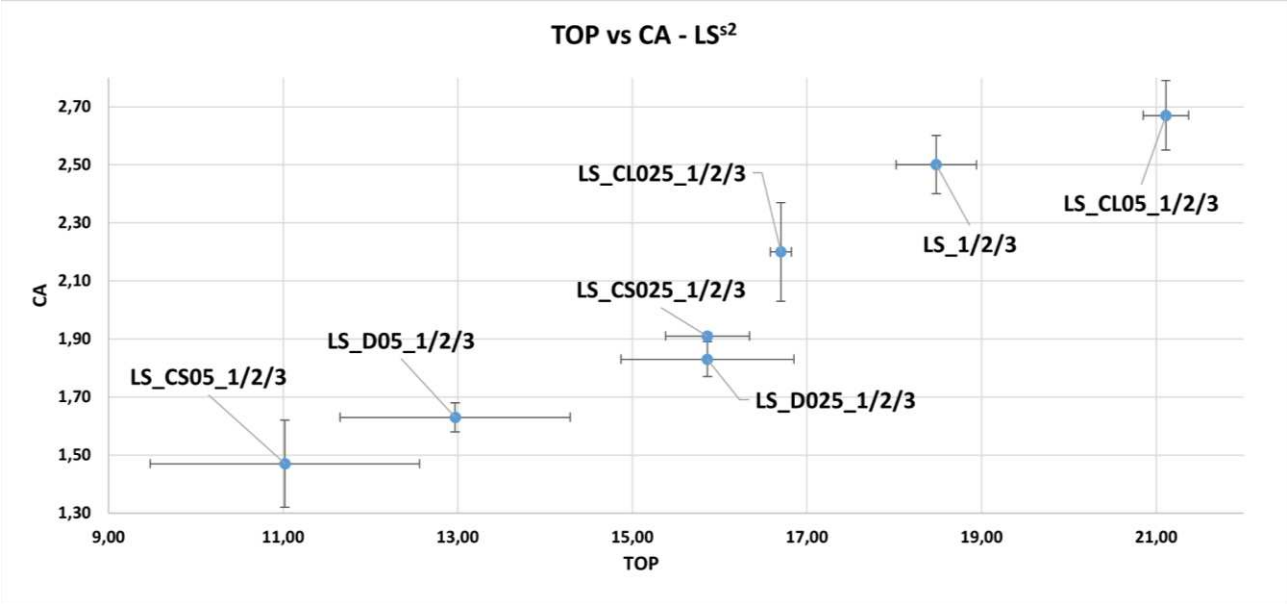

Figure 21 Plotting of TOP vs CA of samples from series 2nd: LS samples.

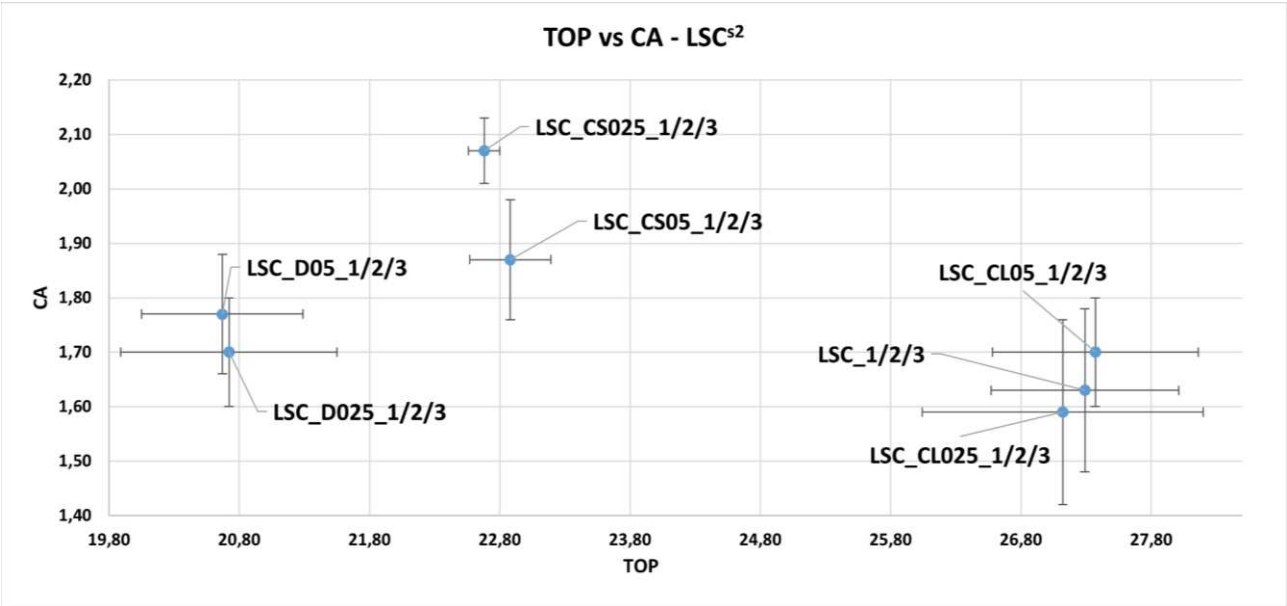

Figure 22 Plotting of TOP vs CA of samples from series 2nd: LSC samples.

The 3rd series characterized by lime, magnesian lime, and sand, added with different percentages of metakaolin, provided interesting results. As seen in Fig.23, there are two almost distinct distributions of two major groups of the lime and sand samples. The TOP of both formulations is affected by the increase in the aggregate ratio, decreasing the more the sand in the mix increases (Tab.15). At the same time, it can be seen that the magnesian lime-based samples (ML...) show more uniform behavior, although not all of them exhibit purely linear behavior in the initial phase (ML07S1M03, ML1S2, ML08S2M02, ML07S2M03) (Fig.24). Here, the presence of metakaolin or the variation in the amount of aggregate does not seem to have generated noteworthy behaviours, resulting in a small variations of CA (0.88±0.1 up to 0.96±0.09) (Tab.15) Metakaolin in high amounts combined with substantial amounts of aggregate helped to produce compact samples, reducing water uptake.

Table 15 Hydric behavior, data regarding water vapor permeability and capillary water absorption of lime and magnesian lime based samples with metakaolin are listed: WDD= density of moisture flow rate; μ = moisture resistance factor; sd = water vapor diffusion equivalent air thickness; CA = coefficient of water absorption by capillarity; TOP = total open porosity as determined by the volume of water absorbed by capillary absorption.

Mock-up ID	**Average TOP (total open porosity)**	**WDD**	**μ**	**sd**	**CA**
	%	**g/(m²•s)**		**m**	**g/cm²•s^{-1}**
L1S1_1/2/3	27,99±0,38	45,21±3,04	18,73±1,31	0,4±0,03	1,18±0,06
L09S1M01_1/2/3	28,91±1,19	94,75±58,79	10,41±5,4	0,22±0,12	1,23±0,07
L08S1M02_1/2/3	27,44±2,4	56,84±15,53	15,35±4,36	0,33±0,09	1,17±0,09
L07S1M03_1/2/3	24,53±0,65	36,8±3,01	23,38±2,13	0,5±0,05	0,9±0,06
L1S2_1/2/3	22,31±0,32	39,71±2,93	21,54±1,74	0,46±0,04	0,85±0,08
L09S2M01_1/2/3	20,75±0,61	76,52±21,98	11,05±3,08	0,24±0,07	0,92±0,05
L08S2M02_1/2/3	19,67±0,29	59,42±18,47	11,13±2,18	0,24±0,05	0,84±0,05
L07S2M03_1/2/3	19,05±0,68	54,64±19,13	11,13±4,81	0,24±0,1	0,76±0,19
L1S3_1/2/3	16,55±0,08	58,12±24,88	10,95±3,85	0,24±0,08	0,75±0,15
L09S3M01_1/2/3	18,89±0,2	63,41±15,76	13,52±3,7	0,29±0,08	0,86±0,03
L08S3M02_1/2/3	20,49±0,82	29,22±8,91	31,47±8,98	0,68±0,19	0,89±0,04
L07S3M03_1/2/3	18,33±0,55	22,09±11,42	46,86±21,35	1,01±0,46	0,82±0,04
ML1S1_1/2/3	28,11±0,59	42,16±12,69	21,34±6,08	0,46±0,13	1,09±0,04
ML09S1M01_1/2/3	29,46±0,23	29,69±7,35	30,37±7,35	0,65±0,16	1,05±0,04

ML08S1M02_1/2/3	26,6±1	29,64±7,64	30,44±7,16	0,65±0,15	1,01±0,03
ML07S1M03_1/2/3	27,96±0,62	79,76±36,61	11,46±4,88	0,25±0,1	0,98±0,03
ML1S2_1/2/3	23,55±0,33	44,64±29,43	28,19±22,71	0,61±0,49	0,96±0,04
ML09S2M01_1/2/3	21,15±0,25	49,17±6,35	17,25±2,26	0,37±0,05	0,92±0,06
ML08S2M02_1/2/3	21,23±0,59	76,52±21,98	11,05±3,08	0,24±0,07	0,93±0,04
ML07S2M03_1/2/3	22,52±0,37	69,99±7,22	11,66±1,36	0,25±0,03	0,96±0,04
ML1S3_1/2/3	20,41±1,61	59,9±9,27	13,99±2,33	0,3±0,05	0,88±0,1
ML09S3M01_1/2/3	22,81±0,48	72,11±22,09	11,9±3,46	0,26±0,07	0,97±0,03
ML08S3M02_1/2/3	21,68±1,52	63,41±15,76	13,52±3,7	0,29±0,08	0,96±0,09
ML07S3M03_1/2/3	21,24±0,15	40,14±6,85	21,63±3,66	0,46±0,08	0,93±0,04

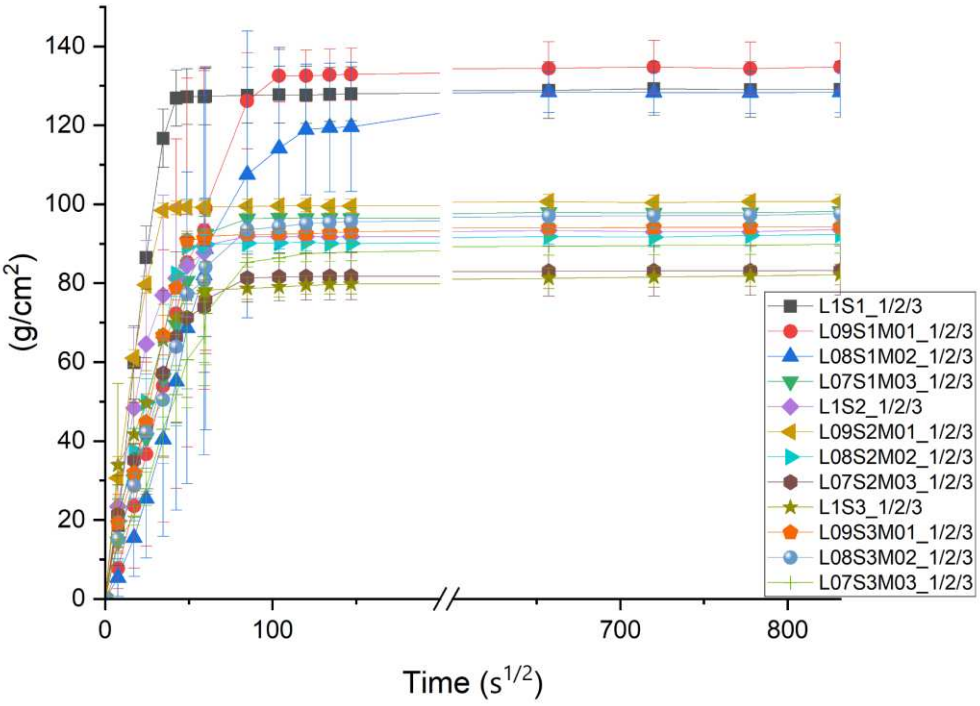

Figure 23 Capillary absorption curve for L samples (3rd Series), showing the measurement until day 8.

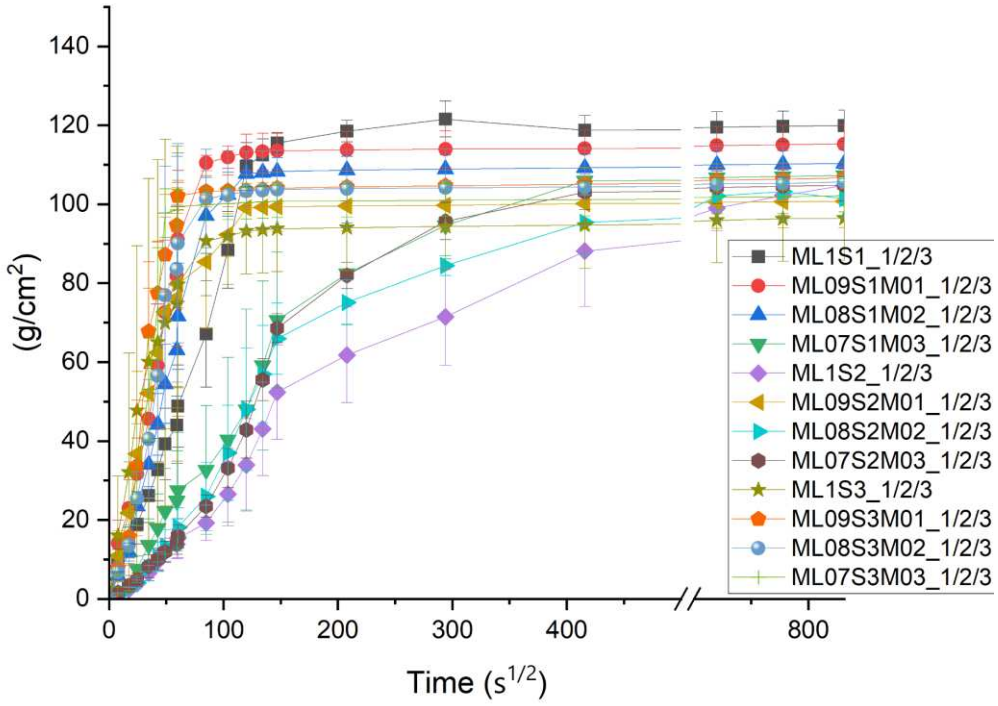

Figure 24 Capillary absorption curve for ML samples (3rd Series), showing the measurement until day 8.

When comparing the variables of permeability (μ) and total open porosity (TOP), two different behaviours were observed following the addition of metakaolin and change in lime: sand ratio between the two basic formulations (traditional lime L and magnesium lime ML) (Fig.25,26). In the first case, the presence of metakaolin has been determined, only in the case of L1S3 and their derived samples L09S3M01, L08S3M02, and L07S3M03 a behavior in line with the general expectations that the increase of TOP corresponds to an increase in permeability resistance. In the case of the other samples, however, it is not possible to describe a precise pattern in relation to the increase in the amount of metakaolin that can explain these behaviours, so much so that in the case of L1S2, metakaolin replacements produce less porous mortars but more permeable (even though the values of permeability resistance do not change between the different metakaolin quantities). In the case of L1S1, the metakaolin at low quantities seems to have an aerating effect (increase of open porosity and permeability) and at high quantities a condensing effect (lowering of TOP and increase of permeability resistance). Focusing on Fig.26, concerning the magnesium mortars (ML...), it is easy to see that in the case of the lime:sand ratio 1:2, the addition of metakaolin has reduced the open porosity still increasing the permeability of the bulk. Meanwhile, considering the case of ML1S1, the lowest amount of substituted metakaolin (ML09S1M01) produces a mortar even though more porous, less

permeable to water vapor while the other substitutions determine lower permeability resistance and lower porosity. ML1S3 shows an improvement in the samples with the lower substitution of metakaolin that generates a more permeable and porous structure (ML09S3M01, ML08S3M02) (Fig.26).

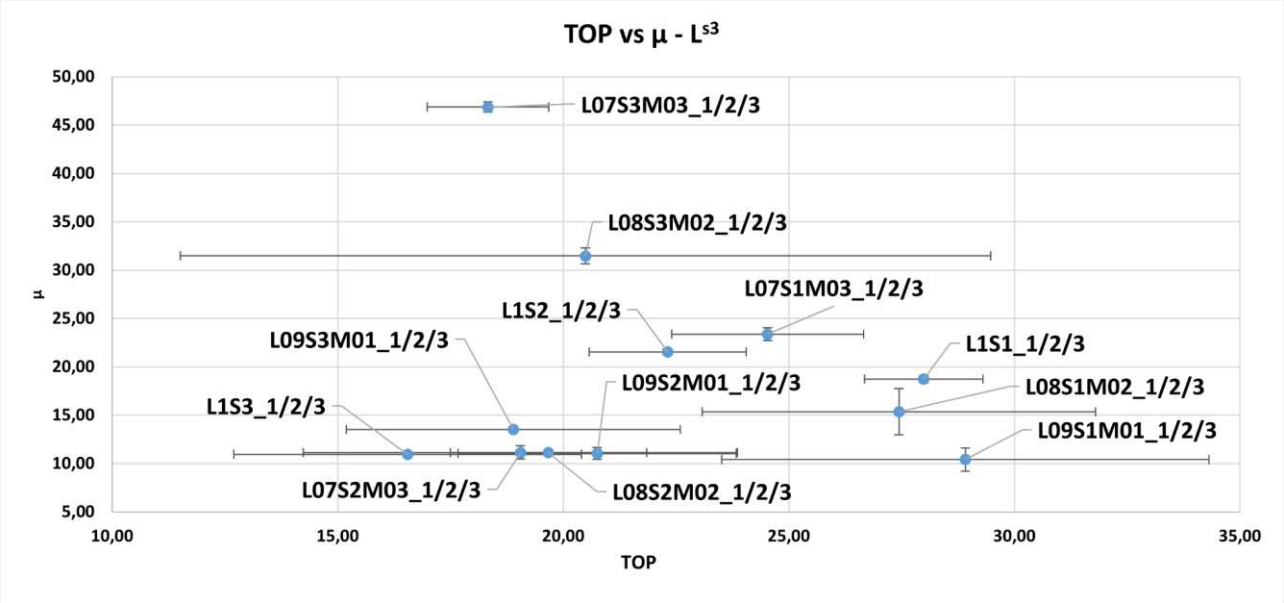

Figure 25 Plotting of TOP vs μ of L samples from series 3rd .

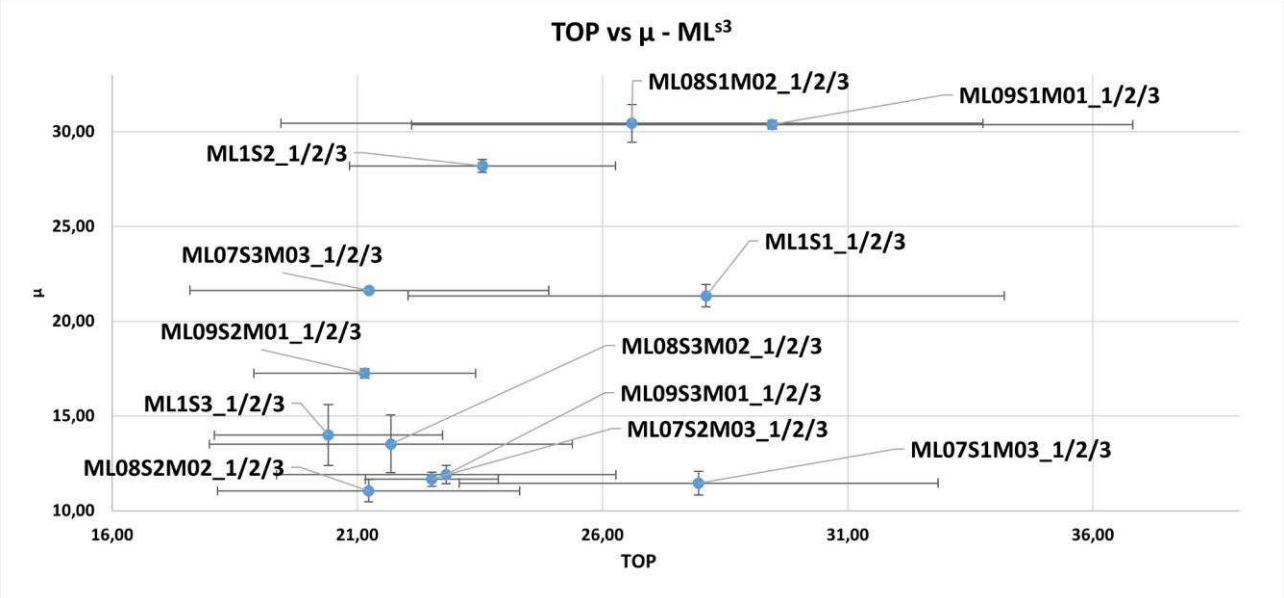

Figure 26 Plotting of TOP vs μ of ML samples from series 3rd.

There is a fairly linear trend in the graphical representation of TOP values against those of CA (Fig.27,28). In both graphs, it is easy to identify an almost linear trend linking the three untreated samples, where capillary absorption values remain unchanged, while total open porosity decreases with increasing aggregate fraction in the mixture. This is caused by the presence of aggregate that increases the compactness

of the mortars, making them more uniform and dense. Again, considering the three families of samples based on different ratios of sand, it is not possible to establish the same behavior in relation to the addition of metakaolin because it causes different effects depending on the ratio. Metakaolin seems to increase the number of open pores only if it is added to a mortar with a ratio of 1:3 and 1:1 but only in the minor amount of substitution (ML09S1M01) while, it probably generates a more closed pore network than normal when it is found in mortars with a ratio of 1:2 (Fig.27,28).

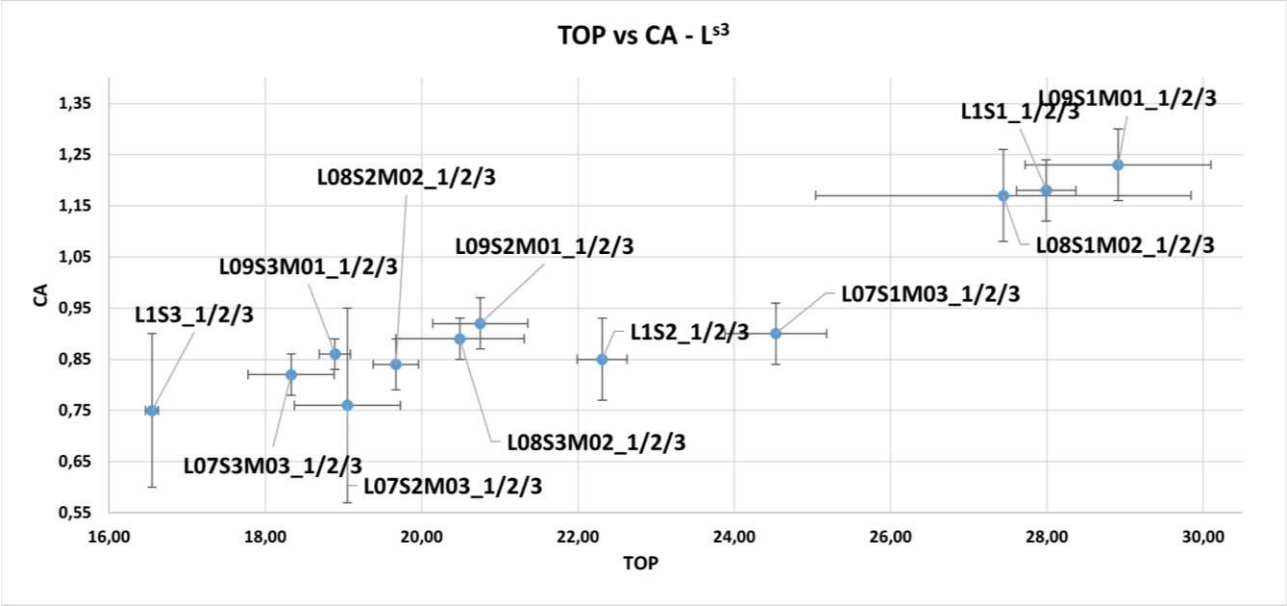

Figure 27 Plotting of TOP vs CA of L samples from series 3rd .

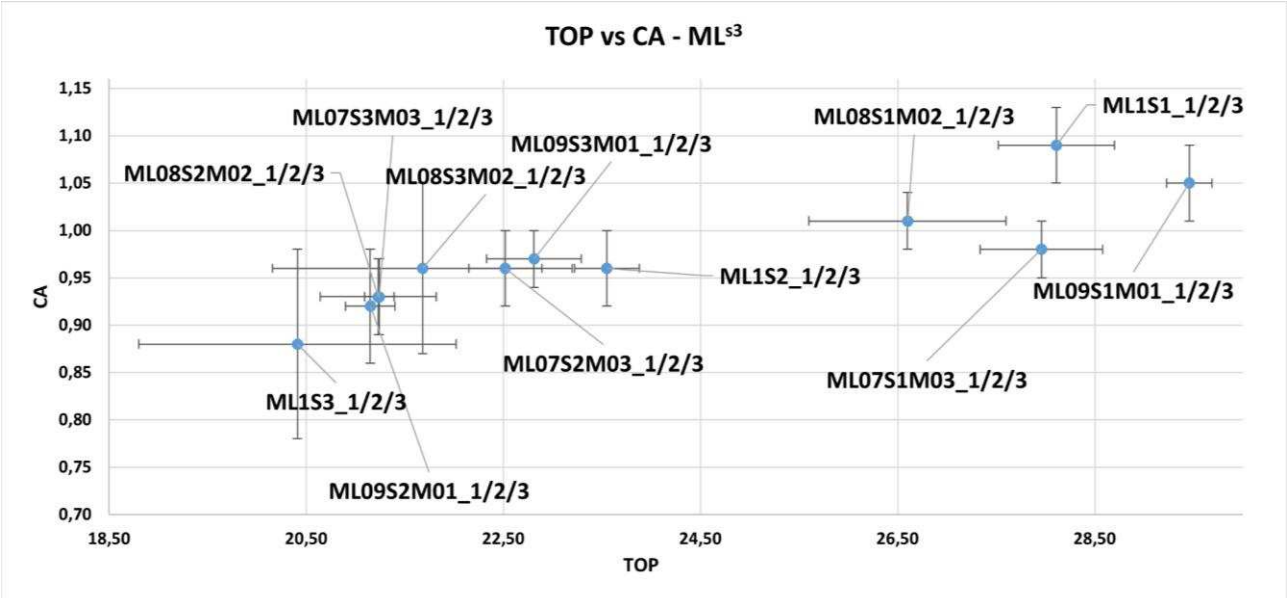

Figure 28 Plotting of TOP vs CA of ML samples from series 3rd.

In conclusion, it is not entirely clear how the different binder:aggregate ratio of the formulation can have such different behaviours with the same metakaolin replacements, abnormal behaviours that do not follow a certain trend, but which are certainly due to metakaolin characteristics that have not been identified in this study. The fourth set of samples features different formulations, designed for application in a humid environment affected by capillary rise. It brings together formulations with the greatest potential from previous experiences along with some new proposals. Among the results obtained, it was possible to observe more clearly how capillary absorption varied among different lime-based mortars. As can be seen from Fig.29, in which the limes mixed with CBP are shown, the trends of traditional (L1S1.7C03), magnesian (ML1S1.7C0.3), and NHL (NHL1S0.7C0.3) limes take on distinct trends. In particular, the aggregate amount variation in traditional lime (L1S0.7C03) seems to have significantly increased the adsorption values compared to the higher lime/ sand ratio (L1S1.7C03) which exhibits a rather low CA (0,69±0,55). Among the new formulations, adding micro hollow glass beads made it possible to observe how these behave when added to a mortar mix (Fig.30). The values of the average porosity and CA shown are markedly low, except for mixtures with liquid chitosan and DTPMP. If in the previous series, DTPMP was able to partially limit water absorption compared to mixes without DTPMP, an increase in absorption values is now observed possibly due to the combination with NHL and micro beads glass. Liquid chitosan instead, maintained values similar to those of the original mixture (Tab.16).

Table 16 Hydric behavior, data regarding water vapor permeability and capillary water absorption are listed: WDD= density of moisture flow rate; μ = moisture resistance factor; sd = water vapor diffusion equivalent air thickness; CA = coefficient of water absorption by capillarity; TOP = total open porosity as determined by the volume of water absorbed by capillary absorption.

Mock-up ID	**Average TOP**	**WDD**	**μ**	**sd**	**CA**
	%	**g/(m²·s)**		**m**	**g/cm²·s⁻¹**
L1S1.7C0.3_1/2/3	18,97±1,34	67,61±8,67	12,17±1,64	0,26±0,04	0,69±0,55
ML1S1.7C0.3_1/2/3	23,21±0,66	86,27±3,10	9,13±0,38	0,2±0,01	2,67±0,21
L1S0.7C0.3_1/2/3	27,32±0,14	78,53±16,88	10,49±2,32	0,23±0,05	2,75±0,24
NHL1S0.7C0.3_1/2/3	27,59±0,42	118,87±15,68	6,33±1,1	0,14±0,02	2,73±1,05
NHL1S3HGMS_1/2/3	20,23±0,4	88,8±12,42	8,97±1,58	0,19±0,03	1,27±0,04
NHL1S3HGMSD_1/2/3	19,97±0,53	124,21±62,98	8,07±6,48	0,17±0,14	1,78±0,40
NHL1S3HGMSCL_1/2/3	18,77±1,05	103,95±30,66	7,82±2,48	0,17±0,05	2,19±0,14

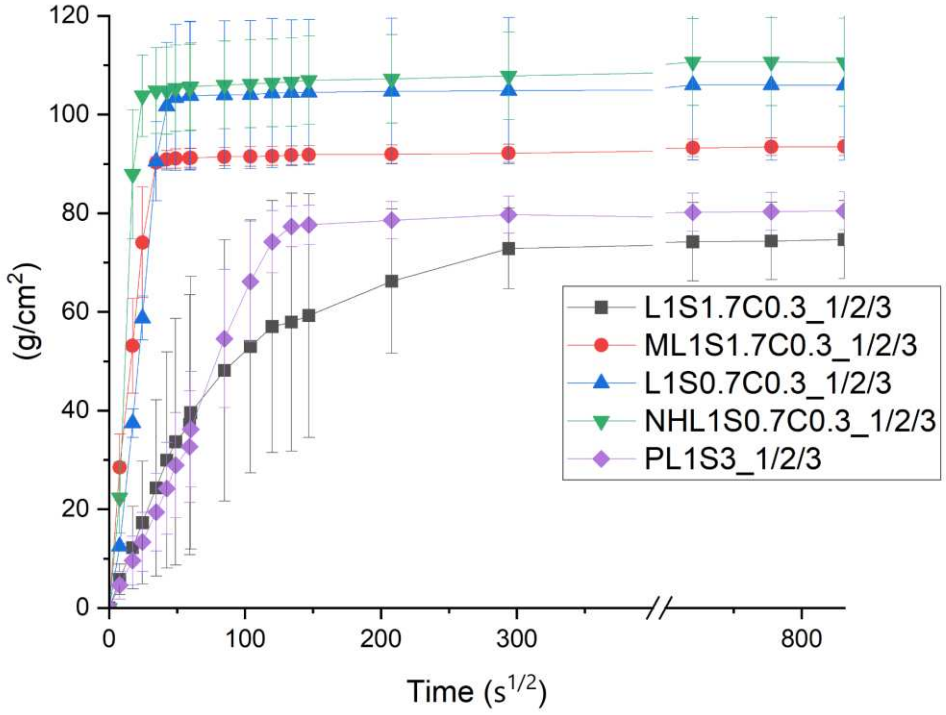

Figure 29 Capillary absorption curve for 4rt Series, showing the measurement until day 8.

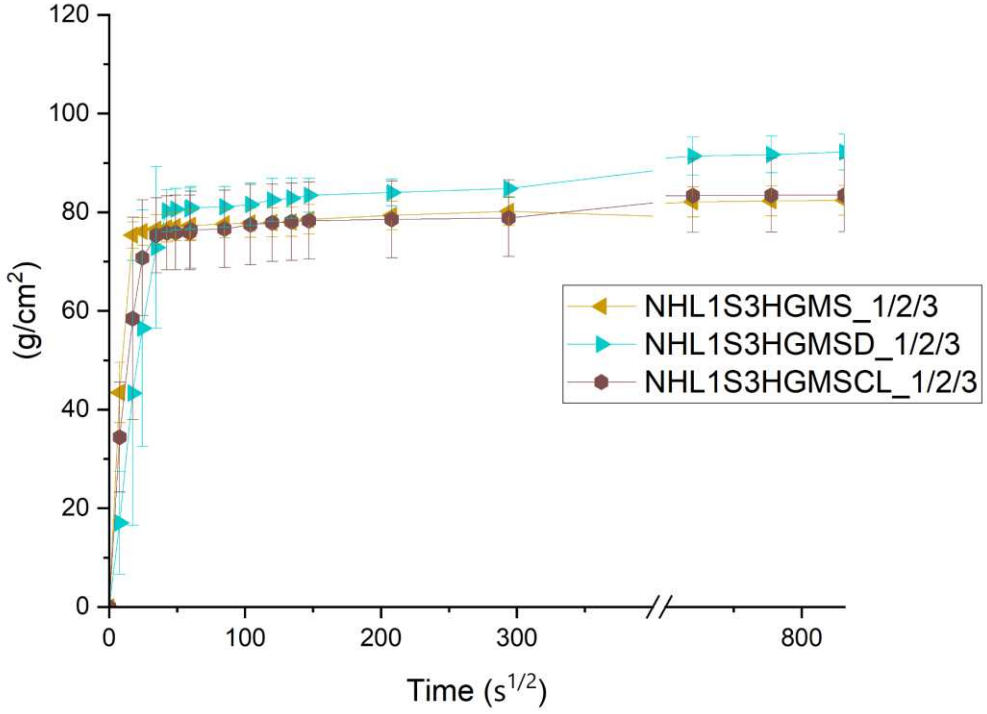

Figure 30 Capillary absorption curve for HGMS added samples (4rt Series), showing the measurement until day 8.

Because Series 4 consists of mixed formulations that are not linked by a common thread, preventing direct comparison at the formulation level, except for the samples added with HGMS and Chitosan or DTPMP, which share the same dough base (NHL1S3), it is difficult to compare graphs between CA and mu values with TOP. Therefore, the usual plotting between TOP vs permeability index and capillary absorption coefficient has not been provided.

The 5th series, on the other hand, illustrates a series of samples based on lime putty mixed with sand and possibly CBP and HGMS (Tab.17). As can be seen from the TOP and CA values assumed by the samples, the SLSC and SLSCH are those with the highest values among all. This behavior is also clearly visible in Fig.31 where the addition of hollow glass microspheres to the mixture seemed to help in lowering the water intake. The graph comparing TOP and μ (Fig.32) demonstrates the existence of a linear relationship between total open porosity and permeability coefficient, where in reality these coefficient should be inversely related as for more porous structures, lower values of μ should correspond(Tab.17).

Table 17 Hydric behavior, data regarding water vapor permeability and capillary water absorption are listed: WDD= density of moisture flow rate; μ = moisture resistance factor; sd = water vapor diffusion equivalent air thickness; CA = coefficient of water absorption by capillarity; TOP = total open porosity as determined by the volume of water absorbed by capillary absorption.

Mock-up ID	**Average TOP**	**WDD**	**μ**	**sd**	**CA**
	%	**g/(m²·s)**		**m**	**g/cm²·s⁻¹**
SLS_1/2/3	14,6±0,33	101,18±16,53	7,72±1,36	0,17±0,03	1,67±0,2
SLSH_1/2/3	16,06±0,4	83,37±20,53	9,9±2,51	0,21±0,05	1,49±0,06
SLSC_1/2/3	15,99±0,05	92,15±18,39	8,7±1,84	0,19±0,04	1,86±0,13
SLSCH_1/2/3	17,16±0,24	74,55±19,11	11,26±2,83	0,24±0,06	1,33±0,05

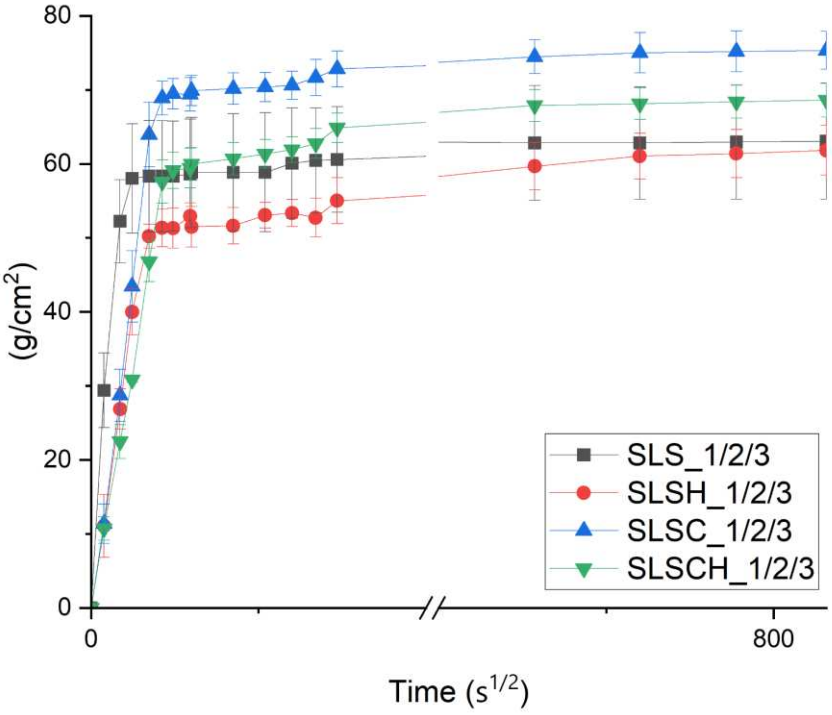

Figure 31 Capillary absorption curve for SL samples (5th Series), showing the measurement until day 8.

The potential of hollow glass microspheres and CBP (Crushed Brick Powder), when added to lime-based mortars (SL), is clearly visible in Fig.18,19. The characteristics of HGMS, often used to produce light and breathable paints, are not entirely reflected in these data, where their silica structure produces a mortar with worse breathability properties than the pure slaked lime sample, due to both μ and TOP high values. In addition, it should be noted that the combination of both aggregates has resulted in an effect where TOP and μ reach higher values than samples with individual additions (Fig.32). Focusing on Fig.33, it's possible to see different behaviours instead. As already observed previously (Tab.10) the presence of CBP contributes to the increase in CA, finding confirmation thanks to the SLSC sample meanwhile the presence of HGMS instead, while contributing to the increase in total porosity like CBP (Crushed brick Powder), does not increase as well the capillary absorption coefficient. This means that the siliceous nature of the microspheres manages to mask the effect of the crushed brick shards, reducing the rate of absorption of liquid water, creating a porous yet lesser permeable mortar (Tab.17).

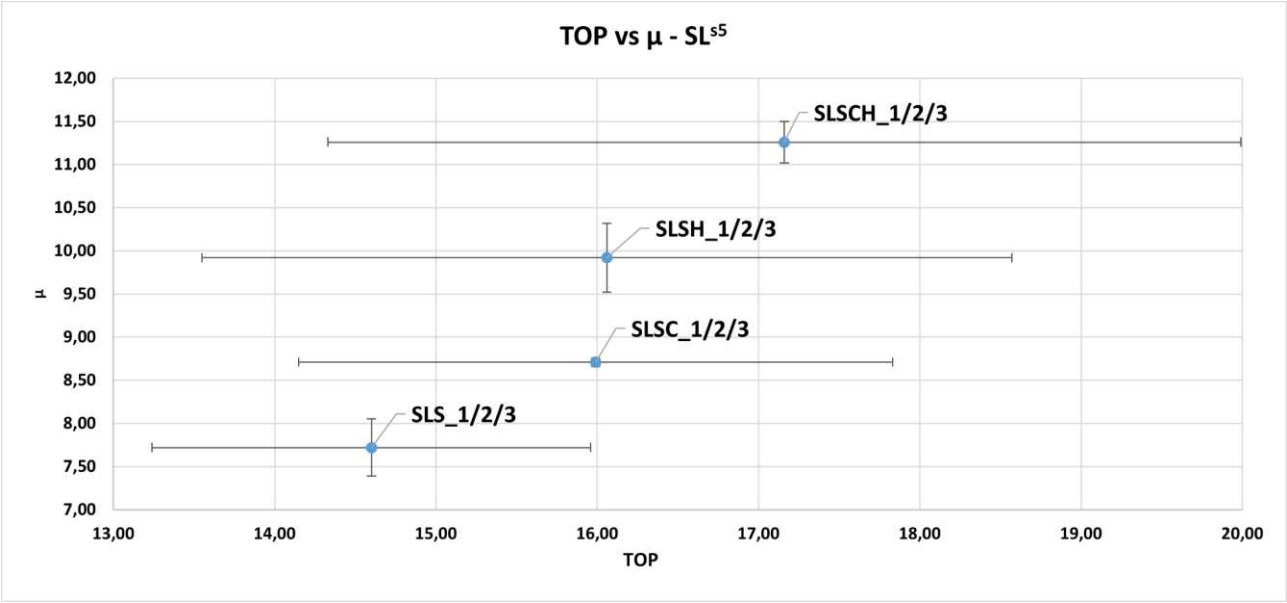

Figure 32 Plotting of TOP vs μ of Series 5th.

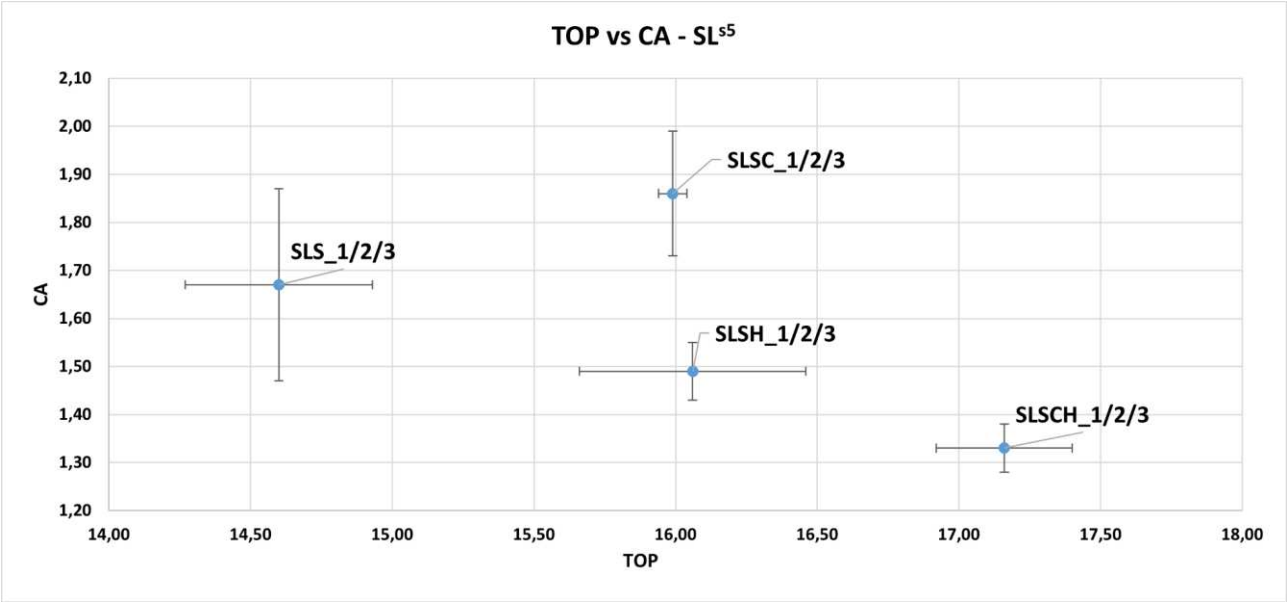

Figure 33 Plotting of TOP vs CA of Series 5th.

Top vs Ca, μ and a Ca vs μ graphs were also produced in order to identify any trends that might associate these values with the nature of the samples themselves, i.e. their composition, type of lime used, additives, etc. The first graph observed (Fig.34), plotted TOP vs μ of all mock-ups. As the observation went on, there was no significant trend to be noted among the scatter plot, showing no apparent correlation between the total open porosity and permeability.

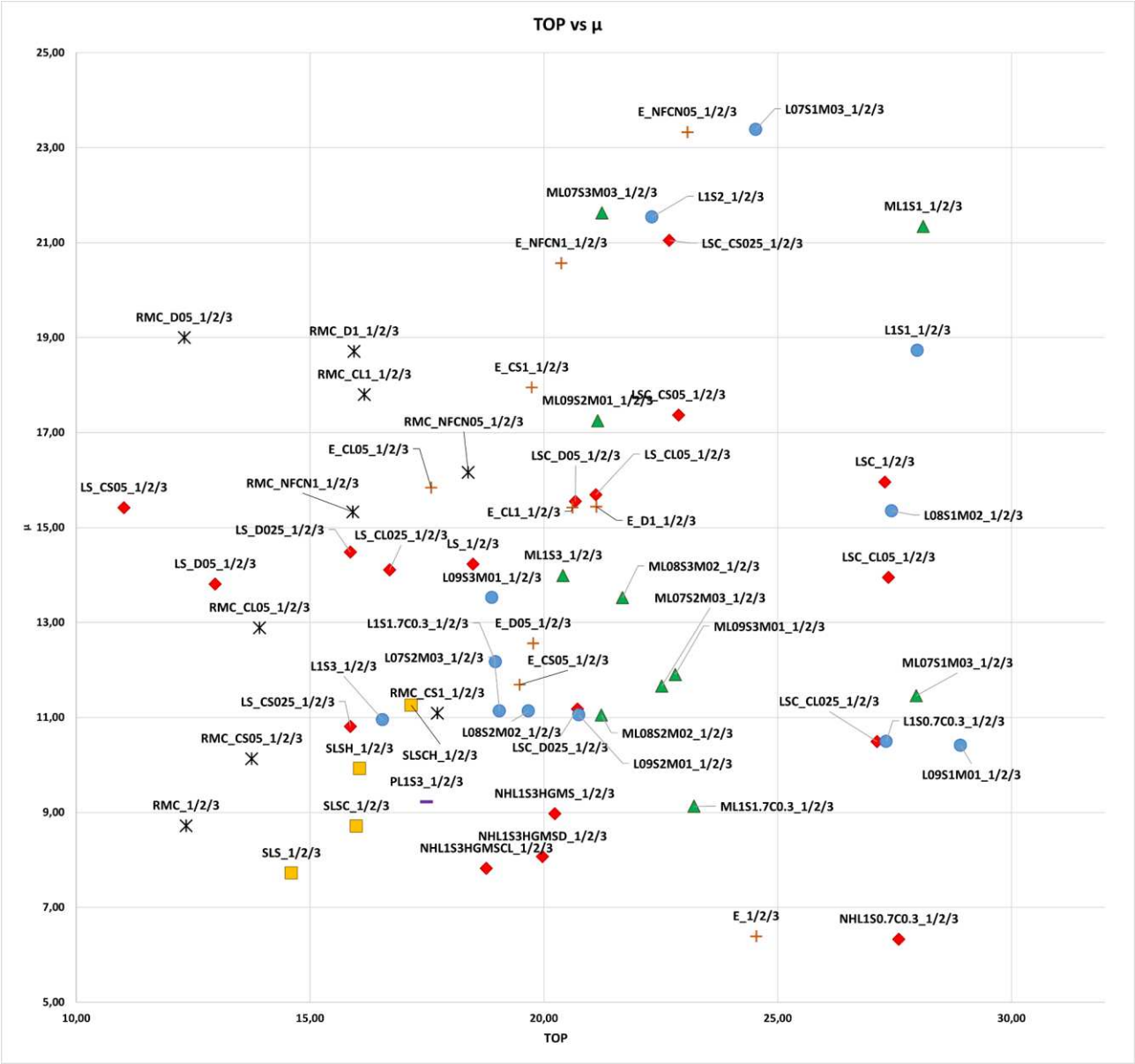

Figure 34 Plotting of global TOP vs μ of all mock-ups.

In the graph showing TOP and overall CA, more defined groupings can be seen (Fig.35). It can be seen that the MAPEI samples (black and orange crosses), of both types present CA with the lowest values of all, with the TOP increasing with the Eco-Risana samples (orange crosses), which by nature are mortars defined as breathable. Interestingly, the presence of additives modifies the total porosity creating a bridge between the untreated RMC_1/2/3 and E_1/2/3 samples. On the other hand, the samples with traditional lime and magnesia lime show a higher average capillary absorption coefficient, which is then exceeded by the samples with slaked lime (yellow square) and NHL Lafarge (red rhombuses).

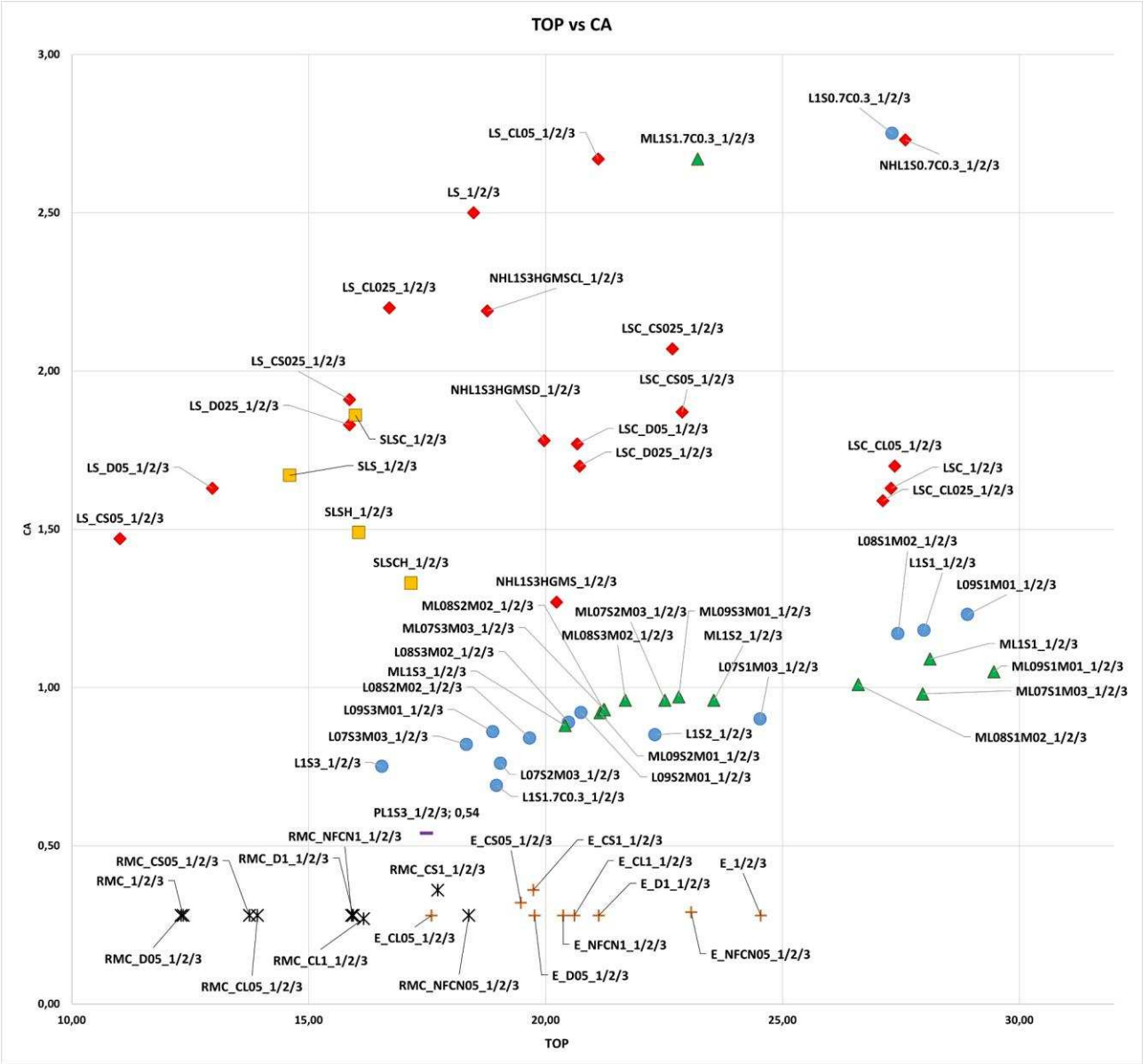

Figure 35 Plotting of global TOP vs CA *of all mock-ups.*

3.2.2 Flexural-Compressive Strength

To assess more fully the true mechanical strength of mortar samples, mechanical strength tests for flexural and compressive strength were used. The mechanical component of a mortar is usually described through a series of tests but for the limitations of this project, we have limited to the two above. The flexural strength of a sample, (sometimes referred to as the breaking modulus) is a measure of tensile strength in bending, carried out on a mortar beam which is loaded at its center point until failure. The highest value reached before the break was then shown in the table. The compressive strength test on the other half, is carried out on smaller samples which are subjected to a compressive load distributed along the whole surface until failure, measuring the highest pressure point. The comparison of these properties is able to provide us not only a prediction of the behavior of the samples under stress but also to identify their applications more closely related to their mechanical properties. This type of analysis also enabled us to determine in what degree the quantities of lime added, the aggregate ratio and the nature of the lime itself would affect the mechanical capacities of the individual samples. This is the case of the samples from Eco-Risana and Rinzaffo+MC where we could see the first applications of Chitosan, DTPMP, and Sodium Iron Cyanide. As can be seen from Tab.18, the resistance values between the two base mortars (E, RMC) are very different, both in the bending and compression form, due to the high-density characteristic of the RMC series compared to a more aerated mortar such as the E samples. The presence of additives has affected both types of mortars, weakening or reinforcing the physical properties of the samples. The presence of chitosan, both in liquid and solid form in the mixture, produced weaker mortars for both force forms in both samples "E" and "RMC", except for samples RMC_CL05 and RMC_CL1 where it was strengthened, with an increase of 4,35%, 8,7% for F module and 20%, 23,08% for C module. Similarly to chitosan, DTPMP also had poor results in both modules, for samples marked "E" and "RMC", this is probably due to an interference of the additive in the maturation phase of the samples which has resulted in a reduction in mechanical strength. As regards sodium iron cyanide, its presence does not seem to have interfered with the sampling phase nor with their maturation. The data obtained are quite similar to those of untreated mortars containing anti-salt products.

Table 18 Average flexural and compressive module with % variations of Series 1st.

Mock-up ID	Average Flessive module (Mpa)	Increase in F module (%)*	Average Compressive module (Mpa)	Increase in C module (%)*
E_1/2/3	0,5±0,01		0,8±0,02	
E_CL05_1/2/3	0,4±0,01	-20	0,6±0,03	-25
E_CL1_1/2/3	0,4±0,02	-20	0,4±0,04	-50
E_CS05_1/2/3	0,4±0,15	-20	0,6±0,12	-25
E_CS1_1/2/3	0,4±0,23	-20	0,6±0,02	-25
E_D05_1/2/3	0,4±0,02	-20	0,7±0,02	-12,5
E_D1_1/2/3	0,4±0,01	-20	0,7±0,01	-12,5
E_NFCN05_1/2/3	0,5±0,01	0	0,8±0,03	0
E_NFCN1_1/2/3	0,5±0,05	0	0,8±0,01	0
RMC_1/2/3	2,3±0,02		6,5±0,12	
RMC_CL05_1/2/3	2,4±0,07	4,35	7,8±0,16	20
RMC_CL1_1/2/3	2,5±0,06	8,7	8±0,15	23,08
RMC_CS05_1/2/3	2,3±0,04	0	6,6±0,09	1,54
RMC_CS1_1/2/3	2,4±0,05	4,35	6,7±0,01	3,08
RMC_D05_1/2/3	2,1±0,02	-8,7	5,4±0,02	-16,92
RMC_D1_1/2/3	2,2±0,05	-4,35	5,3±0,01	-18,46
RMC_NFCN05_1/2/3	2,3±0,15	0	6,5±0,02	0
RMC_NFCN1_1/2/3	2,4±0,02	4,35	6,5±0,01	0

**Increase in module F and C (%) measured in comparison to the respective non admixed mixture (E_1/2/3 for E_ series, RMC_1/2/3 for RMC_ series)*

Having been re-proposed in the second series of samples, Chitosan and DTPMP were analysed, this time on the basis of mortars made with natural hydraulic lime and not pre-mixed mortars (Tab.19). As can be seen, the presence of additives this time has led to an overall increase in the mechanical properties of the samples, with a few exceptions. Chitosan seems to have greatly increased the F and C modules, especially for the LS-type samples, with the exception of sample LSC_CS025 which shows a variation in resistance in the flexure module almost zero. Although no reasons were found, similar behavior can be seen from the DTPMP. This product seems to have increased in general both the flexure and compressive strength but the LS_D025 sample shows a reduction of 3.13% in the F-form. In conclusion, although the salt inhibitors seem to have improved the mechanical properties of the samples, two anomalies persist, the flexure module would appear to be affected, negatively by the presence of DTPMP in lime mortars and not at all from Chitosan in solid form in mortars mixed with CBP.

Table 19 Average flexural and compressive module with % variations of Series 2nd.

Mock-up ID	**Average Flessive module (Mpa)**	**Increase in F module (%)**	**Average Compressive module (Mpa)**	**Increase in C module (%)**
LS_1/2/3	0,32±0,04		4,3±2,35	
LS_CL025_1/2/3	0,54±0,18	68,75	12,13±4,73	182,09
LS_CL05_1/2/3	0,53±0,25	65,63	14,25±9,88	231,4
LS_CS025_1/2/3	0,35±0,17	9,37	5,01±1,79	16,51
LS_CS05_1/2/3	0,53±0,07	65,63	11,04±3,74	156,74
LS_D025_1/2/3	0,31±0,16	-3,13	5,11±6,17	18,84
LS_D05_1/2/3	0,41±0,1	28,13	6,68±2,79	55,35
LSC_1/2/3	0,41±0,12	28,13	14,58±4,62	239,07
LSC_CL025_1/2/3	0,6±0,14	87,5	6,53±2,96	51,86
LSC_CL05_1/2/3	0,41±0,09	28,13	11,46±1,08	166,51
LSC_CS025_1/2/3	0,32±0,12	0	9,23±5,13	114,65
LSC_CS05_1/2/3	0,53±0,15	65,63	6,68±2,86	55,35
LSC_D025_1/2/3	0,41±0,08	28,13	8,57±0,43	99,3

LSC_D05_1/2/3	0,35±0,16	9,37	4,48±2,92	4,19
**Increase in module F and C (%) measured in comparison to the respective non admixed mixture (e.g. LS_1/2/3 for LS_ series, LSC_1/2/3 for LSC_ series)*				

The metakaolin seems to have confirmed the assumptions provided by the a priori research on porcelain mortars. Described as a fundamental element of the above, considered to be the reason for high mechanical and chemical resistance to weather[87,125,126,175-177]. As can be seen from the values given in Tab.20, the modules of both forces seem to have been strengthened by the presence of metakaolin in the case of traditional lime samples. Specifically, this increase in modules F and C seems to increase according to the amount of calcium calcinate itself, as in the case of L09S1M01 from 13.33% to 123.33% of L07S1M03, where the highest percentage of metakaolin is found. As can be seen, the increase in resistance modules based on the metakaolin content is reflected in samples with a lime ratio of 1:2 where the absence of additives allows us to observe a reduction in resistance (L1S2). The same applies to the sample L1S3, where the binder ratio is found: higher aggregate, increasing the amount of sand corresponds to a reduction in the bending modulus. However, if one looks at the modules of the L1S3 series, it can be seen that the increase in resistance due to the higher quantities of additive is only observed in the case of the compression module, while the flexure module shows a bell-shaped pattern, Increasing from 16.67% to 50%, then returning to 43.33% where the metakaolin has a higher content (L07S3M03). The analysis of the samples showed that, with the same formulation (L1S1, Ml1S1), magnesium lime produces a mortar with higher resistance, increasing the flexural modulus by 123.33% and the compression modulus by 63%, and 73%, probably due to the presence of hydro magnesite in the solid matrix. Magnesium-based kicks (whose F and C modules of comparison are those of ML1S1) have shown a reverse trend. In these compositions, it can be seen that, with the increase of the quantity of metakaolin substitute to lime, the flexure module is reduced considerably, much more than the reduction due to the increase of the lime: sand ratio. This trend does not seem to be related to TOP but could be linked to the influence of metakaolin during the maturation phase of the samples.

Table 20 Average flexural and compressive module with % variations of Series 3rd.

Mock-up ID	Average Flessive module (Mpa)	Increase in F module (%)	Average Compressive module (Mpa)	Increase in C module (%)
L1S1_1/2/3	0,3±0,03		2,95±1,05	
L09S1M01_1/2/3	0,34±0	13,33	6,84±0,45	131,86
L08S1M02_1/2/3	0,64±0,02	113,33	14,86±1,52	403,73
L07S1M03_1/2/3	0,67±0,02	123,33	19,94±0,67	575,93
L1S2_1/2/3	0,2±0,04	-33,33	2,91±0,15	-1,36
L09S2M01_1/2/3	0,44±0	46,67	6,04±0,94	104,75
L08S2M02_1/2/3	0,49±0,04	63,33	9,38±2,94	217,97
L07S2M03_1/2/3	0,55±0,05	83,33	13,3±3,36	350,85
L1S3_1/2/3	0,22±0,02	-26,67	1,55±0,61	-47,46
L09S3M01_1/2/3	0,35±0,02	16,67	5,08±0,93	72,2
L08S3M02_1/2/3	0,45±0,07	50	9,59±2,53	225,08
L07S3M03_1/2/3	0,43±0,12	43,33	17,23±1,83	484,07
ML1S1_1/2/3	0,67±0,09	123,33	4,83±0,97	63,73
ML09S1M01_1/2/3	0,48±0,01	-28,36	10,08±0,88	108,7
ML08S1M02_1/2/3	0,37±0,05	-44,78	12,08±2,73	150,1
ML07S1M03_1/2/3	0,25±0	-62,69	12,19±2,75	152,38
ML1S2_1/2/3	0,41±0,05	-38,81	3,35±0,3	-30,64
ML09S2M01_1/2/3	0,62±0,03	-7,46	8,33±0,42	72,46
ML08S2M02_1/2/3	0,44±0,05	-34,33	8,56±1,28	77,23
ML07S2M03_1/2/3	0,27±0,07	-59,7	8,22±1,36	70,19
ML1S3_1/2/3	0,43±0,08	-35,82	2,79±0,39	-42,24
ML09S3M01_1/2/3	0,37±0,03	-44,78	5,98±0,36	23,81

ML08S3M02_1/2/3	0,3±0,03	-55,22	5,22±0,86	8,07
ML07S3M03_1/2/3	0,27±0,04	-59,7	9,93±0,92	105,59
**Increase in module F and C (%) measured in comparison to the respective non admixed mixture (e.g. L1S1_1/2/3 for LxSx_ series, ML1S1_1/2/3 for MLxSx_ series)*				

For the fourth series, some anomalies were found in comparison with previous data. The case of L1S1.7C0.3 and ML1S1.7C0.3 as shown in Tab.21 showed that magnesian limes should provide greater resistance in both force modules (F and C) than a traditional lime, whereas here it was found a decrease of 57.5% in the F module. In the case of the same formulation as the first but with a lower lime ratio: sand, L1S0.7C0.3 was expected to have a higher bending value, but this has also been reduced by 65%. The presence of CBP only increases further doubts, since it has already been ascertained in Tab.19 how both modules increase in the presence of CBP, which suggests that problems have occurred with the maturation of the aforementioned samples. As for the remaining formulations, it was found that the hydraulic lime-based mortars of the Palladio brand compensate for low flexural resistance with excellent compressive strength and that liquid Chitosan, in the presence of HGMS can help the mortar promoting slightly its mechanical properties, probably due to the higher density of the dough.

Table 21 Average flexural and compressive module with % variations of Series 4th.

Mock-up ID	**Average Flessive module (Mpa)**	**Increase in F module (%)**	**Average Compressive module (Mpa)**	**Increase in C module (%)**
L1S1.7C0.3_1/2/3	0,4±0,51		4,95±0,45	
ML1S1.7C0.3_1/2/3	0,17±0,01	-57,5	8,56±1,78	72,92
L1S0.7C0.3_1/2/3	0,14±0,01	-65	8,57±0,23	73,13
NHL1S0.7C0.3_1/2/3	0,11±0,01	-	8,21±0,9	-
PL1S3_1/2/3	0,02±0	-	9,52±0	-
NHL1S3HGMS_1/2/3	0,04±0		1,98±1,03	
NHL1S3HGMSD_1/2/3	0,03±0,01	-25	3,53±0,52	78,28
NHL1S3HGMSCL_1/2/3	0,05±0	25	5,16±0,68	160,60

Increase in module F and C (%) measured in comparison to the respective non admixed mixture (e.g. L1S1.7C0.3_1/2/3 for ML1S1.7C0.3_1/2/3, L1S0.7C0.3_1/2/3 and NHL1S3HGMS_1/2/3 for NHL1S3HGMSD_1/2/3, NHL1S3HGMSCL_1/2/3)

Finally, it was noted that the very nature of lime fat seems to partially shield the influence of CBP and HGMS. The mechanical flexural strength of lime grease is not affected by additives, if at all when combined (SLSCH with an increase of 50%) (Tab.22). However, it seems that the presence of brick dust and microspheres is in contrast to the formation of a compact structure within the lime fat. This may be due to the fact that both HGMS and CBP were observed to make the mixtures more fluid (Tab.10,12) and this would have resulted in an uneven carbonation of the lime during the setting phase.

Table 22 Average flexural and compressive module with % variations of Series 5th.

Mock-up ID	**Average Flessive module (Mpa)**	**Increase in F module (%)**	**Average Compressive module (Mpa)**	**Increase in C module (%)**
SLS_1/2/3	0,02±0	0	4,91±1,27	0
SLSH_1/2/3	0,02±0,01	0	3,41±0,74	-31
SLSC_1/2/3	0,02±0	0	2,97±0,37	-40
SLSCH_1/2/3	0,03±0	50	2,64±0,72	-46
**Increase in module F and C (%) measured in comparison to the respective non admixed mixture (SLS_1/2/3)*				

3.2.3 XRD Analysis

During the course of the project, it was possible to analyse the samples of series 3rd, both traditional and magnesian lime based-mortars, by means of an Empyrean Series 3 diffraction spectrometer (Malvern Panalytical), which provided another perspective on the characterisation of the materials used in the production of mortars. This choice was motivated by the need for information on this type of formulation on which there is unfortunately little information available, namely porcelain and magnesian mortars. The possibility of observing the maturation phase of a self-produced mortar in the laboratory and trying to understand how the presence of metakaolin could interact with the binder, perhaps producing specific phases other than hydromagnesite or magnesite. It was therefore decided to analyze classical *lime+sand* mortars (such as L1S1_1/2/3) in order to obtain reference trends to interpret more complex formulations such as: *lime+sand+metakaolin* and *magnesian lime+sand*, the researched formulas behind the porcelain and magnesian mortars. In order to determine how the different binder/inert ratio influences the XRD patterns, the samples for simple lime-inert mortars were compared together at 28 days of curing, too. As Fig.36 shows, mortars with the lowest lime/sand ratio show small peaks of Portlandite meanwhile, peaks [NN1] for Quartz and Calcite are easier to locate. As the amount of lime grows in the mortar, the intensity of Portlandite grows as well, as the peaks in ratios 1:2 (m5) and 1:3 (m9) are far larger than 1:1 (m1). Although with low intensity, it's possible to locate peaks for mono-carbonates at 11°,12° *2θ*.

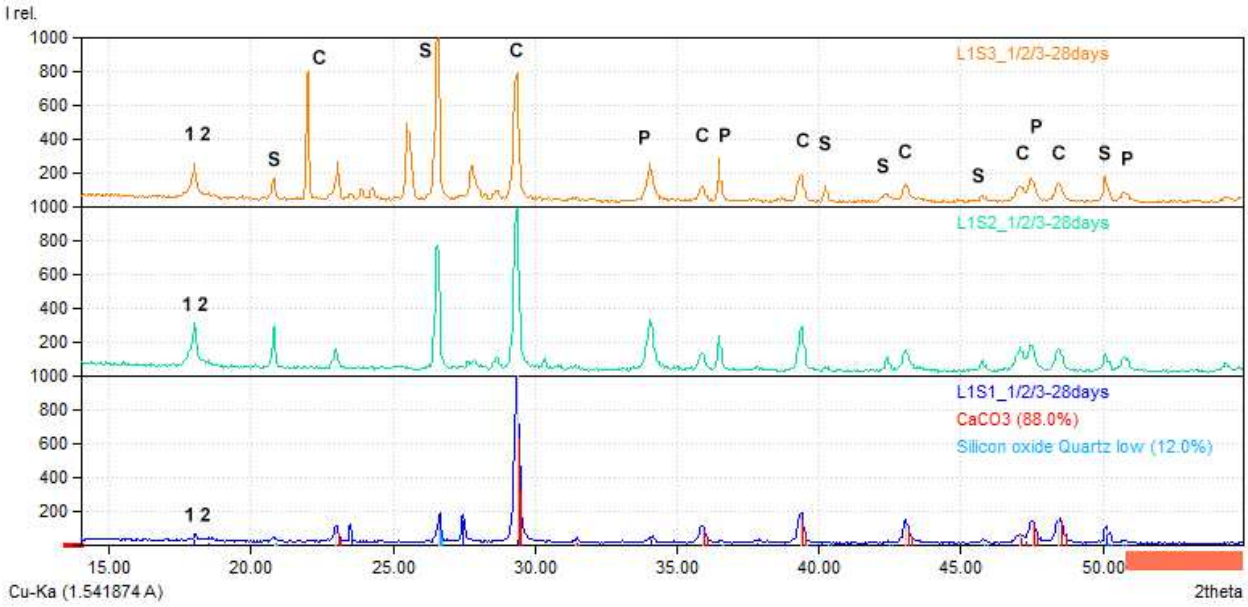

Figure 36 XRD Pattern of 28-days old matured traditional lime mortars with different lime:sand ratio (M1:L1S1_1/2/3; M5:L1S2_1/2/3; M9:L1S3_1/2/3).Quartz(S), Calcite(C) and Portlandite (P) are the main highlighted phases with traces of monocarbonates (1,2).

The evaluation of kaolin and metakaolin powder, produced in the laboratory, was recorded (Fig.37). An optimal match was found with the kaolinite mineral pattern found in the database, alongside other phases such as Illite and β-quartz, therefore, the produced metakaolin powder was not completely pure but resulted in a mixture with few impurities.

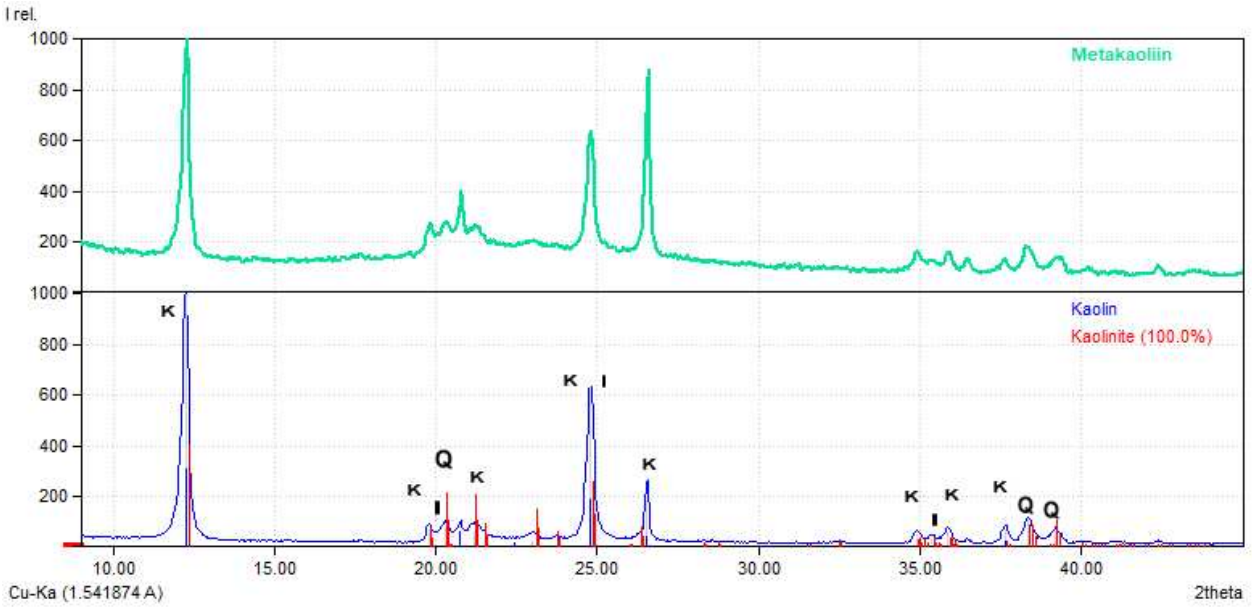

Figure 37 XRD Pattern of Kaolin(bottom) and Metakaolin(above) with highlighted peaks.Different phases are highlighted, Illite (I), Kaolinite (K) and β-quartz (Q).

Notably from Fig.37, some essential peaks can be identified in the characterisation of metakaolin, which, according to literature, possesses a disordered nature, characterised by both an amorphous and crystalline structure[178-181]:

-12.0-13.0° 2Θ: Corresponding to (001) reflection of the amorphous phase, shown as a broad peak;

-20.0-21.0° 2Θ: Corresponding to (110) plane reflection, also typical of the metakaolin's amorphous nature;

-26.0-27.0° 2Θ: Silica amorphous structure peak, its presence is due to the high silica content found in metakaolin due to the breakdown of kaolinite during calcination, which is represented as a broad peak;

The fact that most peaks have an asymmetrical appearance, is motivated by the metakaolin's nature that comprehends both crystalline and amorphous structures. As literature[178-181] pointed out, there may be slight differences between the XRD spectra depending on the production method for metakaolin: calcination temperature and time, impurities and sample preparation are in fact the most influencing factors.

The XRD analyses identified the components present in the formulations with metakaolin. Despite the variation of the physical-mechanical properties of the different formulations, no specific crystal phases produced by the interaction of metakaolin with the binder are identified (Fig.38).

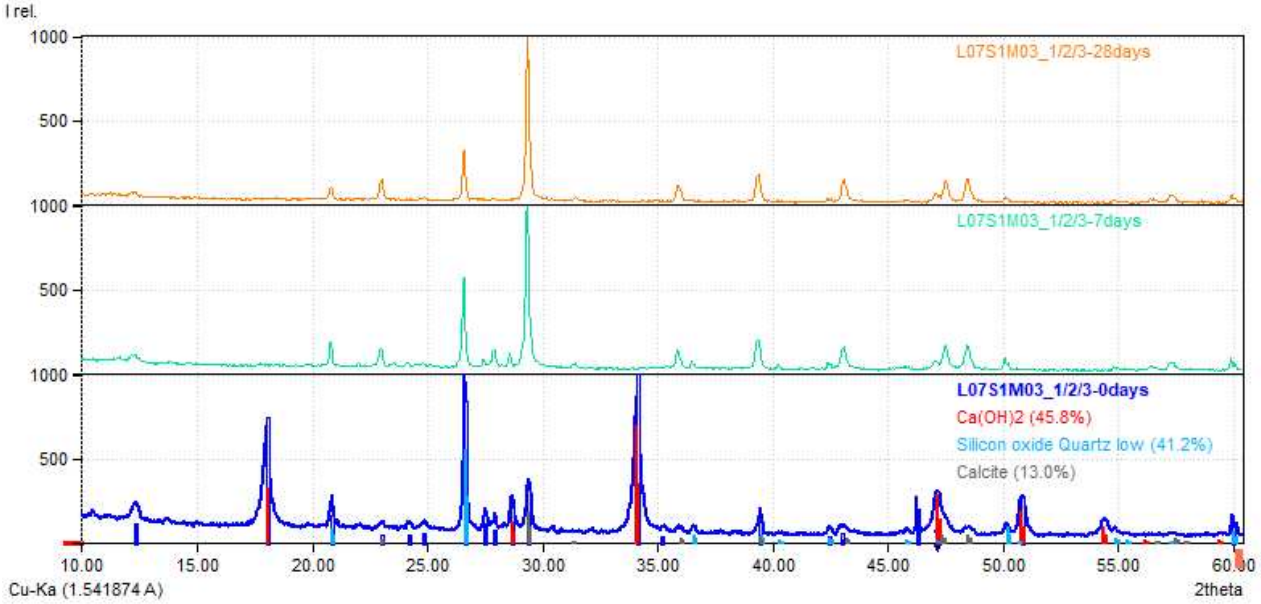

Figure 38 XRD Pattern of 28-days old matured traditional lime mortars added with metakaolin (L07S1M03_1/2/3).

The presence of metakaolin may have induced the greater formation of amorphous phases. From a compositional point of view, the binder reacts forming amorphous and CSH phases which are detected as background increase, this was identified by comparing samples of traditional mortars without the addition of metakaolin to facilitate evaluation[182-186]. As expected, in mortars produced by mixing magnesian lime with inserts, the peaks for calcium hydroxide signals become weaker and weaker as carbonation proceeds, allowing us to detect some previously hidden signals such as those of hydromagnesite (Fig.39).

As was explained in Ch.1.3 a typical feature of magnesian lime maturation was the formation of hydromagnesite $Mg_5(CO_3)_4(OH)_2{\cdot}4H_2O$), a hydrated magnesium carbonate mineral that would give the hardened compound its strength and durability characteristics[187-189]. Among the most important peaks to be found in the graphs are:

-18.0-19.0° 2Θ: Peak for (110) hydromagnesite crystalline structure. Here is represented by a small peak at 28 days, shifted to 17.0° instead of the expected values, but still recognizable even though the $Ca(OH)_2$ peak (18.0° 2Θ) which covers it completely until 7 days;

-28.5-29.5° 2Θ: Peak corresponding to (020) reflection associated with hydromagnesite, it's possible to see how its signal intensity gets broader as the curing time passes, presumably indicating an increase in the hydromagnesite quantity inside the mortar;

-31.0-32.0° 2Θ: This peak, referring to the (130) reflection plane of hydromagnesite shows the same behavior as the previous, as its signal increases during the curing phase, becoming visible around 28 days;

-34.5-35.5° 2Θ: This peak appears presumably shifted to 36.0°, and it's referring to the (131) reflection plane of hydromagnesite;

-42.0-43.0° 2Θ: This peak (132 reflection plane), which remains rather small even at 28 days, is initially covered by the signal of MgO (43.0° 2Θ) which becomes smaller over time;

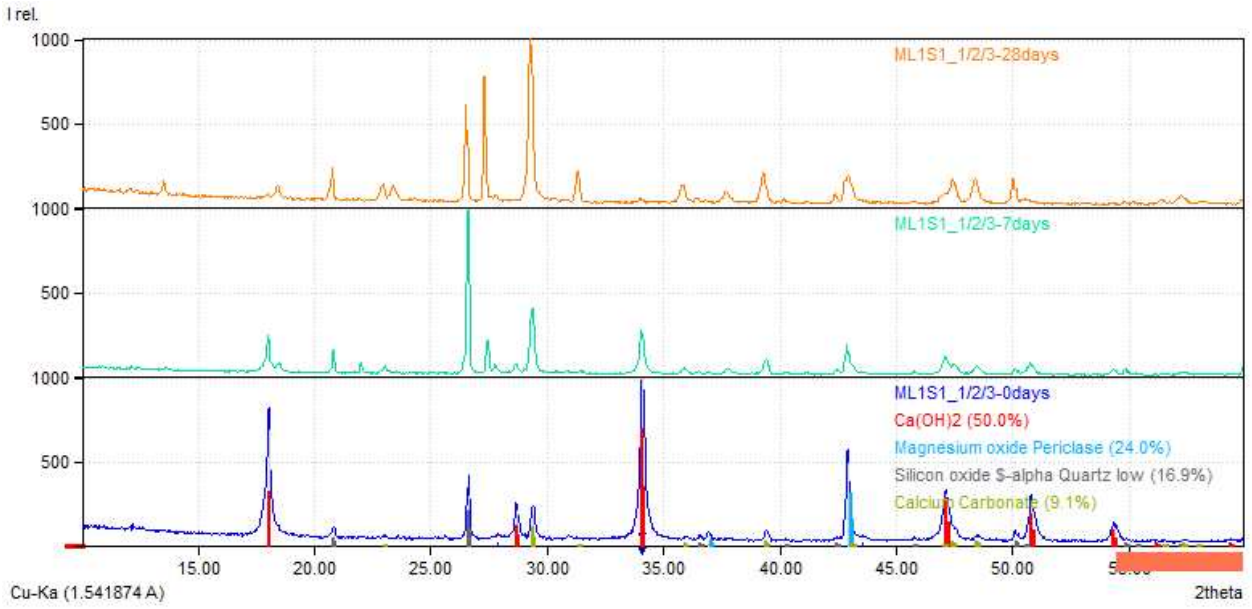

Figure 39 XRD Pattern of curing of magnesian lime mortars (ML1S1_1/2/3).

3.3 Evaluation of mortars undergoing weathering tests

3.3.1 Freeze-Thaw Resistance

Freeze-thaw resistance test is a test designed to identify the physical behavior of porous solid materials subjected to significant difference in temperature (above and below zero) and evaluate their possible use in a continental climate. As described in the previous section, porous materials, depending on their nature, may be more or less susceptible to capillary water absorption, which is directly related to this test, as a wet building element may experience cracking if it undergoes sufficient freeze-thaw cycles. During the freezing phase, ice crystals develop within the porous matrix, and the resulting increase in volume (9%) generates pressure on the inner surfaces of the pores[190-191]. The continuous freezing and subsequent thawing of water in the pores therefore results in the build-up of pressure that can damage the sample even irreparably. The first series of samples was excluded from this type of analysis because a direct approach to soluble salts was preferred. This choice was then followed by a similar weathering test (Freeze-thaw) in order to obtain a more complete overview, which then took place from the second series of samples, whose behavior is shown below (Fig.40,41). During the analysis phase, different trends could be observed depending on the nature of the mortar and the presence of additives, with the addition of crushed brick powder (CBP) proving to be particular.

The LSC mortars (Lime; Sand; Crushed-Brick-Powder) showed a consistent increase in weight during the test, in contrast to the mortars that were not mixed with CBP. This can be explained by the previously observed rather high TOP and water retention rate values (Tab.14). The addition of selected additives was able to inhibit freeze-thaw effects to a greater or lesser extent. The lower weight variation observed with the added CBP suggests that the additives are effective in reducing the effects of the freeze-thawing cycles, particularly LSC_CL05, LSC_D05, and LSC_CS025 achieved the most promising results (Fig.41). The LS mortars, without CBP, showed a much smaller weight variation throughout the test, but the presence of additives seems to have results that are not entirely clear, maintaining a rather uniform behavior, at least up to cycle No. 8. In conclusion, the presence of additives appears to mitigate frost damage in the case of brick dust samples, while LS samples exhibited more uniform weight variation in the added mortars.

By the conclusion of the freeze-thaw cycles, the majority of the samples exhibited slight crushing without significant damage, with the top layer of the LSC_D05 and LS_D05 samples detaching, as illustrated in

Figure 42. The following graphs show the percentage variation of weight in respect to t_0 plotted with the succession of freeze-thaw cycles (The weight is recorded after each freezing period). As can be seen from Fig.40 and Fig.41, due to the weight change trends during the freeze-thaw cycles, the graphs contain a break for ease of reading. In both the lime and sand (LS) and the lime, sand and CBP (Crushed Brick Powder) (LSC) samples, however, a similar trend can be seen by the 4th cycle, where the samples increased their weight after three consecutive cycles of reduction. This can be explained by the accumulation of ice within the sample due to the increasing porosity.

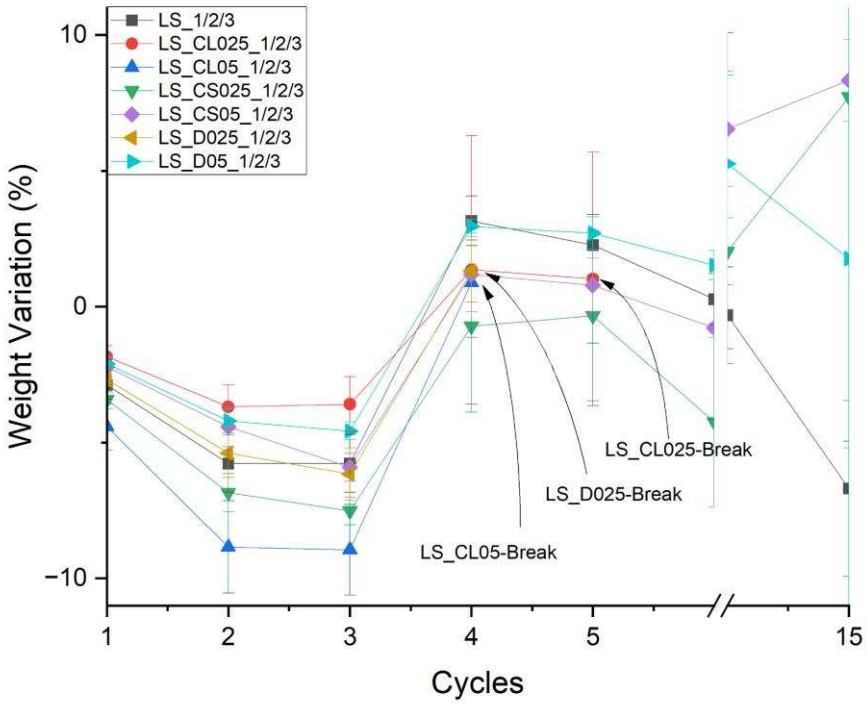

Figure 40 Weight Variation vs Cycles sustained by LS samples 2nd series, weight variation ($(M_i-M_0)/M_0 * 100$) in comparison with the succession of freeze-thaw cycles.

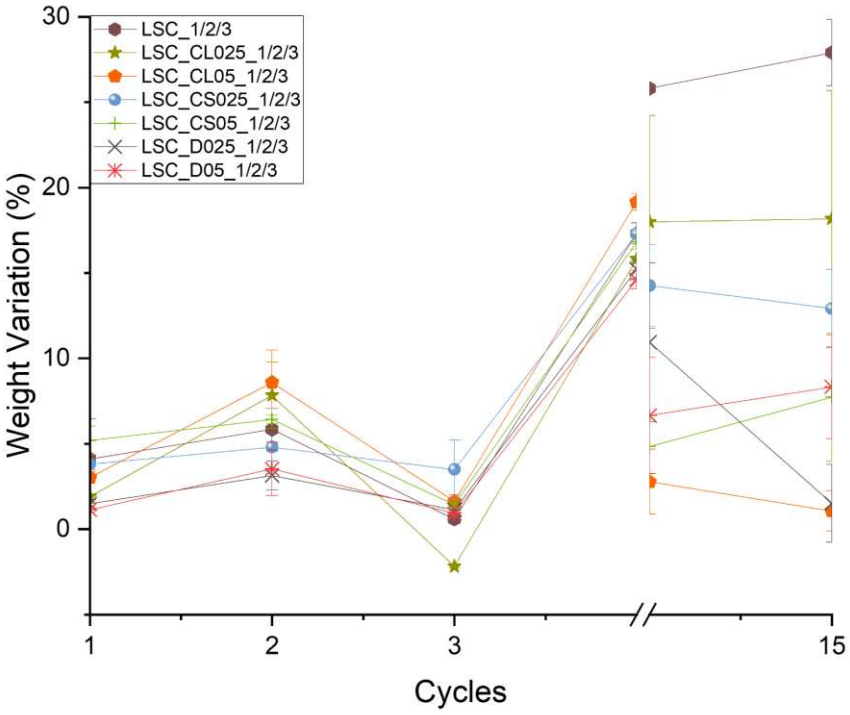

Figure 41 Weight Variation vs Cycles sustained by LSC samples 2nd series.

Figure 42 On the right, LSC_D05 sample before (top-left) and after undergoing freeze-thaw cycles; On the left, LS_D05 sample before (top-left) and after undergoing freeze-thaw cycles.

During the analysis of sample series number three, featuring lime and magnesian lime mixed with different amounts of metakaolin, consistent results were obtained. As can be seen from the table below (Tab.23), not all samples made it through to the end of the test, as they suffered excessive breakage during freeze-thaw

cycles, making it impossible to continue the test. It could be seen that the presence of metakaolin in the formulation is the main reason for the frost resistance. In fact, all samples mixed with metakaolin, regardless of quantity, successfully reached the end of the 14 cycles. This was with the sole exceptions of L09S1M01 and L08S1M02, which broke at the 10th cycle. The weight variations required a distinction between mortars based on traditional and magnesian lime. The former shows a more uniform trend, where the increase of aggregate in the formula contributes to limiting the weight variation during the test (Fig.43). Magnesian mortars, on the other hand, demonstrated two peculiar behaviors, namely, a linear trend of almost perfect weight variation (Fig.44) and a clear branching into two large groups. The mortars with a 1:1 lime-sand ratio (ML1S1; ML09S1M01; ML08S1M02; ML07S1M03) and ML09S2M01 proved to be more susceptible in the first phase to water absorption, which was done as per norm: EN12371 in order to get the samples ready for the first freezing cycle. Except for sample ML09S2M01, the presence of metakaolin, combined with higher sand ratios (1:2; 1:3) determined in the samples a significant resistance to the frost-thaw test, which showed minor damage, without fractures or disintegration.

Table 23 Cycles sustained by series 3rd samples.

Mock-up ID	**Average total Freeze-Thaw cycles sustained**
L1S1_1/2/3	1±0
L09S1M01_1/2/3	10±0
L08S1M02_1/2/3	10±0
L07S1M03_1/2/3	15±0
L1S2_1/2/3	1±0
L09S2M01_1/2/3	15±0
L08S2M02_1/2/3	15±0
L07S2M03_1/2/3	15±0
L1S3_1/2/3	1±0
L09S3M01_1/2/3	15±0
L08S3M02_1/2/3	15±0

L07S3M03_1/2/3	15±0
ML1S1_1/2/3	1±0
ML09S1M01_1/2/3	15±0
ML08S1M02_1/2/3	15±0
ML07S1M03_1/2/3	15±0
ML1S2_1/2/3	1±0
ML09S2M01_1/2/3	15±0
ML08S2M02_1/2/3	15±0
ML07S2M03_1/2/3	15±0
ML1S3_1/2/3	1±0
ML09S3M01_1/2/3	15±0
ML08S3M02_1/2/3	15±0
ML07S3M03_1/2/3	15±0

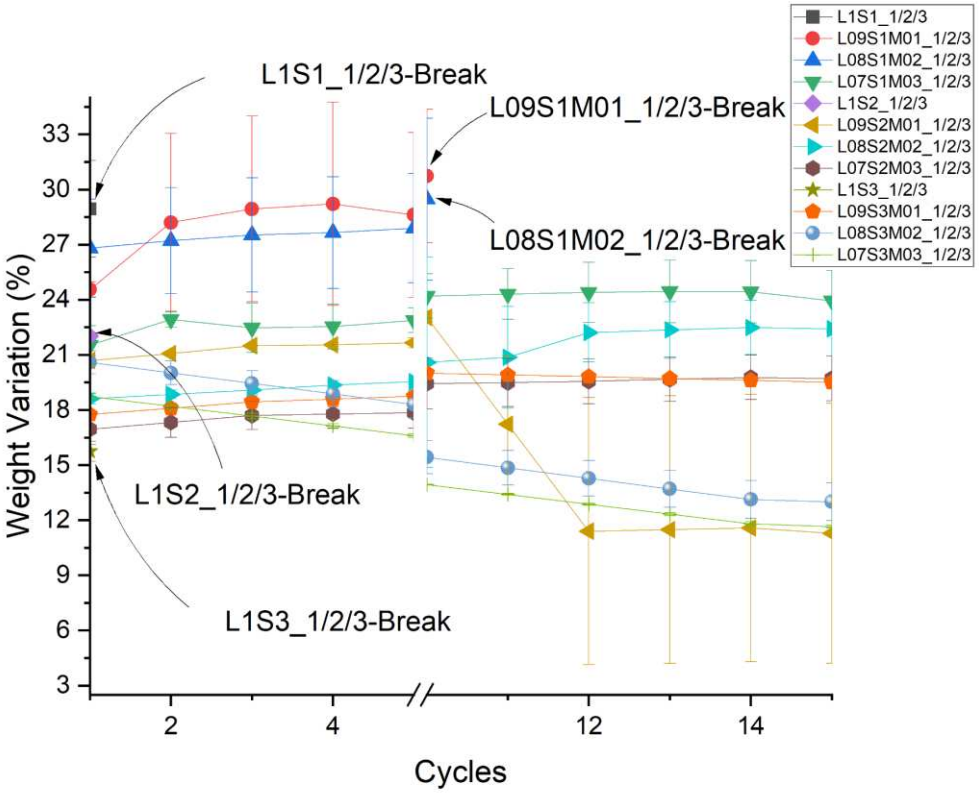

Figure 43 Weight Variation vs Cycles sustained by L samples 3rd series.

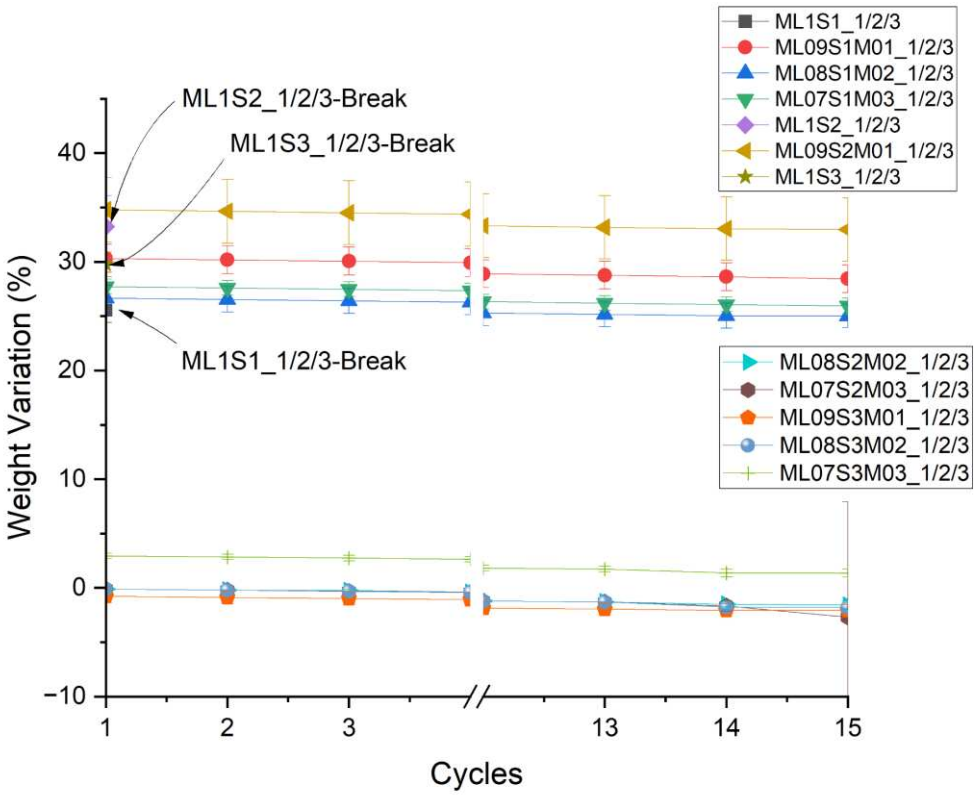

Figure 44 Weight Variation vs Cycles sustained by ML samples 3rd series.

The fourth set is to be considered a revision of previously analysed formulations and the testing of some new proposals with the objective of hypothetical application in a high humidity environment. Specifically, a new additional aggregant (HGMS- Hollow glass microspheres) will be introduced and the potential of a new type of hydraulic lime from Grigolin S.p.A (NHL Palladio, Tab.1) will be tested.

As can be seen from Tab.24, a few samples failed to withstand the freeze-thaw cycles. The combination of lime/magnesian lime and CBP(Crushed Brick Powder) (L1S1.7C0.3, ML1S1.7C0.3, L1S0.7C0.3) was not able to sustain the stress from the test and completely disintegrated during the water thawing phase in the second, fourth and first cycle, respectively. The remaining samples featuring "Palladio" hydraulic mortar and NHL mixed with HGMS survived until the 14th cycle, showing minor and negligible damage to the sample surface. The presence of additives such as Chitosan and DTPMP, in combination with NHL lime and hollow glass microspheres (NHL1S3HGMSCL, NHL1S3HGMSD) influenced the behavior of the sample towards the test. While DTPMP caused consistent weight variations, Chitosan, with a lower TOP (Tab.16) than the pure sample (NHL1S3HGMS) and DTPMP (NHL1S3HGMSD), showed a very low weight variation throughout the test (Fig.45). These results, however, confirm some of the previous assessments. Taking into account series number two and three in particular, we can confirm that already the type of lime at the basis of the formulation greatly influences the future resistance of the mortar to the agents of degradation. From the second series, in which natural hydraulic lime was used but for simplicity was reported only as "L" in the sample code, samples mixed with CBP showed a similar trend to NHL1S0.7C0.3 (although they are different in the ratio of lime: sand).

Table 24 Cycles sustained by series 4th samples.

Mock-up ID	**Average total Freeze-Thaw cycles sustained**
L1S1.7C0.3_1/2/3	2±0
ML1S1.7C0.3_1/2/3	4±1
L1S0.7C0.3_1/2/3	1±0
NHL1S0.7C0.3_1/2/3	15±0
PL1S3_1/2/3	15±0

NHL1S3HGMS_1/2/3	15±0
NHL1S3HGMSD_1/2/3	15±0
NHL1S3HGMSCL_1/2/3	15±0

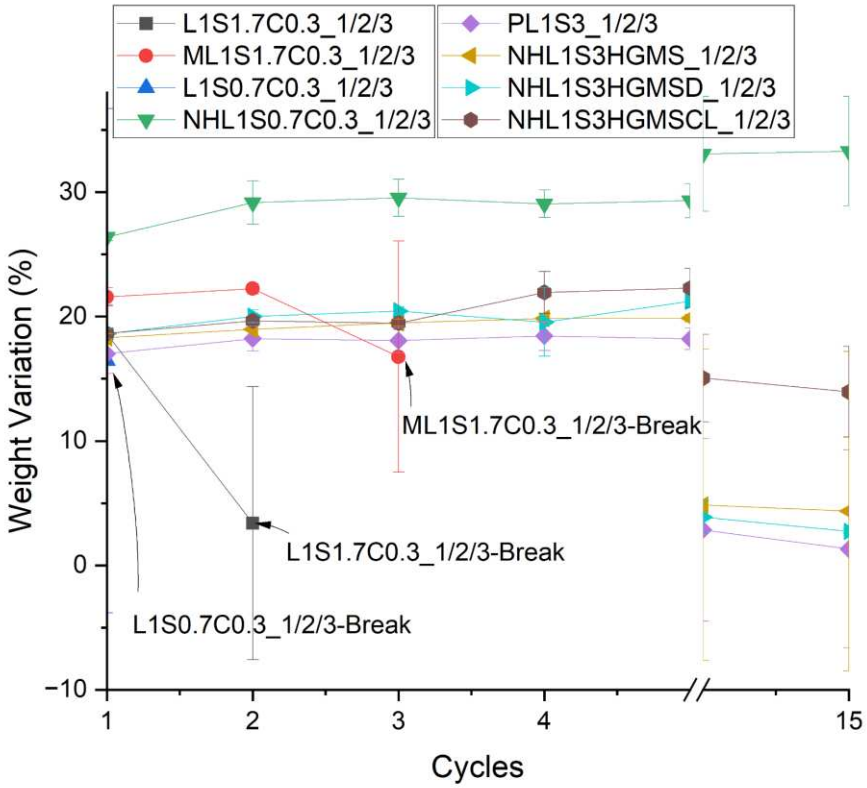

Figure 45 Weight Variation vs Cycles sustained by samples of 4th series.

Observing the lime swatches of the fifth series, we were able to describe different behaviors towards the test (Tab.25). The first crucial element is that none of the samples was able to withstand the damage from the frost-melt cycles until the end of the test, reaching a maximum of 13 out of 15 cycles. Moreover, formulations featuring slaked lime, sand and CBP (SLSC) showed a variable trend, without there being a determining factor for the breakage at the 13th, 4th, and 7th cycles of the single specimen replicas. This can be explained by the tendency of CBP, present in SLS"C" to make samples susceptible to water absorption; however as met in the second series, this should not contribute to the low resistance to the test, the reason why this suggests a not complete maturation of the samples. Nevertheless, looking at Fig.46 it is possible to

see that the variation in weight of the formulation of slaked lime, sand and HGMS (SLSH) is the most contained of all the fifth series, which adds up to the almost uniform trend in the graph.

Table 25 Cycles sustained by series 5th samples.

Mock-up ID	Average total Freeze-Thaw cycles sustained
SLS_1/2/3	13±1
SLSH_1/2/3	13±0
SLSC_1/2/3	8±5
SLSCH_1/2/3	13±0

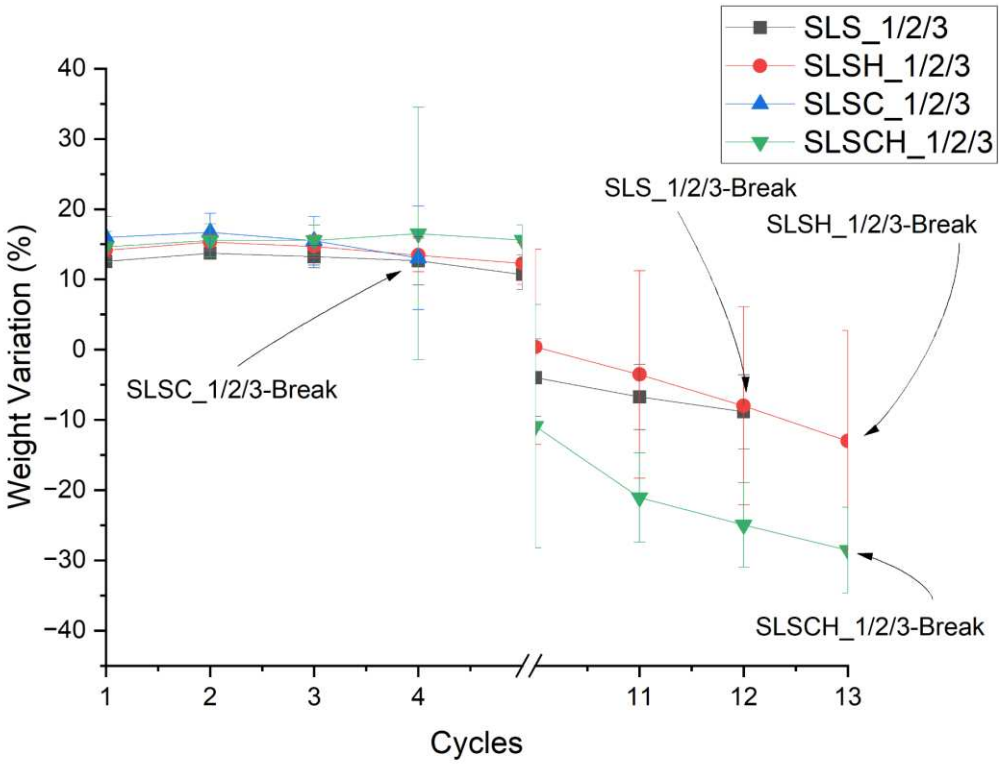

Figure 46 Weight Variation vs Cycles sustained by samples of 5th series.

3.3.2 Soluble Salt Resistance

Saline solutions inside the porous material can damage them in a significant way and compromise the durability of the conservative interventions. This test, as for the Freeze-Thaw test, determines the resistance to the action of soluble salts. It consists of several cycles as the previous and alternates cycles of immersion of the test sample in a saline solution of Na_2SO_4 at 14% then proceeds to the drying phase in the oven until constant weight. As with the formation of ice crystals, salt crystals exert pressure along the walls of the pores, reducing their physical-mechanical resistance and producing fractures, breakages, disintegration, efflorescences, and sub-efflorescences[45,107-114,118-119]. As can be seen from the first series of samples E and RMC, respectively composed by Mapei Eco-Risana, Rinzaffo and MC (made by NHL, Eco-pozzolan, special additives and microfibers, Tab.1) the behavior towards salt cycles showed for both formulations a nearly linear trend in the early stages and then differentiated as the test continued (Fig.47,48). In the case of samples based on Eco-Risana "E" and Rinzaffo-MC "RMC", the presence of chitosan in a non-liquid form produced a linear trend during the test, both in weight variation and damage sustained by the samples themselves, In particular in the case of Eco-Risana, E_CS05, and E_CS1, the samples immediately showed a weight reduction while the samples RMC_CS05 and RMC_CS1 accumulated weight and disintegrated around the eighth cycle (Tab.26). Sodium Iron Cyanide does not appear to have shown any particular effects in comparison with samples containing basic formulations E and RMC, except in the case of RMC_FNCN05, where the weight variations were contained at the beginning, and caused substantial weight loss in the sample from the seventh cycle onwards, induced by efflorescence, fracture, and disintegration. In the case of DTPMP, more consistent results were obtained for samples labeled with E. The product appears to have limited the weight loss of the sample due to damage induced by the absorption of soluble salts, probably due to the partial hydrophobization of the sample as indicated by the the influence of DTPMP on the salt crystallization process[113,192-194]. Although none of the samples passed the test to the end, these results already provide important indications for future applications of salt inhibitors[8].

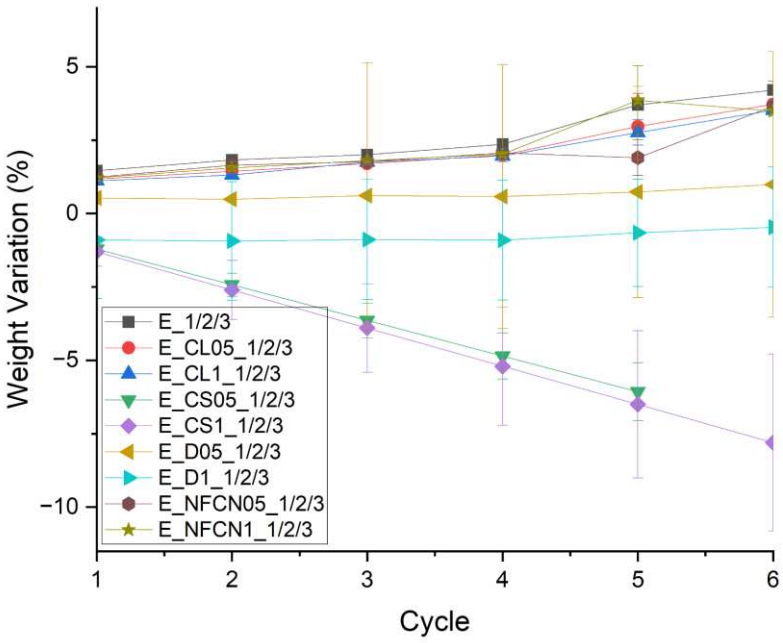

Figure 47 Weight Variation vs Saline Cycles sustained by E_samples of 1st series.

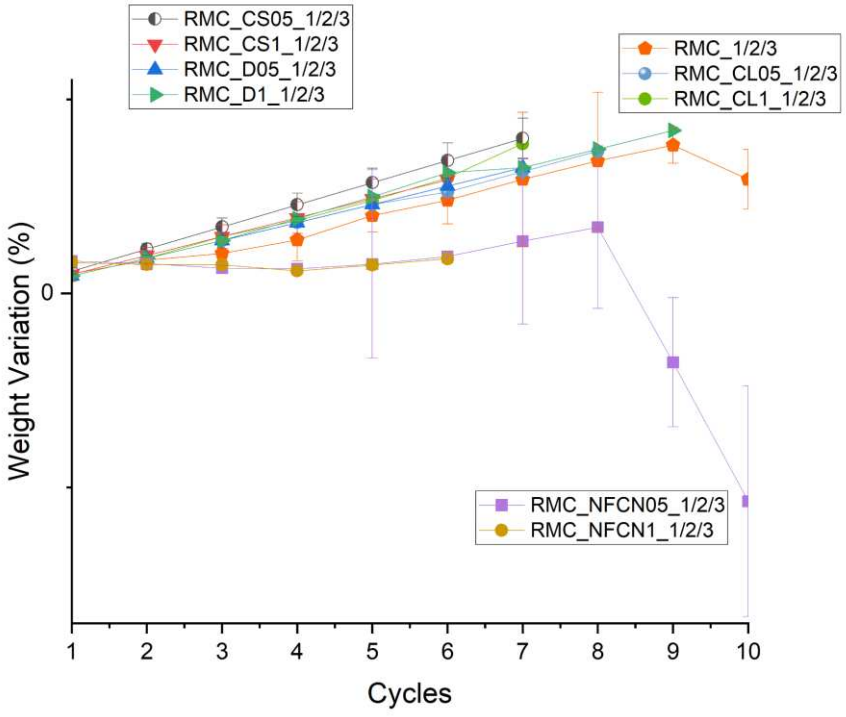

Figure 48 Weight Variation vs Saline Cycles sustained by RMC_samples of 1st series.

Table 26 Total average saline cycles sustained by series 1st.

Mock-up ID	Average total cycles sustained
E_1/2/3	7±0
E_CL05_1/2/3	10±2
E_CL1_1/2/3	7±1
E_CS05_1/2/3	7±1
E_CS1_1/2/3	8±1
E_D05_1/2/3	7±0
E_D1_1/2/3	8±1
E_NFCN05_1/2/3	7±0
E_NFCN1_1/2/3	7±1
RMC_1/2/3	11±0
RMC_CL05_1/2/3	10±1
RMC_CL1_1/2/3	10±2
RMC_CS05_1/2/3	8±1
RMC_CS1_1/2/3	8±1
RMC_D05_1/2/3	10±2
RMC_D1_1/2/3	10±1
RMC_NFCN05_1/2/3	11±1
RMC_NFCN1_1/2/3	8±1

During the first phase of the salt cycles, the LS mortar samples showed great resistance, so much so that they showed a variation of weight almost zero (Fig.49,50). In contrast, samples mixed with CBP, probably due to the higher TOP values induced by the added powder, absorbed a larger amount of saline solution and this may be the cause of the following trend. Not all the samples were able to withstand the salt cycles

until the end of the test, as was the case with LS_D025 and LSCL_025 which, seriously damaged by the efflorescence, ended the test at the 6th and 8th cycles respectively (Fig.51). As can be seen from Fig.49 at the end of the salt cycles, the total weight variation of the LS samples was more consistent than the LSC samples, the former showing a gradual trend, where there seems to be no distinction between samples treated with inhibitors and not, which leads to an ever greater weight reduction (and therefore mass loss). The explanation for this alternating behaviour of weight gain and loss refers to a typical dynamic due to the absorption of soluble salts. Due to the deposition of salt within the pores, the pores become saturated and as a result of the subsequent crystallisation they suffer damage. This rupture of pores, starting with the smallest ones, leads to an increase in the total porosity of the sample, which then becomes more susceptible to the absorption of more salt solution. This dynamic is repeated, causing the sample to absorb more and more salt solution and consequently suffer more and more damage until it breaks. In both cases, the alternating values of weight variation (not shown due to break inserted for better reading of the graph) correspond respectively to weighing on samples that have retained a large quantity of salts, which, remaining within the porous matrix, have increased the overall weight of the sample, which will subsequently undergo a considerable reduction in weight due to the rupture of the pores and therefore the loss of material during the phase of immersion in saline solution.

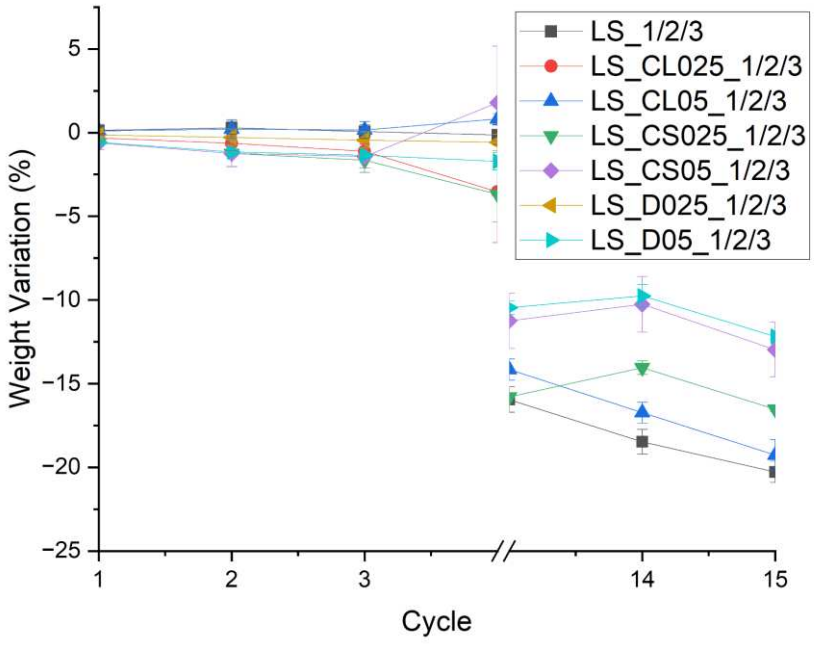

Figure 49 Weight Variation vs Saline Cycles sustained by LS_samples of 2nd series.

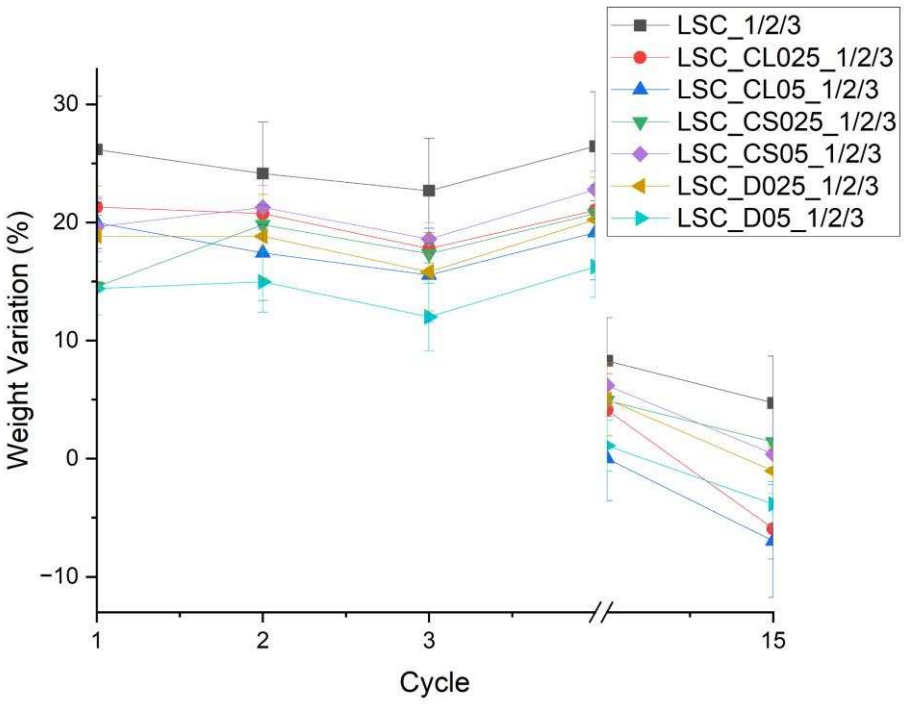

Figure 50 Weight Variation vs Saline Cycles sustained by LSC_samples of 2nd series.

Table 27 Total average saline cycles sustained by series 2nd.

Mock-up ID	Average total cycles sustained
LS_1/2/3	14±0
LS_CL025_1/2/3	14±0
LS_CL05_1/2/3	14±0
LS_CS025_1/2/3	14±0
LS_CS05_1/2/3	14±0
LS_D025_1/2/3	6±0
LS_D05_1/2/3	14±0
LSC_1/2/3	14±0
LSC_CL025_1/2/3	8±0
LSC_CL05_1/2/3	6±0
LSC_CS025_1/2/3	14±0
LSC_CS05_1/2/3	14±0

LSC_D025_1/2/3	14±0
LSC_D05_1/2/3	14±0

Figure 51 Samples LSC_D05 before and after salt cycles.

Although there were remarkable results with the addition of metakaolin in the samples to counter the effect of frost-thaw, the same cannot be said for the resistance to soluble salts. As it is shown by Tab.28, none of the samples could pass the test to the end. Almost all the mortars, both traditional lime and magnesium-based, suffered substantial damage during the cycles so the analysis was interrupted around the 6th, and 7th cycle (Fig.52). Despite the low resistance shown, a trend can be seen in both types of mortar. This characteristic should be attributed to the fact that the base of these samples is not by themselves hydraulic as used in the second series. In fact, a mortar based on NHL lime not added with other elements other than sand was able to withstand the test until completion (LS in Tab.27), probably due to the chemical-physical properties given typical of its nature[9,98,195]. The presence of the different amounts of metakaolin does not seem to have influenced the behaviour of these samples, regardless of the type of mortar from which they are composed or the different lime:sand ratio. An increase in initial weight can be seen starting in both cases in Fig.53 from the very beginning, and then continuing to a more limited extent until the samples break. The function of metakaolin does not therefore appear to have influenced the resistance to soluble salts.

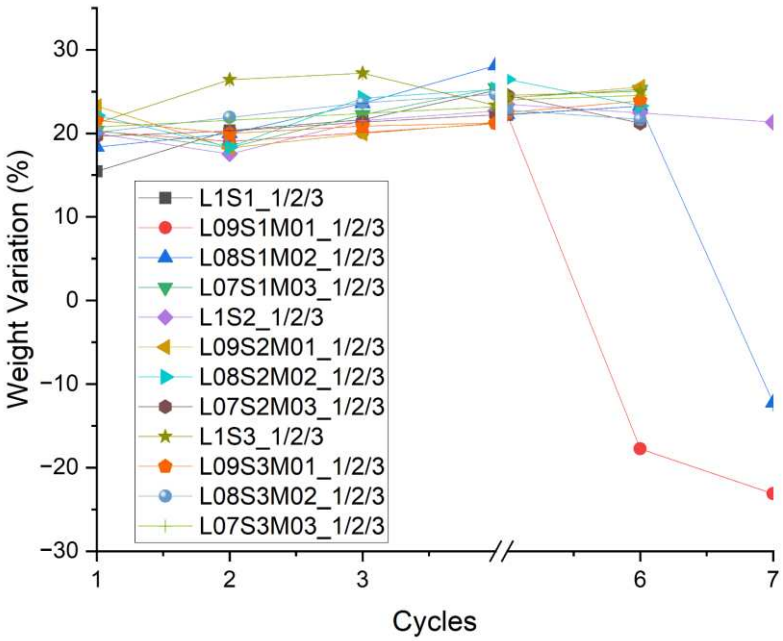

Figure 52 Weight Variation vs Saline Cycles sustained by LxSx_samples of 3rd series.

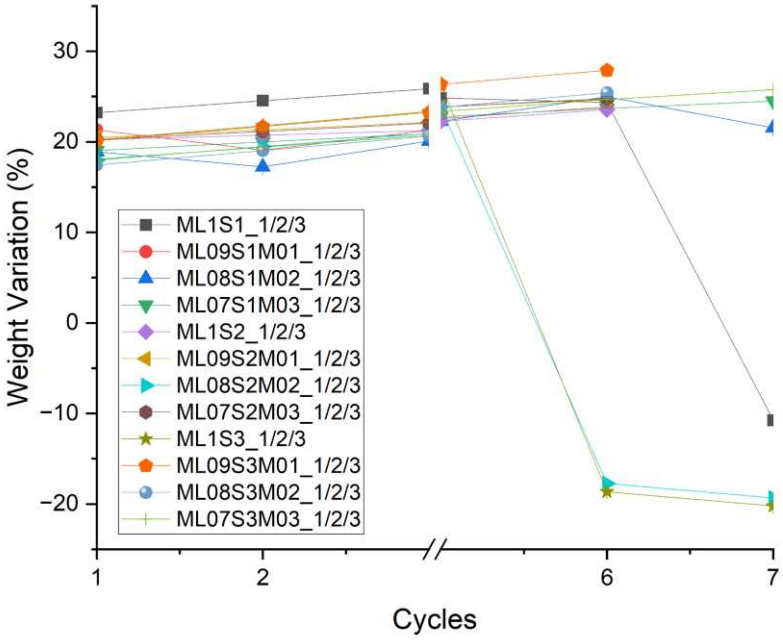

Figure 53 Weight Variation vs Saline Cycles sustained by MLxSx_samples of 3rd series.

Table 28 Total average saline cycles sustained by series 3rd.

Mock-up ID	Average total cycles sustained
L1S1_1/2/3	6±1,00
L09S1M01_1/2/3	7±1,00
L08S1M02_1/2/3	7±1,00
L07S1M03_1/2/3	6±0,00
L1S2_1/2/3	7±2,00
L09S2M01_1/2/3	6±1,00
L08S2M02_1/2/3	6±1,00
L07S2M03_1/2/3	6±0,00
L1S3_1/2/3	6±1,00
L09S3M01_1/2/3	6±0,00
L08S3M02_1/2/3	6±0,58
L07S3M03_1/2/3	6±0,58
ML1S1_1/2/3	7±1,15
ML09S1M01_1/2/3	6±0,58
ML08S1M02_1/2/3	7±0,58
ML07S1M03_1/2/3	7±0,58
ML1S2_1/2/3	6±0,00
ML09S2M01_1/2/3	6±0,00
ML08S2M02_1/2/3	7±0,58
ML07S2M03_1/2/3	6±0,00
ML1S3_1/2/3	7±1,00
ML09S3M01_1/2/3	6±0,58
ML08S3M02_1/2/3	6±0,58

ML07S3M03_1/2/3	7±1,15

As described above, the fourth series is characterized by elements with different formulations, thus limiting comparisons between results and composition (Tab.29). From the graph below (Fig.54) it can be seen that not all samples exhibited the same resistance to the action of soluble salts. In particular, NHL1S3HGMSCL has already been disintegrated in the second cycle. This abnormal behavior, given the already mentioned resistance of NHL mortar to the action of salts (and of the sample NHL1S0.7C0.3), could be explained by an anomaly in the maturation phase of the sample, where the components of sand HGMS and chitosan, have not effectively bonded (RESULTS OF PRESSURE). The behavior of NHL1S3HGMSD, in the same way, was probably caused by a poor interaction between the single components of the mortar. In particular, the untreated NHL1S3HGMS dough has indeed shown higher strength. Among the remaining samples, PL1S3 (made from Palladio natural hydraulic lime), and NHL1S0.7C0.3 (made with Lafarge natural hydraulic lime) showed more consistent results, with a change in weight almost negligible during the whole test until the samples broke. It was already noted by the third series that a natural non-hydraulic lime (LS Tab.28) could withstand about 5-6 total cycles of saline solution before breaking down. In this series, the fact that the sample of natural lime L1S1.7C0.3 (the same as LS), has withstood up to 11 cycles is a test of the strengthening properties of ground brick powder (CBP) on the physical characteristics of the mortars.

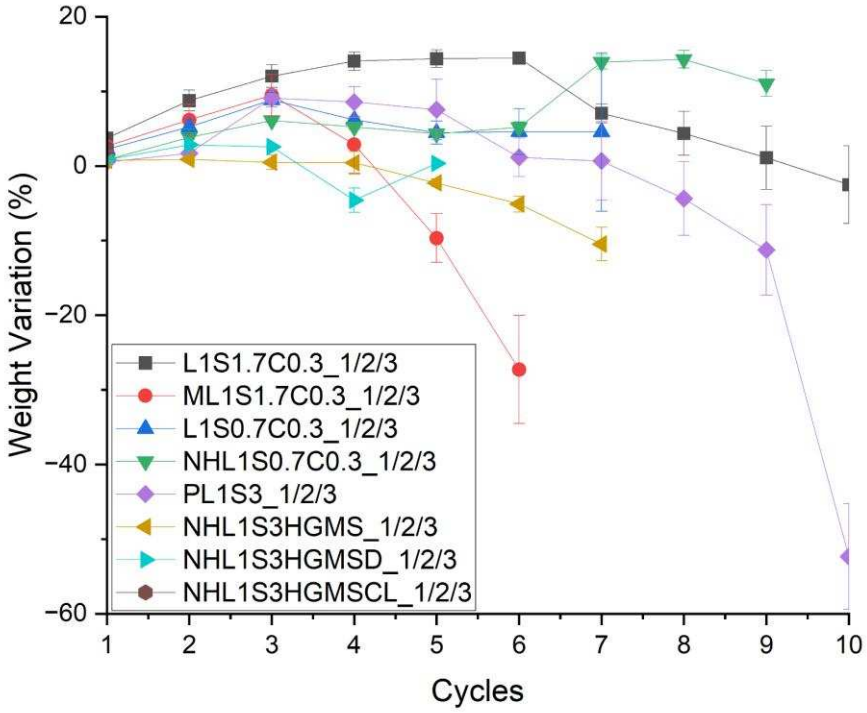

Figure 54 Weight Variation vs Saline Cycles sustained by samples of 4th series.

Table 29 Total average saline cycles sustained by series 4th.

Mock-up ID	Average total cycles sustained
L1S1.7C0.3_1/2/3	11±0
ML1S1.7C0.3_1/2/3	7±0
L1S0.7C0.3_1/2/3	9±1,15
NHL1S0.7C0.3_1/2/3	10±0,58
PL1S3_1/2/3	11±0
NHL1S3HGMS_1/2/3	8±0,58
NHL1S3HGMSD_1/2/3	6±6
NHL1S3HGMSCL_1/2/3	2±0

The fifth series, on the contrary, proposes a series of samples bound by the slaked lime base, possibly enriched by CBP or HGMS. It can be seen immediately that there is a uniform behavior on the part of the samples enriched with either of the two products mentioned above. Both the presence of hollow glass microspheres (SLSH, SLSCH) and crushed brick powder (SLSC, SLSCH) determine an initial spike in the graph that is successively canceled until the samples are broken (Fig.55). This initial weight gain may be due to the hydrophilic properties of CBP and HGMS, supported by the values of TOP, higher than that of the untreated sample SLS (Tab.17). Despite everything, none of the samples reached the end of the 14 salt cycles without undergoing complete disintegration. The samples which have been able to maintain structural integrity, albeit with a significant loss of weight, are those in which the hollow glass microspheres (SLSH, SLSCH) have been added. Here too the presence of cocciopesto seems to have confirmed the previous results, increasing the resistance to the effect of soluble salts in mortar. It is sufficient to note that SLS has reached 6 cycles total while SLSC 11. The same observations can be made for the addition of HGMS which seems to obtain the same properties to mortars treated with CBP.

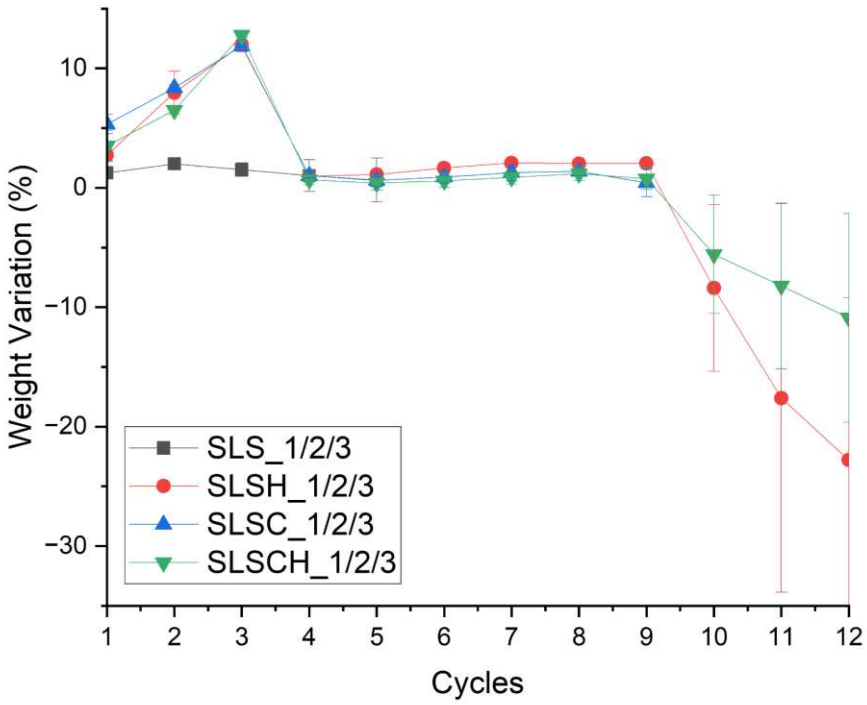

Figure 55 Weight Variation vs Saline Cycles sustained by samples of 5th series.

Table 30 Total average saline cycles sustained by series 5th.

Mock-up ID	Average total cycles sustained
SLS_1/2/3	6±0,58
SLSH_1/2/3	13±0,58
SLSC_1/2/3	11±1,53
SLSCH_1/2/3	13±0,58

Chapter 4. Discussion

In this chapter the analysis of the results illustrated in chapter 3 are reported. As there are many interconnected variables regarding the properties of the mortars developed, it was decided to organize this discussion by presenting the performance of Mapei premixed mortars and each lime-based product, reporting its potential and the shortcomings detected during the experimentation.

The focus of this project is the development of mortars for the architectural heritage and has resulted in the development of several formulations, the ultimate aim of which was to deal with different problems characteristic of the world of architectural buildings, first and foremost, the problem of soluble salts. To this perspective was added in parallel an in-depth study, from both a historical and experimental research point of view, of little-known mortar formulations, such as magnesian mortars and 'porcelain' mortars, cited for their marked durability against deterioration agents. In conclusion, the influence of hollow glass microspheres in mortars as an inert additive, used in painting to create breathable, light and moisture-resistant layers, was investigated.

To summarize, the research focused on several aspects:

- Study of the properties of fresh mortar, workability, spreading, specific gravity;
- Study of the physical properties of hardened mortar, with reference to its behavior with respect to capillary absorption and water vapor permeability;
- Study of the behavior of mortars against freezing/thawing;
- Evaluation of the mechanical properties of flexural and compressive modulus.
- Study of the behavior of mortars against crystallization of soluble salts;

One of the aspects we focused on the most was the relationship that mortars showed towards water, so we went to consider how a hypothetical masonry could primarily come into contact with the elements mainly responsible for damage due to frost and thaw and the crystallization of soluble salts. In order to assess the amount of potentially damaging material transport in the masonry matrix, two main parameters can be considered: the capillary absorption coefficient and water vapor permeability. The tendency of the sample to absorb water by capillarity without the application of external pressure, expressed by means of a

coefficient (CA), makes it possible to identify those mortars that will be more sensitive to this phenomenon. Permeability resistance (μ), on the other hand, is a dimensionless factor indicating how much greater the resistance to the diffusion of water vapor of a material is with respect to a volume of air of equal thickness (for air μ =1). We can define permeability as the extent to which a mortar will allow the wall substrate to 'breathe'. A good breathability of a protective layer guarantees the maintenance of structural integrity in the long term, limiting the accumulation of potentially damaging material at the interface between the masonry substrate and mortar[196-201]. From a sustainability point of view, investing in masonry and mortar that 'breathes' would not only improve the condition of the building but also improve quality of life and save energy. By maintaining optimal humidity levels and preventing the formation of mold, living spaces would be healthier and more comfortable by improving indoor air quality, and the reduced dependence on heating, ventilation and air conditioning systems would help minimize energy consumption[198].

Generally, one should aim for the development of mortars that tend to absorb and transport a limited volume of water and have a high breathability, which would allow the protective layer to easily dry itself and the substrate to which it is attached. It is therefore important to avoid selecting mortars that are not very breathable or insulating, as this would lead to the accumulation of soluble salts and water at the wall-mortar interface, subsequently causing detachments, cracks, efflorescence and undesirable bio-growth.

In this first part, we will evaluate the first two series, Mapei' and 'Cocciopesto', because of the nature of the formulations. What distinguishes the first formulations from the following ones lies in the fact that the soluble salt resistance was modify by adding the mixtures with specific compounds and is not an inherent property of the lime or inert material used. As these were introduced into the mix in the form of an aqueous solution, which replaced the mixing water, at different concentrations, the first effect evaluated was the influence on the rheology of the mixes. This aspect is fundamental since, however effective a mortar may be in counteracting saline action, an excessive softness or hardness of the mix and a lack of adhesion to the wall substrate would nullify its usefulness. Following this characteristic, Chitosan was the least performing product, both when added in liquid form and in dry flakes, as it negatively influenced the rheology of the fresh mortar, making it denser and pastier. This negative influence is evident in all samples between the first and second series, but especially in the samples E^{s1} and RMC^{s1} where uneven structures full of gaps were created (Fig.56) such that, in some cases among the Mapei samples RMC^{s1}, a detachment from the substrate of Rinzaffo (Fig.57).

Figure 56 Close up of sample E_CL1, it is noticeable the presence of voids in the sample matrix

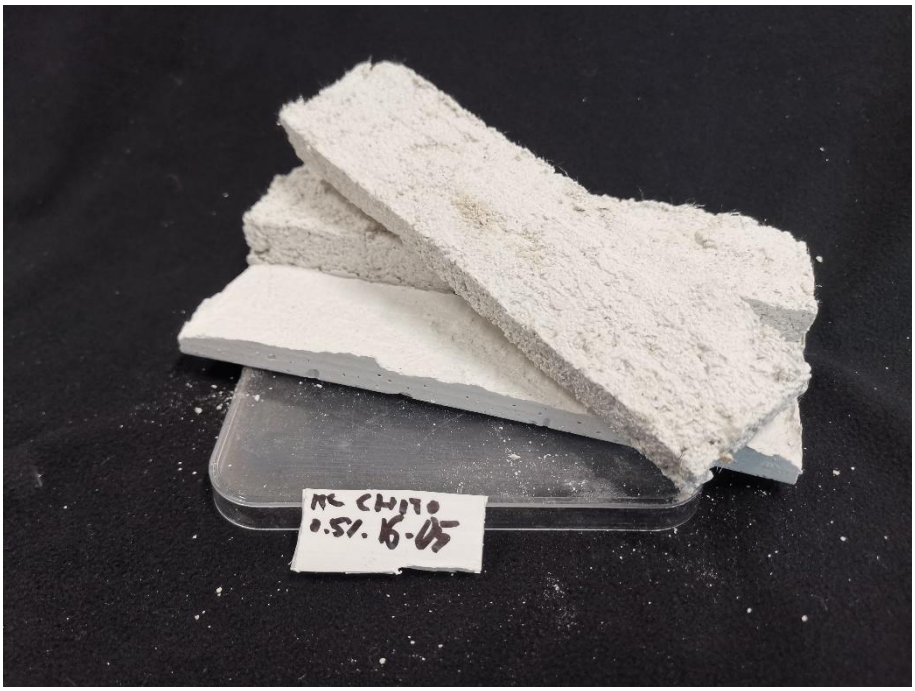

Figure 57 Parallelepiped sample of RMC_CL05 with detachment between parts of MC and Rinzaffo

As can be seen from the previous photos, the structures of the samples are in fact not as compact and uniform as one would expect but present voids in several places, an element that leaves doubts as to a hypothetical application on a large scale and that will influence subsequent tests, especially those of mechanical strength. The uncompact and airy nature of these samples is probably due to the coarse texture

of the dough obtained from premixed components and the chitosan, since the same structures do not reappear in the second series 'Cocciopesto' where instead the admixed samples present more uniform and void-free structures (Fig.58).

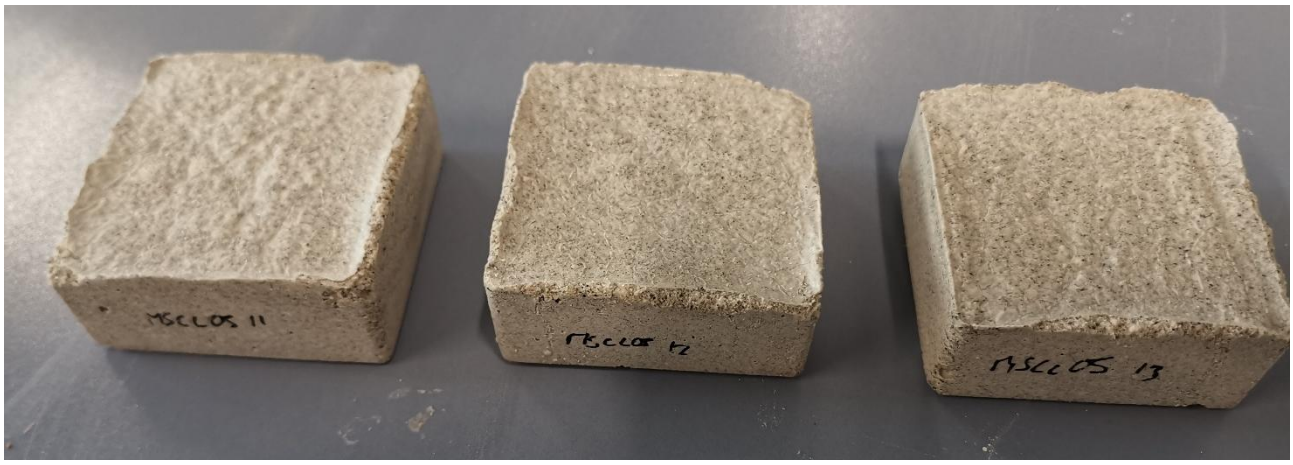

Figure 58 LSC_CL05 samples with uniform, void-free appearance

DTPMP, on the contrary, acted as a fluidifying agent even at low concentrations (Tab.9,10) to such an extent that the combinations with Mapei Eco-Risana^{s1}, RMC^{s1}, LS^{s2} and LSC^{s2} were somewhat complicated to handle within the time indicated for the setting phase, especially at higher concentrations. The mortars thus composed presented a soft, semi-liquid appearance with a high degree of brittleness and a slightly yellow-beige color, due to the shade of the DTPMP solution itself. In contrast to the Chitosan, these mortars presented much greater uniformity and the almost total absence of voids, creating well compacted and uniform looking samples, however, as in the previous cases shown in Fig.56,57, there were cases of detachment in the RMC^{s1} samples between the Rinzaffo and MC part (Fig.59) probably due to the partially hydrophobic nature of the DTPMP seen in Chapter 3, particularly in the capillary absorption tests (Tab.5).

Figure 59 Sample of RMC_D05 with detachment between parts of MC and Rinzaffo

On the contrary, the mortars whose aqueous mixing solution contained a percentage of potassium ferrocyanide (Tab.9) showed rather variable behavior depending on the type of premix. The combination with the product Eco-Risana, a breathable and dehumidifying product, led to a reduction in workability, similar to what was seen with Chitosan in liquid form. The foamy and light texture of the standard pre-mixed lime became denser and harder to spread, while in the case of the pre-mixed MC, it slightly improved the workability of the mixture, promoting a uniform and compact consistency that improved the pouring procedure in the moulds and subsequent levelling. In both formulations of the first series, the ferrocyanide kept the appearance and structures of the original mixes intact, without generating changes in colour or shape. The presence of most anti-salt additives therefore actively influenced the rheology of the slurries, something that had not been theorized during the design phase and which created minimal difficulties during the sample production phase.

Once the prescribed curing time had been completed, the analysis focused on the physical and mechanical properties of the mortars as planned. The study of the physical properties in relation to water (capillary absorption, water vapor permeability), provided results that were not entirely promising. The three anti-salt products did not have any particular effects on the formulations, except for the presence of chitosan

flakes, which instead seems to have made the mortars more susceptible to water absorption and thus to the forms of degradation linked to it. DTPMP also had variable results, where it showed a reduced water absorption therefore, it was able to give partial hydrophobicity to the samples to which it was added, particularly in the samples LS_D025 ^{s2}, LS_D05 ^{s2} (Tab.14). It is worth mentioning the effects that these products, with the exception of ferrocyanide, had on freeze-thaw resistance, data that can only be observed in the second series, however, and only with the products Chitosan and DTPMP. When considering the samples consisting of lime and sand (LS_series ^{s2}), variable effects were observed: The presence of chitosan flakes at both concentrations and DTPMP at a concentration of 05% allowed the samples to reach the end of the test almost intact, increasing their weight compared to the initial weight. The rest of the additives, i.e. Chitosan at both concentrations and DTPMP (0.25%) induced a lower strength in the samples, causing them to break down around the 4th-5th cycle. In the case of the specimens mixed with brick powder (LSC_series ^{s2}), the presence of the additives induced a higher resistance to freeze-thaw cycles, significantly reducing the weight change compared to the respective mix without additive (LSC_1/2/3 ^{s2}). These do not seem to have influenced in any way either the weight variation of the samples between the various cycles or the total number of cycles sustained, so much so that at the end of the tests, all the samples in the series showed only superficial damage.

Turning our attention to the salt crystallization resistance tests, and thus to the focal point of this study, the results unfortunately did not meet the expectations set. Chitosan, DTPMP and potassium ferrocyanide do not appear to have consistently increased the physical-mechanical properties of the first and second series samples to such an extent as to justify their addition to the mixing water. The number of cycles sustained and the condition of the samples at the end of the tests leave little room for further consideration. However, there are some exceptions such as the samples RMC_CS05 ^{s1}, RMC_CS1 ^{s1}, LSC_CL025 ^{s1} e LSC_CL05 ^{s1} which withstood fewer salt cycles than the reference sample RMC ^{s1} e E_CL05 ^{s1} which instead endured 3 more cycles than the reference sample E ^{s1}. From this it can be deduced that the presence of a thickening product such as chitosan is detrimental to the matrix of mortars, whether pre-mixed or not, as it reduces the compactness of the whole, being ineffective in counteracting salt crystals growth within the pores. Since it is now known that a relationship exists between porosity and mechanical resistance of the porous structures of mortars rather interesting results had been expected from the mechanical strength tests[202-206]. If we consider the tables of the compressive and flexural strength moduli of the first two series of samples (Tab.18,19), we can see that the effects of the anti-salt products are rather limited in the case of

pre-mixed mortars. The samples consisting of Mapei Eco-Risana (E^{s1}) reacted negatively to the products Chitosan, DTPMP and ferrocyanide, that worsened their performance in both compression and flexural moduli. On the contrary, those consisting of Mapei Rinzaffo+MC (RMC^{s1}) improved from the presence of all the products, particularly in the higher concentrations, except for DTPMP which decreased the strength of both modules. The difference in these results is probably due to the nature of the pre-mixed mortars themselves, which generated an improvement in the case of the Mapei Rinzaffo+MC (RMC^{s1}) given their inherently more solid and compact structure than the lightweight and aerated Mapei Eco-Risana (E^{s1}). If, on the other hand, one looks at the data of the same test on the second series, i.e. on non-packed mortars, the results are slightly different. Overall, a modest improvement in the mechanical properties can be noted, particularly in the presence of the chitosan in liquid and flake form, with the exception, however, of the concentration in flakes at 0.25% (LS_CS025, LSC_CS025), which resulted in a minor or almost non-existent increase in the compressive and flexural moduli, without any apparent motivation. It can also be assumed that the choice to reduce the concentration of the additives in the mixing solutions would not have led to different results in the first series. In fact, the nature of pre-mixed products makes it difficult to organize possible improvements from a formula point of view, which is why series 1 was considered as a basis on which to organize subsequent formulae. Taking into consideration the data obtained, we can therefore conclude that Chitosan, DTPMP, and Potassium Ferrocyanide are not an entirely suitable choice for limiting the damage caused by soluble salts nor for improving mortars in their overall performance other than in their purely mechanical properties. The variable behavior of the samples and the uncertainty as to the real efficacy of anti-salts in mortar matrices meant that this approach to mortars mixed with an anti-salt solution was abandoned in favor of new perspectives. One of the questions posed in the post-production stages, and which led to the emergence of the subsequent series, was the long-term efficacy of anti-salt products. If one considers in particular the nature of how salt inhibitors and salt modifiers work, it is possible to assume that the addition of a product within a mortar, assuming that it does not change during the hardening and maturation phase, has a temporary rather than a lasting effect. On the other hand, the applications of this type of product are mostly oriented towards brushing the surface to be cleaned, or bundling in special poultices to clean masonry surfaces should they need it, rather than keeping efflorescence damage to a minimum.

Following this, the project focused on the rediscovery and reworking of two ancient and little-known types of mortar, in particular, the properties of metakaolin as a pozzolanic addition to traditional lime and

magnesian lime. The properties of metakaolin are well known, especially in its use as an additive to Portland cement, but documentation for traditional lime and even more so for magnesian lime is lacking[207-208]. The third series 'Metakaolin' consists of traditional and magnesian lime-based mortars with varying lime/sand ratios and varying amounts of metakaolin, used as a partial substitute for lime. According to references in the scarce bibliography[85-88]. An attempt was made to recreate the ancient formulations of mortars with extraordinary physical and chemical properties and innate durability. No noteworthy differences were found when analyzing the rheological appearance of the fresh mortars (Ch.2.5.1), with the exception of the magnesium lime mixtures, which appeared denser and more adhesive than the traditional ones, making them very useful for application on sloping surfaces (Fig.60).

Figure 60 Evaluation of fresh mortar workability on tilted surface

Although the samples were studied during the course of the curing phase by means of XRD analysis, no notable preferential patterns or peaks could be emphasized, and no relevant conclusions regarding the presence of metakaolin emerged on the basis of the different concentrations. The same about their behavior with water, both capillary absorption and water vapor permeability of lime and magnesian- lime was found to be similar. The compression test gave good results for both formulations in which metakaolin was added.

The presence of metakaolin positively influenced not only the compressive strength modulus of the mortars but also the resistance to freeze/thaw cycles, making the mortars more resistant and limited to minor damage. Unfortunately, the same cannot be said about the resistance to crystallization of soluble salts; in fact, the formulations of the third series (traditional and magnesian lime added with metakaolin), regardless of composition, suffered such a damage that the it was not possible to reach 15 crystallization-immersion cycles, the test was stopped prematurely due to cubes crumbling (Fig.60). Behind this phenomenon, the possibility of incomplete curing was ruled out, as all samples were stored in the same place and for a sufficient period of time to develop optimal physical and mechanical characteristics.

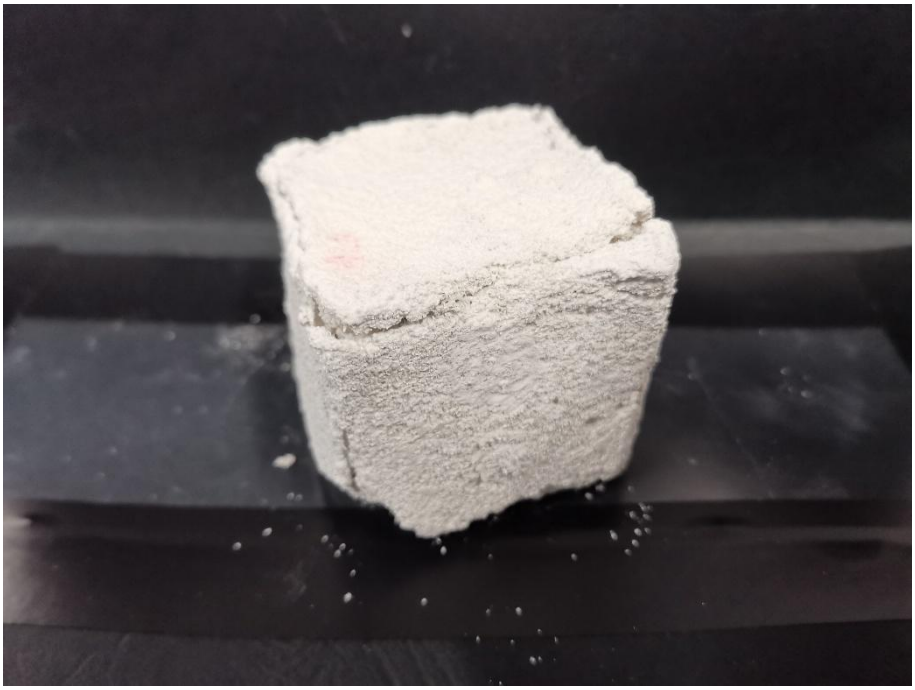

Figure 60 Sample L1S1 just after the 4th cycle

Although this sensitivity to salts may appear to be a characteristic of these formulations, historical information regarding porcelain mortars suggests that they are highly resistant to the saline environment, able to withstand salt without exhibiting any particular damage over the years. It is worth mentioning that for the project, the reproduction of these mortars was deprived of the alum component, on which there was no certainty of effectiveness, using only metakaolin. It is therefore possible that the presence of alum promotes an increase in resistance to the action of salts, but this will be the subject of future studies and research in order to determine the range of its effects and the best way to incorporate it.

As a further study element, this project implemented the addition of glass microspheres in the mortar matrix, to improve its performance in a wet environment. First and foremost, it was noted that this inert material produces mixes that are easy to work, frothy, and improve the compactness and uniformity of the whole, which resulted in a reduction in total open porosity. Very pleasingly, it has been noted that the presence of the microspheres also reduces the medium specific weight and increases the permeability to water vapor, resulting in lighter and more breathable mortar layers that allow the underlying masonry to breathe (Tab.16,17). These mortars also demonstrate good resistance to freeze/thaw and salt cycles, but not optimal, forcing the test to stop two cycles earlier than expected. Overall, the mortars suffered uniform weight reductions during the progression of each test, ending in extremely damaged rather than pulverized samples (Tab.25,30). A weak aspect of these formulations is certainly the area of mechanical strength. As can be seen from Tab.22, which shows a variable behavior of the flexural modulus, increasing only in the presence of CPB (SLSCH^{s5}), and a rather substantial reduction in that of compression up to 46%. In conclusion, this Project was able to illustrate a wide selection of materials including limes, sands, and additives in a complex series of formulations aimed at protecting the environment and safeguarding architectural heritage. Various aspects were explored, including composition, physical-mechanical properties and frost/thaw resistance capabilities, and first and foremost, resistance to crystallization of soluble salts. The potential of several components including metakaolin and hollow glass microspheres has been studied and demonstrated. Porcelain mortars could be an excellent starting point for future studies, this time considering more in-depth research and the inclusion of alum as a part of the production.

5. Conclusions

This Project had the opportunity to deepen and illustrate the production phases of mortars, the study and research of their composition, and their evaluation in the laboratory, with the aim of identifying formulations that could be useful in the field of Architectural Cultural Heritage. Italy and Europe are characterized by a wide variety of architectural elements that have been or are currently the subject of studies and research aimed at their maintenance and preservation. A mortar compatible with historic masonry must be breathable, porous, made from materials similar to the original (be them air lime or NHL etc.) and easily removable or reversible, if possible. These characteristics can be identified with the different physical-mechanical properties already discussed in Ch.3 and Ch.4 and can be found in the table below (Tab.31), drawn up with the aim of providing a general guideline for the hypothetical application of the individual formulations. What has become clear from this project is the importance of the choice of starting materials with which to develop a particular mortar. The type of lime, the relationship with any type of binder, and the presence of certain additives constitute highly characterizing elements that will influence not only the characteristics of the fresh mortar during processing, but especially those of the hardened mortar. Specifically, various properties have been identified to describe these porous building materials, which can also act as protection for the brickwork of the building, preventing most damage due to deterioration agents. Pre-mixed mortars were a great help in being able to observe and obtain initial information, without excessive preparation time, on the main methods of using and producing mortars. Thanks to this, different types of mortars were developed and produced from the selection of materials according to the desired characteristics of the hardened product. Mortars based on lime, sand, and earthenware were studied, the performance of which demonstrated an excellent versatility of formulation, also in resistance to freeze-thaw and salt crystallization. Another highlight of this thesis was the study of porcelain and magnesian mortars, also aimed at drawing the attention of future research to these types of mortars, of which there is a scarce and incomplete bibliography, but which are cited for their durability over time against frost and soluble salts. Although the results of the latter were not further investigated, lacking the study of the alum element in the alleged ancient formulation, what could be seen provided an excellent starting point for further developments. The same can be said for the addition of HGMS to the mortar mix to give new characteristics to the mortars, including breathability and resistance to humidity, properties similar to those obtained today when the same microspheres are added to interior paints. The

wide variety of formulations analyzed during the three years of the project has therefore allowed us to explore topics that are daily discussed in the field of Cultural Heritage and that should also be fundamental in today's building industry, helping the development of an innovative point of view based on aspects of durability and environmental and economic sustainability.

Table 31 Overview of main mortars properties in relation to building sector. Composition= weight ratio; Sd=breathability expressed as Sd(m); TOP= Total open porosity (%)**; CS= mechanical compressive strength (MPa)***; FTR= Freeze-thaw resistance, SR=Salt Resistance (Cycles sustained)****.*

Sample	Composition	Sd*	TOP**	CS***		FTR****		SR****	
E_1/2/3	EcoRisana(Mapei)	0,14	24,5	4,3	4	ND	ND	7	M
E_CL05_1/2/3	EcoRisana(Mapei)_LiquidChitosan(0,5%)	0,34	17,5	12,1	6	ND	ND	10	H
E_CL1_1/2/3	EcoRisana(Mapei)_LiquidChitosan(1%)	0,33	20,6	14,2	6	ND	ND	7	M
E_CS05_1/2/3	EcoRisana(Mapei)_SolidChitosan(0,5%)	0,25	19,4	5,01	5	ND	ND	7	M
E_CS1_1/2/3	EcoRisana(Mapei)_SolidChitosan(1%)	0,39	19,7	11	6	ND	ND	8	M
E_D05_1/2/3	EcoRisana(Mapei)_DTPMP(0,5%)	0,27	19,7	5,11	5	ND	ND	7	M
E_D1_1/2/3	EcoRisana(Mapei)_DTPMP(1%)	0,33	21,1	6,68	5	ND	ND	8	M
E_NFCN05_1/2/3	EcoRisana(Mapei)_Na4Fe(CN)6·H_2O(0,5%)	~~0,5~~	23,0	14,5	6	ND	ND	7	M
E_NFCN1_1/2/3	EcoRisana(Mapei)_Na4Fe(CN)6·H_2O(1%)	0,44	20,3	6,53	5	ND	ND	7	M
RMC_1/2/3	RinzaffoMC(Mapei)	0,19	12,3	11,4	6	ND	ND	11	H
RMC_CL05_1/2/3	RinzaffoMC(Mapei)_LiquidChitosan(0,5%)	0,28	13,9	9,23	6	ND	ND	10	H
RMC_CL1_1/2/3	RinzaffoMC(Mapei)_LiquidChitosan(1%)	0,38	16,1	6,68	5	ND	ND	10	H
RMC_CS05_1/2/3	RinzaffoMC(Mapei)_SolidChitosan(0,5%)	0,22	13,7	8,57	6	ND	ND	8	M
RMC_CS1_1/2/3	RinzaffoMC(Mapei)_SolidChitosan(1%)	0,24	17,7	4,48	4	ND	ND	8	M
RMC_D05_1/2/3	RinzaffoMC(Mapei)_DTPMP(0,5%)	0,41	12,3	2,95	3	ND	ND	10	H
RMC_D1_1/2/3	RinzaffoMC(Mapei)_DTPMP(1%)	0,4	15,9	6,84	5	ND	ND	10	H
RMC_NFCN05_1/2/3	RinzaffoMC(Mapei)_Na4Fe(CN)6·H_2O(0,5%)	0,35	18,3	14,8	6	ND	ND	11	H
RMC_NFCN1_1/2/3	RinzaffoMC(Mapei)_Na4Fe(CN)6·H_2O(1%)	0,33	15,9	19,9	6	ND	ND	8	M
LS_1/2/3	Lime1Sand2	0,3	18,4	2,91	3	15	H	14	H
LS_CL025_1/2/3	Lime1Sand2_LiquidChitosan(0,25%)	0,3	16,7	6,04	5	5	M	14	H
LS_CL05_1/2/3	Lime1Sand2_LiquidChitosan(0,5%)	0,34	21,1	9,38	6	4	L	14	H
LS_CS025_1/2/3	Lime1Sand2_SolidChitosan(0,25%)	0,23	15,8	13,3	6	15	H	14	H
LS_CS05_1/2/3	Lime1Sand2_SolidChitosan(0,5%)	0,33	11,0	1,55	2	15	H	14	H
LS_D025_1/2/3	Lime1Sand2_DTPMP(0,25%)	0,31	15,8	5,08	5	4	L	6	M

LS_D05_1/2/3	Lime1Sand2_DTPMP(0,5%)	0,3	12,9	9,59	6	15	H	14	H
LSC_1/2/3	Lime1Sand2_CrushedBrickPowder	0,34	27,2	17,2	6	15	H	14	H
LSC_CL025_1/2/3	Lime1Sand2_CrushedBrickPowder_LiquidChitosan(0,25%)	0,23	27,1	4,83	4	15	H	8	M
LSC_CL05_1/2/3	Lime1Sand2_CrushedBrickPowder_LiquidChitosan(0,5%)	0,3	27,3	10	6	15	H	6	M
LSC_CS025_1/2/3	Lime1Sand2_CrushedBrickPowder_SolidChitosan(0,25%)	0,45	22,6	12	6	15	H	14	H
LSC_CS05_1/2/3	Lime1Sand2_CrushedBrickPowder_SolidChitosan(0,5%)	0,38	22,8	12,1	6	15	H	14	H
LSC_D025_1/2/3	Lime1Sand2_CrushedBrickPowder_DTPMP(0,25%)	0,24	20,7	3,35	4	15	H	14	H
LSC_D05_1/2/3	Lime1Sand2_CrushedBrickPowder_DTPMP(0,5%)	0,33	20,6	8,33	6	15	H	14	H
L1S1_1/2/3	Lime1Sand1	0,4	27,9	8,56	6	1	L	6	M
L09S1M01_1/2/3	Lime09Sand1_Metakaolin01 (0.9:1:0.1 in weight)	0,22	28,9	8,22	6	10	H	7	M
L08S1M02_1/2/3	Lime08Sand1_Metakaolin02 (0.8:1:0.2 in weight)	0,33	27,4	2,79	3	10	H	7	M
L07S1M03_1/2/3	Lime07Sand1_Metakaolin03 (0.7:1:0.3 in weight)	~~0,5~~	24,5	5,98	5	15	H	6	M
L1S2_1/2/3	Lime1Sand2	0,46	22,3	5,22	5	1	L	7	M
L09S2M01_1/2/3	Lime09Sand2_Metakaolin01 (0.9:2:0.1 in weight)	0,24	20,7	9,93	6	15	H	6	M
L08S2M02_1/2/3	Lime08Sand2_Metakaolin02 (0.8:2:0.2 in weight)	0,24	19,6	4,95	4	15	H	6	M
L07S2M03_1/2/3	Lime07Sand2_Metakaolin03 (0.7:2:0.3 in weight)	0,24	19,0	8,56	6	15	H	6	M
L1S3_1/2/3	Lime1Sand3	0,24	16,5	8,57	6	1	L	6	M
L09S3M01_1/2/3	Lime09Sand3_Metakaolin01 (0.9:3:0.1 in weight)	0,29	18,8	8,21	6	15	H	6	M
L08S3M02_1/2/3	Lime08Sand3_Metakaolin02 (0.8:3:0.2 in weight)	~~0,68~~	20,4	9,52	6	15	H	6	M
L07S3M03_1/2/3	Lime07Sand3_Metakaolin03 (0.7:3:0.3 in weight)	~~1,01~~	18,3	1,98	2	15	H	6	M
ML1S1_1/2/3	MagnesianLime1Sand1	0,46	28,1	3,53	4	1	L	7	M
ML09S1M01_1/2/3	MagnesianLime09Sand1_Metakaolin01 (0.9:1:0.1 in weight)	~~0,65~~	29,4	5,16	5	15	H	6	M
ML08S1M02_1/2/3	MagnesianLime08Sand1_Metakaolin02 (0.8:1:0.2 in weight)	~~0,65~~	26,6	4,91	4	15	H	7	M
ML07S1M03_1/2/3	MagnesianLime07Sand1_Metakaolin03 (0.7:1:0.3 in weight)	0,25	27,9	3,41	4	15	H	7	M
ML1S2_1/2/3	MagnesianLime1Sand2	~~0,61~~	23,5	2,97	3	1	L	6	M
ML09S2M01_1/2/3	MagnesianLime09Sand2_Metakaolin01 (0.9:2:0.1 in weight)	0,37	21,1	2,64	3	15	H	6	M
ML08S2M02_1/2/3	MagnesianLime08Sand2_Metakaolin02 (0.8:2:0.2 in weight)	0,24	21,2	0,8	1	15	H	7	M
ML07S2M03_1/2/3	MagnesianLime07Sand2_Metakaolin03 (0.7:2:0.3 in weight)	0,25	22,5	0,6	1	15	H	6	M

ML1S3_1/2/3	MagnesianLime1Sand3	0,3	20,4	0,4	1	1	L	7	M
ML09S3M01_1/2/3	MagnesianLime09Sand3_Metakaolin01 (0.9:3:0.1 in weight)	0,26	22,8	0,6	1	15	H	6	M
ML08S3M02_1/2/3	MagnesianLime08Sand3_Metakaolin02 (0.8:3:0.2 in weight)	0,29	21,6	0,6	1	15	H	6	M
ML07S3M03_1/2/3	MagnesianLime07Sand3_Metakaolin03 (0.7:3:0.3 in weight)	0,46	21,2	0,7	1	15	H	7	M
L1S1.7C0.3_1/2/3	Lime1Sand1.7_CrushedBrickPowder0.3	0,26	18,9	0,7	1	2	L	11	H
ML1S1.7C0.3_1/2/3	MagnesianLime1Sand1.7_CrushedBrickPowder0.3	0,2	23,2	0,8	1	4	L	7	M
L1S0.7C0.3_1/2/3	Lime1Sand0.7_CrushedBrickPowder0.3	0,23	27,3	0,8	1	1	L	9	M
NHL1S0.7C0.3_1/2/3	NHLime1Sand0.7_CrushedBrickPowder0.3	0,14	27,5	6,5	5	15	H	10	H
PL1S3_1/2/3	PalladioNHLime1Sand3	0,2	17,4	7,8	6	15	H	11	H
NHL1S3HGMS_1/2/3	NHL1Sand3Microspheres50g	0,19	20,2	8	6	15	H	8	M
NHL1S3HGMSD_1/2/3	NHL1Sand3Microspheres50gDTPMP40g	0,17	19,9	6,6	5	15	H	6	M
NHL1S3HGMSCL_1/2/3	NHL1Sand3Microspheres50gChitosan20g	0,17	18,7	6,7	5	15	H	2	L
SLS_1/2/3	SlakedLime1Sand3	0,17	14,6	5,4	5	13	H	6	M
SLSH_1/2/3	SlakedLime1Sand3HGMS0.03	0,21	16,0	5,3	5	13	H	13	H
SLSC_1/2/3	SlakedLime1Sand2.7CruchedBrickPowder0.3	0,19	15,9	6,5	5	8	M	11	H
SLSCH_1/2/3	SlakedLime1Sand2.7CruchedBrickPowder0.3HGMS0.03	0,24	17,1	6,5	5	13	H	13	H

* Sd values < 0.5 m is recommended in order to prevent condensation and degradation (e.g. efflorescence, mold), Sd values > 0.5 m = ~~Not Suitable~~ (Low breathability)[209,210]; **A TOP ≥ 30% is generally recommended for the restoration of historic masonry[210-211]; *** See Tab.32[212-213]; ****H: High resistance, M= Medium resistance, L= Low resistance[132-133].

Table 32 Guide to mortar applications related to their compressive strength resistance value

ID	Range	Application in building sector
1	≤ 1 MPa	Restoration of ancient masonry (aerial lime), decorative surfaces, historic plasterwork
2	1 – 2 MPa	Conservative reconstruction, stitching, bedding compatible with historic solid brickwork
3	2 – 3 MPa	Light structural restoration, reintegration in consolidated old masonry
4	3 – 5 MPa	New lightweight construction, unreinforced load-bearing masonry in modern buildings
5	5 – 7 MPa	Mortars for reinforced masonry, light seismic zones
6	> 7 MPa	Structural mortars, anti-seismic interventions, load-bearing reinforced masonry and modern high-performance technologies

6. References

1. European Commission. (2023). The European Green Deal. In Directorate-General for Communication. Publications Office of the European Union. Retrieved from https://commission.europa.eu/strategy-and-policy/priorities-2019-2024/european-green-deal_en
2. Potts, A. (2021). Executive Summary. European Cultural Heritage Green Paper. Retrieved from https://openarchive.icomos.org/id/eprint/2552/1/2021_European%20Heritage%20Green%20Paper_full%20paper.pdf
3. Turner, B. L., Lambin, E. F., & Reenberg, A. (2007). The emergence of land change science for global environmental change and sustainability. In Proceedings of the National Academy of Sciences, 104(52), 20666–20671. https://doi.org/10.1073/pnas.0704119104
4. Grimm, N. B., et al (2008). Global Change and the Ecology of Cities. In Science, 319(5864), 756–760. https://doi.org/10.1126/science.1150195
5. Mannheimer, R. (2023). Edifici sostenibili: la percezione degli italiani. La Responsabilità Del Cambiamento per Il Benessere Delle Persone. Retrieved from https://gbcitalia.org/2024/01/30/green-building-gbc-italia-indaga-la-percezione-dei-cittadini-italiani/
6. Monosilio, F., et al (2024). Osservatorio congiunturale sull'industria delle costruzioni. ANCE. Retrieved from https://ance.it/wp-content/uploads/allegati/20250128_Osservatorio_Ance_-_Gennaio_2025.pdf
7. Perinelli C. (2023). 51 Statistiche sull'Edilizia Sostenibile. Greenmarketing.
8. Melià, P., Ruggieri, G., Sabbadini, S., & Dotelli, G. (2014). Environmental impacts of natural and conventional building materials: A case study on earth plasters. In Journal of Cleaner Production, 80, 179–186. https://doi.org/10.1016/j.jclepro.2014.05.073
9. Destefani, M., Falchi, L., & Zendri, E. (2023). Proposal of New Natural Hydraulic Lime-Based Mortars for the Conservation of Historical Buildings. In Coatings. 13(8). https://doi.org/10.3390/coatings13081418
10. Lazell, E. W. (2023). *Hydrated Lime: History, Manufacture and Uses in Plaster, Mortar, Concrete; a Manual For the Architect, Engineer, Contractor and Builder*. London:Sothis Press.
11. Papayianni, I., & Stefanidou, M. (2003). Mortars for intervention in monuments and historical buildings. WIT Press. Retrieved from https://www.witpress.com/Secure/elibrary/papers/STR03/STR03006FU.pdf
12. Pires, J. (2015). Simple analysis of historical lime mortars. In Journal of Chemical Education, 92(3), 521–523. https://doi.org/10.1021/ed500336p
13. Luxán, M. P., et al (1999). Torroja Institute, the historie building: conservation and characteristics of the materials of its façade, 49(255), 41–48. In Construction Materials. https://doi.org/10.3989/mc.1999.v49.i255.441
14. Montoya, C., et al (2001, January). Characterization of Ancient Dolomitic Binding Materials from Zamarce, in Navarre (Spain). ResearchGate. Retrieved from https://www.researchgate.net/publication/273105035
15. Montoya, C., et al (2003). Study of ancient dolomitic mortars of the church of Santa María de Zamarce in Navarra (Spain): comparison with simulated standards. In Thermochimica Acta, 398(1–2), 107–122. https://doi.org/10.1016/S0040-6031(02)00321-0

16. Olmedo, C., Calle, A., & Antuña, J. (2022). What is built and what is taught: The difference between teaching and professional practice in building structures. In Architecture, Structures and Construction, 2(4), 685–698. https://doi.org/10.1007/s44150-022-00056-7
17. Torroja E. (2018). Concrete and Spain's Indigenous Structural Types. SAHANZ. Retrieved from https://www.sahanz.net/wp-content/uploads/SAHANZ18_paper_Tippey.pdf
18. Varas, M. J., de Buergo, M. A., & Fort, R. (2007). The origin and development of natural cements: The Spanish experience. In Construction and Building Materials, 21(2), 436–445. https://doi.org/10.1016/j.conbuildmat.2005.07.011
19. Cardoso, I., et al (2014). A multidisciplinary approach to the study of archaeological mortars from the town of Ammaia in the Roman Province of Lusitania (Portugal). In Archaeometry, 56(1), 1–24. https://doi.org/10.1111/arcm.12020
20. Rodriguez-Navarro, C., Ruiz-Agudo, E., Burgos-Cara, A., Elert, K., & Hansen, E. F. (2017). Crystallization and Colloidal Stabilization of Ca(OH)2 in the Presence of Nopal Juice (Opuntia ficus indica): Implications in Architectural Heritage Conservation. In Langmuir, 33(41), 10936–10950. https://doi.org/10.1021/acs.langmuir.7b02423
21. Binda, L., Saisi, A., & Tiraboschi, C. (2000). Investigation procedures for the diagnosis of historic masonries. In Construction and Building Materials 14(4), 199-233. https://doi.org/10.1016/S0950-0618(00)00018-0
22. Copsey, N. (2019). *Hot Mixed Lime and Traditional Mortars: A Practical Guide to Their Use in Conservation and Repair*. Marlborough: The Crowood Press.
23. Cowper, A. (1998). *Lime and Lime Mortars*. London: Routledge.
24. Groot, C., Hughes, J. J., Groot, C. J. W. P., & Bartos, P. J. M. (1999). Historic mortars: characteristics and tests-Concluding summary and state-of-the-art. https://www.researchgate.net/publication/319015279
25. Hendry, E. A. W. (2001). Masonry walls: materials and construction. In Construction and Building Materials 15(8), 323-330. https://doi.org/10.1016/S0950-0618(01)00019-8.
26. Hughes, J. J. (Eds.) (2019). *Historic Mortars: Advances in Research and Practical Conservation*. Berlin: Springer.
27. Lanas, J., & Alvarez, J. I. (2003). Masonry repair lime-based mortars: Factors affecting the mechanical behavior. In Cement and Concrete Research, 33(11), 1867–1876. https://doi.org/10.1016/S0008-8846(03)00210-2
28. Ventol, L., Vendrell, M., Giraldez, P., & Merino, L. (2011). Traditional organic additives improve lime mortars: New old materials for restoration and building natural stone fabrics. In Construction and Building Materials, 25(8), 3313–3318. https://doi.org/10.1016/j.conbuildmat.2011.03.020
29. Weyer, A. (2016). *EwaGlos: European Illustrated Glossary of Conservation Terms for Wall Paintings and Architectural Surfaces*. Petersberg: Michael Imhof Verlag.
30. Elsen, J. (2006). Microscopy of historic mortars-a review. In Cement and Concrete Research 36(8), 1416–1424. https://doi.org/10.1016/j.cemconres.2005.12.006
31. Callebaut, K., Elsen, J., van Balen, K., & Viaene, W. (2001). Nineteenth century hydraulic restoration mortars in the Saint Michael's Church (Leuven, Belgium) Natural hydraulic lime or cement? In Cement and Concrete Research 31(3), 397-403. https://doi.org/10.1016/S0008-8846(00)00499-3.
32. Aceto, M. (2021). Pigments—the palette of organic colourants in wall paintings. In Archaeological and Anthropological Sciences 13(10). https://doi.org/10.1007/s12520-021-01392-3

33. Acharya, A. (2017). Role of Additives in Mortars: Historic Precedents. In International Journal of Engineering Research and Applications, 7(2), 7–12. Ijera. https://doi.org/10.9790/9622-0702050712
34. Delle, A., Antiche, M., Pecchioni, E., Fratini, F., & Cantisani, E. (2014). *Atlante delle malte antiche in sezione sottile al microscopio ottico*. Firenze: Nardini Editore.
35. la Russa, M. F., & Ruffolo, S. A. (2021). Mortars and plasters - How to characterize mortar and plaster degradation. In Archaeological and Anthropological Sciences 13 (10). https://doi.org/10.1007/s12520-021-01405-1
36. Monaco, M., Aurilio, M., Tafuro, A., & Guadagnuolo, M. (2021). Sustainable mortars for application in the cultural heritage field. In Materials, 14(3), 1–17. https://doi.org/10.3390/ma14030598
37. Papayianni, I., & Hughes, J. (2018). Testing properties governing the durability of lime-based repair mortars. In RILEM Technical Letters, 3, 135–139. https://doi.org/10.21809/rilemtechlett.2018.81
38. Adriano, P., Santos Silva, A., Veiga, R., Mirão, J., & Candeias, A. E. (2009). Microscopic characterisation of old mortars from the Santa Maria Church in Évora. In Materials Characterization, 60(7), 610–620. https://doi.org/10.1016/j.matchar.2008.11.008
39. Alberghina, M. F., et al (2020). The Tomb of the Diver and the frescoed tombs in Paestum (southern Italy): New insights from a comparative archaeometric study. PLoS ONE, 15(4). https://doi.org/10.1371/journal.pone.0232375
40. Arizzi, A., & Cultrone, G. (2021). Mortars and plasters—how to characterise hydraulic mortars. In Archaeological and Anthropological Sciences (Vol. 13, Issue 9). https://doi.org/10.1007/s12520-021-01404-2
41. Carran, D., Hughes, J., Leslie, A., & Kennedy, C. (2012). A short history of the use of lime as a building material beyond Europe and North America. In International Journal of Architectural Heritage 6(2), 117–146. https://doi.org/10.1080/15583058.2010.511694
42. Zhang, K., et al (2021). Effects of sticky rice addition on the properties of lime-tile dust mortars. In Heritage Science, 9(1). https://doi.org/10.1186/s40494-020-00475-z
43. Falchi, L., Slanzi, D., Balliana, E., Driussi, G., & Zendri, E. (2018). Rising damp in historical buildings: A Venetian perspective. In Building and Environment, 131, 117–127. https://doi.org/10.1016/j.buildenv.2018.01.004
44. Sabbioni, C., Bonazza, A., & Zappia, G. (2002). Damage on hydraulic mortars: the Venice Arsenal. Journal of Cultural Heritage, 3(1), 83-88. https://doi.org/10.1016/S1296-2074(02)01163-9
45. Serandrei Barbero, R., Albani, A. D., & Bonardi, M. (2004). Ancient and modern salt marshes in the Lagoon of Venice. In Palaeogeography, Palaeoclimatology, Palaeoecology, 202(3–4), 229–244. https://doi.org/10.1016/S0031-0182(03)00636-9
46. Menicali, U. (1992). *I materiali dell'edilizia storica. Tecnologia e impiego dei materiali tradizionali.* Roma: Carocci.
47. Vecchiattini, R., & Mannoni, T. (2024). *La civiltà della calce. Storia, scienza, restauro*. Genova: De Ferrari.
48. Davey, N. (1971). *A History of Building Materials*. Devon: Drake Publishers Ltd.
49. Spataro, G. (2018). Timeline of Concrete Through History. Retrieved from https://www.concreterenovations.co.uk/news/timeline-of-concrete-through-history/
50. Trout, E. A. R. (2019). The history of calcareous cements. In Lea's Chemistry of Cement and Concrete, 1–29. https://doi.org/10.1016/B978-0-08-100773-0.00001-0

51. Artioli, G., Secco, M., & Addis, A. (2019). The vitruvian legacy: Mortars and binders before and after the Roman world. In European Mineralogical Union Notes in Mineralogy, 20, 151–202. https://doi.org/10.1180/EMU-notes.20.4
52. Vitruvius Marcus Pollio. (1997). De architectura (Corso A. & Romano E., Eds.; Vol. 5). Torino:Einaudi.
53. Traini, L. (2013). La lavorazione della calce dall'antichità al medioevo. Roma e le province dell'Impero. Roma: Scienze e Lettere.
54. Myking, T., Hertzberg, A., & Skrøppa, T. (2005). History, manufacture and properties of lime bast cordage in northern Europe. In Forestry, 78(1), 65–71. https://doi.org/10.1093/forestry/cpi006
55. Speweik, J. (2008). The History of Masonry Mortar in America 1720-1995. Retrieved from https://www.canadamasonrydesigncentre.com/research/the-history-of-masonry-mortar-in-america-1720-1995/
56. Grassi, M. (2005). *Calchere*. Milano: Elle Libri.
57. Jordan, J. W. (2005). Lime mortar and the conservation of historic structures. In Australian Journal of Multi-Disciplinary Engineering, 3(1), 35–42. https://doi.org/10.1080/14488388.2005.11464731
58. Lanciato, A. Q. (2001). Val Canzoi, fornaci da calce. Comitato Calchere. https://www.ilmortodafeltre.it/shop/storia-locale/belluno-e-provincia/val-canzoi-fornaci-da-calce-recupero-di-tipologie-locali-ripristino-e-riuso-di-una-calchera/
59. Pagnucco, D., & Baccinchet, M. (2005). *Fornaci da calce in Tramonti di Sopra*. Tramonti di Sopra: Pro Loco Tramonti di Sopra.
60. van Balen, K. (2005). Carbonation reaction of lime, kinetics at ambient temperature. In Cement and Concrete Research, 35(4), 647–657. https://doi.org/10.1016/j.cemconres.2004.06.020
61. Yur'ev, B. P., & Spirin, N. A. (2012). Thermophysical properties of limestone and lime on heating. In Steel in Translation, 42(4), 308–311. https://doi.org/10.3103/S0967091212040195
62. Ezziane, K., Bougara, A., Kadri, A., Khelafi, H., & Kadri, E. (2007). Compressive strength of mortar containing natural pozzolan under various curing temperature. In Cement and Concrete Composites, 29(8), 587–593. https://doi.org/10.1016/j.cemconcomp.2007.03.002
63. Oates, J. A. H. (1998). *Lime and Limestone : Chemistry and Technology, Production and Uses*. https://doi.org/10.1002/9783527612024
64. Pachta, V., Triantafyllaki, S., & Stefanidou, M. (2018). Performance of lime-based mortars at elevated temperatures. In Construction and Building Materials, 189, 576–584. https://doi.org/10.1016/j.conbuildmat.2018.09.027
65. Pavlík, V., & Užáková, M. (2016). Effect of curing conditions on the properties of lime, lime-metakaolin and lime-zeolite mortars. In Construction and Building Materials, 102, 14–25. https://doi.org/10.1016/j.conbuildmat.2015.10.128
66. Balksten, K., & Lindqvist, J.E. (2016). Two-hundred year old lime putty found in the ground explaining the character of fat historic lime mortars. Retrieved from https://www.academia.edu/35805086/Two_hundred_year_old_lime_putty_from_barrels_found_in_the_ground_explaining_the_character_of_fat_historic_lime_mortar
67. Holmes, S., & Wingate, M. (2002). *Building With Lime: A Practical Introduction*. Torino: ITDG Publishing
68. Taşcı, B., & Böke, H. (2018). Properties of Roman lime mortars in ancient Lycia region. Recent Advances on Environment, Chemical, Engineering and Materials. 2022 (1). https://doi.org/10.1063/1.5060692

69. Elsen, J., van Balen, K., & Mertens, G. (2012). Hydraulicity in Historic Lime Mortars: A Review. In Historic Mortars, 125–139. https://doi.org/10.1007/978-94-007-4635-0_10
70. Grilo, J., et al (2014). New natural hydraulic lime mortars - Physical and microstructural properties in different curing conditions. In Construction and Building Materials, 54, 378–384. https://doi.org/10.1016/j.conbuildmat.2013.12.078
71. Grilo, J., Santos Silva, A., Faria, P., Gameiro, A., Veiga, R., & Velosa, A. (2014). Mechanical and mineralogical properties of natural hydraulic lime-metakaolin mortars in different curing conditions. In Construction and Building Materials, 51, 287–294. https://doi.org/10.1016/j.conbuildmat.2013.10.045
72. Parra-Fernández, C., Arizzi, A., Secco, M., & Cultrone, G. (2024). The manufacture of natural hydraulic limes: Influence of raw materials' composition, calcination and slaking in the crystal-chemical properties of binders. In Cement and Concrete Research, 185. https://doi.org/10.1016/j.cemconres.2024.107631
73. Garijo, L., Zhang, X., Ruiz, G., Ortega, J. J., & Yu, R. C. (2017). Advanced mechanical characterization of NHL mortars and cohesive simulation of their failure behavior. In Construction and Building Materials, 153, 569–577. https://doi.org/10.1016/j.conbuildmat.2017.07.127
74. Chever, L., Pavía, S., & Howard, R. (2010). Physical properties of magnesian lime mortars. In Materials and Structures, 43(1–2), 283–296. https://doi.org/10.1617/s11527-009-9488-9
75. Diekamp, A., Konzett, J., & Peter, M. (2009, March). Magnesian lime mortars - identification of magnesium-phases in medieval mortars and plasters with imaging techniques. In Conference: 12th Euroseminar on Microscopy Applied to Building Materials, Kassel. Retrieved from https://www.researchgate.net/publication/236875128_Magnesian_lime_mortars_-_identification_of_magnesium-phases_in_medieval_mortars_and_plasters_with_imaging_techniques
76. Lanas, J., Pérez Bernal, J. L., Bello, M. A., & Alvarez, J. I. (2006). Mechanical properties of masonry repair dolomitic lime-based mortars. In Cement and Concrete Research, 36(5), 951–960. https://doi.org/10.1016/j.cemconres.2005.10.004
77. Lackner, K. S., Wendt, C. H., Butt, D. P., Joyce, E. L., & Sharp, D. H. (1995). Carbon dioxide disposal in carbonate minerals. In Energy, 20(11), 1153–1170. https://doi.org/10.1016/0360-5442(95)00071-N
78. Bruni, S., Cariati, F., Fermo, P., Pozzi, A., & Toniolo, L. Characterization of ancient magnesian mortars coming from northern Italy. In Thermochimica Acta, 321 (1-2), 161,165. https://doi.org/10.1016/S0040-6031(98)00455-9
79. Pavía, S., Fitzgerald, B., & Howard, & R. (2005). Evaluation of properties of magnesian lime mortar Structural Studies, Repairs and Maintenance of Heritage Architecture IX 375. https://www.researchgate.net/publication/237225843_Evaluation_of_properties_of_magnesian_lime_mortar
80. Pistilli, A. (2012). Determinazione del rapporto aggregato/legante di malte: affidabilità dello studio petrografico in sezione sottile. Bachelor Thesis, Padua university, Science Faculty, 2011-2012, C.Mazzoli. Retrieved from https://thesis.unipd.it/handle/20.500.12608/20617
81. Athira, V. S., & Manohar, S. (2023). Carbonation of air lime mortars under natural and accelerated conditions – A systematic review. In Materials Today: Proceedings. https://doi.org/10.1016/j.matpr.2023.04.082

82. Sheila, D., Sankaran, C., & Khangaonkar, P. R. (1991). Studies on the extraction of magnesia from low grade magnesites by carbon dioxide pressure leaching of hydrated magnesia. In Minerals Engineering, 4(1), 79–88. https://doi.org/10.1016/0892-6875(91)90120-K
83. Dheilly, R. M., Bouguerra, A., Beaudoin, B., Tudo, J., & Queneudec, M. (1999). Hydromagnesite development in magnesian lime mortars. In Materials Science and Engineering (Vol. 268).
84. Brunello, V. (2020). Mortars: a complex material in cultural heritage. In Materials Science and Engineering: A, 268 (1-2), 127-131. https://doi.org/10.1016/S0921-5093(99)00085-4
85. Branca, G. (2010). Manuale d'architettura. Research Library, The Getty Research Institute. Retrieved from http://www.archive.org/details/architeturadigioOObran
86. Mannoni, T. (1975). *Saggi di scavo dei livelli medievali delle "stufe di San Calogero" (Sciacca). In Archeologia medievale*. 2, 389–392.
87. Cabona Ferrando, I., Mannoni, T., (1988). *Liguria, ritratto di una regione*. Genova: SAGEP Editori Srl.
88. Middleton, R., & Baudouin-matuszek, M. (2007). *Jean Rondelet: The Architect As Technician*. London: Yale University Press
89. Bakolas, A., & Aggelakopoulou, E. (2019). Pozzolanic activity of natural pozzolan–lime pastes and physicomechanical characteristics. In Journal of Thermal Analysis and Calorimetry, 135(6), 2953–2961. https://doi.org/10.1007/s10973-018-7612-1
90. Becerra-Duitama, J. A., & Rojas-Avellaneda, D. (2022). Pozzolans: A review. In Engineering and Applied Science Research, 49(4), 495–504. https://doi.org/10.14456/easr.2022.49
91. Ghrici, M., Kenai, S., & Meziane, E. (2006). Mechanical and durability properties of cement mortar with Algerian natural pozzolana. In Journal of Materials Science, 41(21), 6965–6972. https://doi.org/10.1007/s10853-006-0227-0
92. Ghrici, M., Kenai, S., & Said-Mansour, M. (2007). Mechanical properties and durability of mortar and concrete containing natural pozzolana and limestone blended cements. In Cement and Concrete Composites, 29(7), 542–549. https://doi.org/10.1016/j.cemconcomp.2007.04.009
93. Tagnit-Hamou, A., Petrov, N., & Luke, K. (2003). Properties of Concrete Containing Diatomaceous Earth. ACI Materials Journal, 100, 73–78. DOI: 10.14359/51712250
94. Martín, C. M., Scarponi, N. B., Villagrán, Y. A., Manzanal, D. G., & Piqué, T. M. (2021). Pozzolanic activity quantification of hollow glass microspheres. Cement and Concrete Composites, 118. https://doi.org/10.1016/j.cemconcomp.2021.103981
95. Perfilov, V. A., Oreshkin, D. V., & Zemlyanushnov, D. Yu. (2016). Concrete Strength and Crack Resistance Control. Procedia Engineering, 150, 1474–1478. https://doi.org/10.1016/j.proeng.2016.07.085
96. Verweij, H., de With, G., & Veeneman, D. (1985). Hollow glass microsphere composites: preparation and properties. In Journal of Materials Science, 20, 1069-1078. https://doi.org/10.1007/BF00585751
97. Xie, Y., McAllister, S. D., Edwards, D. B., & Cheng, I. F. (2011). Fabrication of porous hollow glass microspheres. Journal of Power Sources, 196(24), 10727–10730. https://doi.org/10.1016/j.jpowsour.2011.07.049
98. Falchi, L., et al (2013). Influence and effectiveness of water-repellent admixtures on pozzolana-lime mortars for restoration application. In Construction and Building Materials, 49, 272–280. https://doi.org/10.1016/j.conbuildmat.2013.08.030

99. Walker, R., & Pavía, S. (2011). Physical properties and reactivity of pozzolans, and their influence on the properties of lime-pozzolan pastes. In Materials and Structures, 44(6), 1139–1150. https://doi.org/10.1617/s11527-010-9689-2
100. Spackman, C. (1929). *Some Writers on Lime and Cement: From Cato to Present Time*. Cambridge: W. Heffer & sons Limited.
101. Newby, F. (2016). *Early Reinforced Concrete* (Taylor & Francis, Ed.; Vol. 11). London: Routledge.
102. Sickels-Taves, L. B., & Allsopp, P. D. (2005). Lime And Its Place In The 21st Century: Combining Tradition, Innovation and Science in Building Preservation. In Adcances in Geosciences, 45, 19-24. DOI:10.5194/adgeo-45-19-2018
103. Fang, S. Q., Zhang, H., Zhang, B. J., & Zheng, Y. (2014). The identification of organic additives in traditional lime mortar. In Journal of Cultural Heritage, 15(2), 144–150. https://doi.org/10.1016/j.culher.2013.04.001
104. Lindqvist, J. E., et al (2006). Analysis of mortars with additives. In SP Building Technology and Mechanics SP REPORT.
105. Quintaliani, C., et al (2022). Vegetal Fiber Additives in Mortars: Experimental Characterization of Thermal and Acoustic Properties. In Sustainability, 14(3). https://doi.org/10.3390/su14031260
106. Rampazzi, L., Colombini, M. P., Conti, C., Corti, C., Lluveras-Tenorio, A., Sansonetti, A., & Zanaboni, M. (2016). Technology of Medieval Mortars: An Investigation into the Use of Organic Additives. Archaeometry, 58(1), 115–130. https://doi.org/10.1111/arcm.12155
107. Cardinali, F., Bracciale, M. P., Santarelli, M. L., & Marrocchi, A. (2021). Principal component analysis (PCA) combined with naturally occurring crystallization inhibitors: An integrated strategy for a more sustainable control of salt decay in built heritage. Heritage, 4(1), 220–229. https://doi.org/10.3390/heritage4010013
108. Delgado, J. M. P. Q., Guimarães, A. S., de Freitas, V. P., Antepara, I., Kočí, V., & Černý, R. (2016). Salt Damage and Rising Damp Treatment in Building Structures. In Advances in Materials Science and Engineering (Vol. 2016). Hindawi Limited. https://doi.org/10.1155/2016/1280894
109. Diaz Gonçalves, T. (2024). Salt Decay and Salt Mixtures in the Architectural Heritage: A Review of the Work of Arnold and Zehnder. In International Journal of Architectural Heritage, 18(1), 125–149. https://doi.org/10.1080/15583058.2022.2117670
110. Lubelli, B., Aguilar, A. M., Beck, K., de Kock, T., Desarnaud, J., Franzoni, E., Gulotta, D., Ioannou, I., Kamat, A., Menendez, B., Rörig-Dalgaard, I., & Sassoni, E. (2022). A new accelerated salt weathering test by RILEM TC 271-ASC: preliminary round robin validation. In Materials and Structures/Materiaux et Constructions, 55(9). https://doi.org/10.1617/s11527-022-02067-8
111. Lopez-Arce, P., Doehne, E., Greenshields, J., Benavente, D., & Young, D. (2009). Treatment of rising damp and salt decay: the historic masonry buildings of Adelaide, South Australia. In Materials and Structures/Materiaux et Constructions, 42(6), 827–848. https://doi.org/10.1617/s11527-008-9427-1
112. Lubelli, B. (2006). Development of a new accelerated salt crystallization test. Research Gate. Retrieved from https://www.researchgate.net/publication/27352080
113. Lubelli, B., & van Hees, R. P. J. (2007). Effectiveness of crystallization inhibitors in preventing salt damage in building materials. In Journal of Cultural Heritage, 8(3), 223–234. https://doi.org/10.1016/j.culher.2007.06.001

114. Selwitz, C., & Doehne, E. (2002). The evaluation of crystallization modifiers for controlling salt damage to limestone. In Journal of Cultural heritage, 3 (3), 205-216. https://doi.org/10.1016/S1296-2074(02)01182-2.
115. Kamat, A., Lubelli, B., & Schlangen, E. (2023). Leaching behaviour of a crystallisation inhibitor in mortars. In Journal of Building Engineering, 79, 107933. https://doi.org/10.1016/j.jobe.2023.107933
116. Muxika, A., Etxabide, A., Uranga, J., Guerrero, P., & de la Caba, K. (2017). Chitosan as a bioactive polymer: Processing, properties and applications. In International Journal of Biological Macromolecules, 105, 1358–1368. https://doi.org/10.1016/j.ijbiomac.2017.07.087
117. Padaki, M., Isloor, A. M., Fernandes, J., & Prabhu, K. N. (2011). New polypropylene supported chitosan NF-membrane for desalination application. In Desalination, 280(1–3), 419–423. https://doi.org/10.1016/j.desal.2011.06.032
118. Granneman, S. J. C., Lubelli, B., & van Hees, R. P. J. (2019). Mitigating salt damage in building materials by the use of crystallization modifiers – a review and outlook. In Journal of Cultural Heritage 40, 183–194). https://doi.org/10.1016/j.culher.2019.05.004
119. Renso, M. (2020). Analysis of the effectiveness of inhibitors of crystallization of soluble salts and consolidation of plaster in marine environment. Bachelor Thesis, Ca'Foscari University, 2019-2020. Zendri, E.
120. Sabir, B. B., Wild, S., & Bai, J. (n.d.). Metakaolin and calcined clays as pozzolans for concrete: a review. In Cement and Concrete Composites, 23 (6), 441-454. https://doi.org/10.1016/S0958-9465(00)00092-5.
121. Samet, B., Mnif, T., Chaabouni, M., 2007. Use of a kaolinitic clay as a pozzolanic material for cements: Formulation of blended cement. In Cement & Concrete Composites 29, 741-749. https://doi.org/10.1016/j.cemconcomp.2007.04.012
122. Tironi, A., Trezza, M. A., Irassar, E. F., & Scian, A. N. (2012). Thermal Treatment of Kaolin: Effect on the Pozzolanic Activity. In Procedia Materials Science, 1, 343–350. https://doi.org/10.1016/j.mspro.2012.06.046
123. Anugrah, R. I., & Rasjad, S. S. (2010). Pretreatment of kaolin into metakaolin. In Indonesian mining journal 13(3).
124. Smiley et al., (1998). Method of Producing Metakaolin. Patent (106/484). Retrieved from https://patents.google.com/patent/US5792251A/en
125. Zada Farhan, K., & Gul, W. (2017). Impact of metakaolin on cement mortar and concrete: A review. International Journal of Civil Engineering and Technology, 8 (4), 2157–2172. Retrieved from https://www.researchgate.net/publication/317215896_Impact_of_metakaolin_on_cement_mortar_and_concrete_A_review
126. Siddique, R., & Klaus, J. (2009). Influence of metakaolin on the properties of mortar and concrete: A review. In Applied Clay Science 43 (3–4), 392–400. https://doi.org/10.1016/j.clay.2008.11.007
127. Tafraoui, A., Escadeillas, G., & Vidal, T. (2016). Durability of the Ultra High Performances Concrete containing metakaolin. In Construction and Building Materials, 112, 980–987. https://doi.org/10.1016/j.conbuildmat.2016.02.169

128. UNI EN-1015/6, 2007. Metodi di prova per malte per opere murarie - Parte 6: Determinazione della massa volumica apparente della malta fresca. Retrieved from https://store.uni.com/uni-en-1015-6-2007

129. UNI EN-1015/3, 2007. Metodi di prova per malte per opere murarie - Parte 3: Determinazione della consistenza della malta fresca (mediante tavola a scosse). Retrieved from https://store.uni.com/uni-en-1015-3-2007

130. UNI EN-15801, 2010. Conservazione dei beni culturali - Metodi di prova - Determinazione dell'assorbimento dell'acqua per capillarità. Retrieved from https://store.uni.com/uni-en-15801-2010

131. UNI EN 1015/19, 2008. Metodi di prova per malte per opere murarie - Parte 19: Determinazione della permeabilità al vapore d'acqua delle malte da intonaco indurite. Retrieved from https://store.uni.com/uni-en-1015-19-2008

132. UNI EN 12370, 2020. Metodi di prova per pietre naturali - Determinazione della resistenza alla cristallizzazione dei sali. Retrieved from https://store.uni.com/uni-en-12370-2020

133. UNI EN 12371, 2010. Metodo di prova per pietre naturali - Determinazione della resistenza al gelo. Retrieved from https://store.uni.com/uni-en-12371-2010

134. UNI EN-1015-11, 2019. Metodi di prova per malte per opere murarie - Parte 11: Determinazione della resistenza a flessione e a compressione della malta indurita. Retrieved from https://store.uni.com/uni-en-1015-11-2019

135. Mape Antique Eco Risana, Mapei S.p.A, SDS. 9018998; v.2; UFI: KRS0-Q09U-V009-5DUT; MAPEI S.p.A. - Via Cafiero, 22 - 20158 Milano.

136. Mape Antique Rinzaffo, Mapei S.p.A, SDS. 901891; v.3; UFI: J0F0-F017-K00E-GR0R; MAPEI S.p.A. - Via Cafiero, 22 - 20158 Milano.

137. Mape Antique MC, Mapei S.p.A, SDS 901851; v.3; UFI: 0H92-J0G6-T000-PFEY; MAPEI S.p.A. - Via Cafiero, 22 - 20158 Milano.

138. White lime Lafarge, SDS. R0200010; Via Piave 20/22 - 36077 Altavilla Vicentina (VI). Retrieved from https://ctsconservation.com/it/calce-lafarge/3961-calce-bianca-lafarge-nhl-35-conf-25-kg.html

139. PALLADIO Grigolin, SDS. CAS:85117-09-5; 1708010004; v.5; Fornaci Calce Grigolin S.p.A. Via Foscarini 2-31040 Treviso. Retrieved from https://www.fornacigrigolin.it/bio-edilizia-palladio/calce-idraulica-naturale/calce-natura.html

140. CALCE IDRATA CL 80 Grigolin, SDS. CAS 1305-62-0; 1708010003; v.3; Fornaci Calce Grigolin S.p.A. Via Foscarini 2-31040 Treviso. Retrieved from https://www.fornacigrigolin.it/costruzione-tradizionale/calce/calce-idrata-cl-80.html

141. CALCE IDRATA MAGNESIACA Grigolin, SDS. CAS 58398-71-3; 1708010002; v.3; Fornaci Calce Grigolin S.p.A. Via Foscarini 2-31040 Treviso. Retrieved from https://www.fornacigrigolin.it/costruzione-tradizionale/calce/calce-idrata-magnesiaca.htm

142. Slaked lime Fassa Bortolo S.r.l, SDS. CAS:1305-62-0; 01-2119475151-45-xxxx; v.3; FASSA Srl Via Lazzaris, 3 - 31027 Spresiano (TV)

143. Ticino Sand, Siliceous sand by Vaga S.r.l. Construction materials. SDS. Retrieved from https://www.edilportale.com/prodotti/vaga/sabbia-di-fiume/sabbia-ticino-mm-01%C3%B709_43799.html
144. Chitosan; CAS:9012-76-4; 448877; v.7.3; Merk Life Science S.r.l.: Via Monte Rosa 93 I-20149 MILANO, 2022.04.26;
145. DTPMP; REACH:1907/2006; 36818; v.7.5; Merk Life Science S.r.l.: Via Monte Rosa 93 I-20149 MILANO, 2022.04.26;
146. Sodium ferrocyanide decahydrate; Retrieved from https://rehsiffscientific.com/products/code/R09666 (accessed:19/03/2025)
147. Sodium ferrocyanide decahydrate; CAS:14434-22-1; 13425; v.6.3; Merk Life Science S.r.l.: Via Monte Rosa 93 I-20149 MILANO, 2022.04.26;
148. BS EN 1015, MPA Mortar:Methods of test for mortar for masonry. Retrieved from https://mortar.org.uk/documents/LT08-Mortar-Testing.pdf (accessed:19/03/2025).
149. Chenite, A. (2001). Rheological characterisation of thermogelling chitosan/glycerol-phosphate solutions. Carbohydrate Polymers, 46(1), 39–47. https://doi.org/10.1016/S0144-8617(00)00281-2
150. Ramachandran, V. S., & Wise, T. (1995). The Effect of phosphonic acid on the slump loss in superplasticized mortar. Il Cemento, 92(1), 3–14. Retrieved from https://nrc-publications.canada.ca/eng/view/ft/?id=10b563f0-e54e-4e5b-8754-8cad33e04e25
151. Younes, M. et.al., (2018). Re-evaluation of sodium ferrocyanide (E 535), potassium ferrocyanide (E 536) and calcium ferrocyanide (E 538) as food additives. In EFSA Journal, 5616(7). https://doi.org/10.2903/j.efsa.2018.5374
152. Gail, E. et.al., (2011). Cyano Compounds, Inorganic. In Ullmann's Encyclopedia of Industrial Chemistry. https://doi.org/10.1002/14356007.a08_159.pub3
153. Holleman A. F., & Wiberg E. (2001). Inorganic Chemistry. London: Academic Press.
154. Giosuè, C., Mobili, A., di Perna, C., & Tittarelli, F. (2019). Performance of lightweight cement-based and alkali-activated mortars exposed to high-temperature. In Construction and Building Materials, 220, 565–576. https://doi.org/10.1016/j.conbuildmat.2019.05.193.
155. Nežerka supervisor, V., Zeman, J., & Tesárek, P. (2015). Modeling and Design of Modern Cocciopesto Mortars. PhD Thesis, Faculty of Civil Engineering, Czech Technical University, Prague.
156. Nežerka, V., & Zeman, J. (2012). A micromechanics-based model for stiffness and strength estimation of cocciopesto mortars. In Acta polytechnica, 52(6), 29-37. https://doi.org/10.48550/arXiv.1210.5857
157. Miriello, D., et al (2018). New compositional data on ancient mortars and plasters from Pompeii (Campania – Southern Italy): Archaeometric results and considerations about their time evolution. In Materials Characterization, 146, 189–203. https://doi.org/10.1016/j.matchar.2018.09.046
158. Böke, H., Akkurt, S., Ipekoğlu, B., & Uğurlu, E. (2006). Characteristics of brick used as aggregate in historic brick-lime mortars and plasters. In Cement and Concrete Research, 36(6), 1115–1122. https://doi.org/10.1016/j.cemconres.2006.03.011
159. Baronio, G., Bindat, L., & Lombardini, N. (1997). The role of brick pebbles and dust in conglomerates based on hydrated lime and crushed bricks*. In Consfruction and Building Materials (Vol. 11, Issue I).

160. Uğurlu, E., & Böke, H. (2009). The use of brick-lime plasters and their relevance to climatic conditions of historic bath buildings. In Construction and Building Materials, 23(6), 2442–2450. https://doi.org/10.1016/j.conbuildmat.2008.10.005
161. Torres, I., Matias, G., & Faria, P. (2020). Natural hydraulic lime mortars - The effect of ceramic residues on physical and mechanical behaviour. In Journal of Building Engineering, 32. https://doi.org/10.1016/j.jobe.2020.101747.
162. Farih, M., Omar, C., Abudaqqa, W. S. K., & Messaoud, B. (2024). Rheological, mechanical and durability properties of mortar containing brick waste as a partial replacement of sand. In Case Studies in Construction Materials, 21, e04043. https://doi.org/10.1016/j.cscm.2024.e04043
163. Cheng, Y., Cong, P., Hao, H., Zhao, Q., Mei, L., Zhang, A., Han, Z., & Hu, M. (2022). Improving workability and mechanical properties of one-part waste brick power based-binders with superplasticizers. In Construction and Building Materials, 335, 127535. https://doi.org/10.1016/j.conbuildmat.2022.127535
164. Ayaz Khan, M. N., Liaqat, N., Ahmed, I., Basit, A., Umar, M., & Khan, M. A. (2018). Effect of Brick Dust on Strength and Workability of Concrete. In IOP Conference Series: Materials Science and Engineering, 414, 012005. https://doi.org/10.1088/1757-899X/414/1/012005
165. Liu, Q., Singh, A., Xiao, J., Li, B., & Tam, V. W. (2020). Workability and mechanical properties of mortar containing recycled sand from aerated concrete blocks and sintered clay bricks. In Resources, Conservation and Recycling, 157, 104728. https://doi.org/10.1016/j.resconrec.2020.104728
166. Groot, C., Veiga, R., Papayianni, I. et al. RILEM TC 277-LHS report: lime-based mortars for restoration–a review on long-term durability aspects and experience from practice. Mater Struct 55, 245 (2022). https://doi.org/10.1617/s11527-022-02052-1
167. Fusade, L., & Viles, H. A. (2019). A comparison of standard and realistic curing conditions of natural hydraulic lime repointing mortar for damp masonry: Impact on laboratory evaluation. In Journal of Cultural Heritage, 37, 82–93. https://doi.org/10.1016/j.culher.2018.11.011
168. Margalha, G., Veiga, R., Silva, A. S., & de Brito, J. (2011). Traditional methods of mortar preparation: The hot lime mix method. In Cement and Concrete Composites, 33(8), 796–804. https://doi.org/10.1016/j.cemconcomp.2011.05.008
169. Alsadik, S. M., Ibrahim, E. L., & Jaber, H. A. (2020). Performance of Cement Mortar Exposed to Different Temperature and Curing Methods. In Civil Engineering Journal, 6(1), 174–185. https://doi.org/10.28991/cej-2020-03091462
170. Lucía Garijo, Xiaoxin Zhang, Gonzalo Ruiz, José J. Ortega, Age effect on the mechanical properties of natural hydraulic and aerial lime mortars, In Construction and Building Materials, Volume 236, 2020, 117573, ISSN 0950-0618, https://doi.org/10.1016/j.conbuildmat.2019.117573.
171. Rucińska, T. (2018). Sustainable cement mortars. In E3S Web of Conferences, 49, 00090. https://doi.org/10.1051/e3sconf/20184900090
172. Paiva, H., Velosa, A., Veiga, R., & Ferreira, V. M. (2010). Effect of maturation time on the fresh and hardened properties of an air lime mortar. In Cement and Concrete Research, 40(3), 447–451. https://doi.org/10.1016/j.cemconres.2009.09.016

173. İnce, İ., Bozdağ, A., Barstuğan, M., & Fener, M. (2021). Evaluation of the relationship between the physical properties and capillary water absorption values of building stones by regression analysis and artificial neural networks. In Journal of Building Engineering, 42, 103055. https://doi.org/10.1016/j.jobe.2021.103055
174. Yang, L., Gao, D., Zhang, Y., Tang, J., & Li, Y. (2019). Relationship between sorptivity and capillary coefficient for water absorption of cement-based materials: theory analysis and experiment. In Royal Society Open Science, 6(6), 190112. https://doi.org/10.1098/rsos.190112
175. Khatib, J. M., & Wild, S. (1998). Sulphate Resistance of Metakaolin Mortar. In Cement and Concrete research. https://doi.org/10.1016/S0008-8846(97)00210-X
176. Khatib, J. M., Negim, E. M., & Gjonbalaj, E. (2012). High Volume Metakaolin as Cement Replacement in Mortar. In World Journal of Chemistry, 7(1), 7–10. https://doi.org/10.5829/idosi.wjc.2012.7.1.251
177. Courard, L., et al (2003). Durability of mortars modified with metakaolin. Cement and Concrete Research, 33(9), 1473–1479. https://doi.org/10.1016/S0008-8846(03)00090-5
178. Minghua Zhang, et al. (2021). Characterization of metakaolin from kaolin clay for use in geopolymer production. In Construction and Building Materials, 272. https://doi.org/10.1016/j.conbuildmat.2020.121938.
179. B. S. S. H. Bhatty, (1993). Metakaolin as a Supplementary Cementing Material, ACI Materials Journal.
180. T. C. M. I. Raj and G. R. S. L. Chithra, (2018). XRD and FTIR studies of metakaolin and its effect on the properties of geopolymer concrete. In Materials Science and Engineering.
181. R. C. M. Silva, et al. (2012). The influence of kaolin on metakaolin-based geopolymers," Journal of the European Ceramic Society.
182. Marfo, K. K., et al (2020). The physico-mechanical influence of dehydroxylized activated local kaolin: A supplementary cementitious material for construction applications. In Case Studies in Construction Materials, 12, e00306. https://doi.org/10.1016/j.cscm.2019.e00306
183. Sánchez, I., de Soto, I. S., Casas, M., Vigil de la Villa, R., & García-Giménez, R. (2020). Evolution of Metakaolin Thermal and Chemical Activation from Natural Kaolin. In Minerals, 10(6), 534. https://doi.org/10.3390/min10060534
184. Abiodun, Y., & Adeosun, S. (2023). Kaolin-Metakaolin Crystallographic Transformation and the Durability of Metakaolin-Based Geopolymer Concrete. In The Egyptian International Journal of Engineering Sciences and Technology, 41(1), 27–39. https://doi.org/10.21608/eijest.2022.136365.1154
185. Andrejkovičová, S., Ferraz, E., Velosa, A. L., Silva, A. S., & Rocha, F. (2011). Fine sepiolite addition to air lime-metakaolin mortars. In Clay Minerals, 46(4), 621–635. https://doi.org/10.1180/claymin.2011.046.4.621
186. Zunino, F., & Scrivener, K. (2021). The reaction between metakaolin and limestone and its effect in porosity refinement and mechanical properties. In Cement and Concrete Research, 140, 106307. https://doi.org/10.1016/j.cemconres.2020.106307
187. K. B. Tits, et al., (1995). Hydromagnesite: A Hydrated Magnesium Carbonate. In American Mineralogist.
188. A. L. C. Pereira, et al., (2012) Magnesium Carbonates: Synthesis, Characterization, and Applications. In Minerals Engineering.
189. J. M. D. Coombs, et al., (1997). X-ray Diffraction Studies of Hydromagnesite and Other Magnesium Carbonates. In Canadian Mineralogist.

190. Esmaeeli, H. S., Farnam, Y., Bentz, D. P., Zavattieri, P. D., & Weiss, W. J. (2017). Numerical simulation of the freeze–thaw behavior of mortar containing deicing salt solution. In Materials and Structures/Materiaux et Constructions, 50(1). https://doi.org/10.1617/s11527-016-0964-8

191. Nunes, C., & Slížková, Z. (2016). Freezing and thawing resistance of aerial lime mortar with metakaolin and a traditional water-repellent admixture. In Construction and Building Materials, 114, 896–905. https://doi.org/10.1016/j.conbuildmat.2016.04.029

192. Simonelli, G., Sidoti, G., Ruggiero, L., Calia, A., Quarta, G., Aramini, F., & Mezzadri, P. (2024). The Use of Phosphonates to Inhibit Salt Crystallization: A Laboratory Study for the Sustainable Conservation of Mural Paintings in the Hypogea Context. In Sustainability, 16(22), 9745. https://doi.org/10.3390/su16229745

193. Ruiz-Agudo, E., Rodriguez-Navarro, C., & Sebastián-Pardo, E. (2006). Sodium Sulfate Crystallization in the Presence of Phosphonates: Implications in Ornamental Stone Conservation. In Crystal Growth & Design, 6(7), 1575–1583. https://doi.org/10.1021/cg050503m

194. Tomson, B., Kan, A. T., & Oddo, J. E. (1994). Acid/Base and Metal Complex Solution Chemistry of the Polyphosphonate DTPMP versus Temperature and Ionic Strength. In Langmuir (Vol. 10). https://pubs.acs.org/sharingguidelines

195. Gulotta, D., Goidanich, S., Tedeschi, C., & Toniolo, L. (2015). Commercial NHL-containing mortars for the preservation of historical architecture. Part 2: Durability to salt decay. In Construction and Building Materials, 96, 198–208. https://doi.org/10.1016/j.conbuildmat.2015.08.006

196. Gonçalves, H., Gonçalves, B., Silva, L., Vieira, N., Raupp-Pereira, F., Senff, L., & Labrincha, J. A. (2014). The influence of porogene additives on the properties of mortars used to control the ambient moisture. In Energy and Buildings, 74, 61–68. https://doi.org/10.1016/j.enbuild.2014.01.016

197. Künzel, H. M., & Holm, A. H. (2009). Moisture Control and problem analysis of heritage constructions. Research Gate. Retrieved from https://www.researchgate.net/publication/228523467_Moisture_Control_and_problem_analysis_of_heritage_constructions

198. Kuru, Z., & Aksoy, K. (2024). A Review of Breathable Walls and Breathable Paints: Innovations and Sustainability in Building Materials. The European Journal of Research and Development, 4(4), 58–100. https://doi.org/10.56038/ejrnd.v4i4.515

199. Pavlík, Z., Vejmelková, E., Fiala, L., & Černý, R. (2009). Effect of moisture on thermal conductivity of lime-based composites. International Journal of Thermophysics, 30(6), 1999–2014. https://doi.org/10.1007/s10765-009-0650-y

200. Wu, Y., Gong, G., Yu, C. W. F., & Fang, P. (2014). The hygroscopic properties of wood fibre, sepiolite and expanded perlite-based breathable wall for moderating the humidity environment. In Indoor and Built Environment, 23(2), 299–312. https://doi.org/10.1177/1420326X13505105

201. Yu, C. W. F. (2011). Breathable Walls — Sustainable Innovation for Future Built Environment. In Indoor and Built Environment, 20(2), 203–205. https://doi.org/10.1177/1420326X11407121
202. Liu, Y., Deng, H., Jiang, Z., Tian, G., Wang, P., & Yu, S. (2024). Research on influence laws of aggregate sizes on pore structures and mechanical characteristics of cement mortar. In Construction and Building Materials, 442, 137606. https://doi.org/10.1016/j.conbuildmat.2024.137606
203. Lyu, K., Garboczi, E. J., & Liu, X. (2022). A quantitative characterization of spatial arrangement of air voids in mortars via X-ray CT and numerical calculations. In Construction and Building Materials, 360, 129550. https://doi.org/10.1016/j.conbuildmat.2022.129550
204. Martínez-García, R., Sánchez de Rojas, M. I., Jagadesh, P., López-Gayarre, F., Morán-del-Pozo, J. M., & Juan-Valdes, A. (2022). Effect of pores on the mechanical and durability properties on high strength recycled fine aggregate mortar. In Case Studies in Construction Materials, 16, e01050. https://doi.org/10.1016/j.cscm.2022.e01050
205. Marulitua, B., Muslim, F., & Sagita, L. (2021). Effects of Void Characteristics on Compressive Strength of Permeable Mortar Paver and Design Recommendation for Parking Area. IOP Conference Series: Earth and Environmental Science, 794(1), 012048. https://doi.org/10.1088/1755-1315/794/1/012048
206. Santos, A. R., Veiga, M. do R., Santos Silva, A., & de Brito, J. (2020). Microstructure as a critical factor of cement mortars' behaviour: The effect of aggregates' properties. In Cement and Concrete Composites, 111, 103628. https://doi.org/10.1016/j.cemconcomp.2020.103628
207. Frías, M., Sánchez De Rojas, M. I., & Cabrera, J. (2000). The effect that the pozzolanic reaction of metakaolin has on the heat evolution in metakaolin-cement mortars. In Cement and Concrete Research, 30 (2), 209-216. https://doi.org/10.1016/S0008-8846(99)00231-8.
208. Kostuch, J. A., Walters, G. V., & Jones, T. R. (1993). High Performance Concrete Incorporating Métakaolin—A Review. In infrastructure, research, new applications, 2. Retrieved from https://www.tib.eu/en/search/id/BLCP:CN002551949/High-performance-concretes-incorporating-metakaolin/
209. UNI EN ISO 12572, 2006. Prestazione igrotermica dei materiali e dei prodotti per edilizia - Determinazione delle proprietà di trasmissione del vapore d'acqua. Retrieved from https://store.uni.com/uni-en-iso-12572-2006
210. UNI 11432, 2011. Beni culturali - Materiali lapidei naturali ed artificiali - Misura della capacità di assorbimento di acqua mediante spugna di contatto. Retrieved from https://conto.uni.com/uni-11432-2011
211. UNI EN 1015-10, 2007. Metodi di prova per malte per opere murarie - Parte 10: Determinazione della massa volumica apparente della malta indurita essiccata. Retrieved from https://store.uni.com/uni-en-1015-10-2007
212. UNI EN 998-2, 2016. Specifiche per malte per opere murarie - Parte 2: Malte da muratura. Retrieved from https://store.uni.com/uni-en-998-2-2016
213. NTC, 2018. Decreto della Repubblica Italiana. Nuove norme sismiche per il calcolo strutturale. Retrieved from https://www.studiopetrillo.com/ntc2018.html

Special thanks

I would like to thank Professor Elisabetta Zendri and Dr Laura Falchi for their advice, support and guidance throughout these three years of PhD as well as the entire research group of Cultural Heritage Conservation at Ca'Foscari university.

I would also like to thank the team of the company Mapei S.p.A, in particular Mr. Donato Stefano, Mr. Bandera Davide and Mr. Valsasina Marco for their helpfulness, guidance and support during the research periods carried out in the company.

I also thank my girlfriend, friends and family for their encouragement during this experience.

Abstract for doctoral thesis

The abstract (max. 1000 characters) must be written in both Italian and English and in any foreign language indicated by the Board of teachers.

The abstract must be signed and bound as the last sheet of the thesis.

Student: Destefani Marco _____ mat.number: 858827 _____

PhD: Environmental Sciences: DEVELOPMENT OF NEW PLASTERS FOR THE CONSERVATION OF ARCHITECTURAL HERITAGE _____

Cicle: PON n°37 ____

Thesis title[1] : Exploring Innovative Formulations for Coastal Heritage Preservation Inspired by Ancient Mortars _____

Abstract:

The main objective of this PhD project, in collaboration with Mapei S.p.A., is the design of new mortars aimed at safeguarding traditional masonry by ensuring greater durability, especially in coastal regions. Durability is to be considered a fundamental point at the basis of sustainability and structures that have stood the test of time over the centuries provide valuable information on this. By increasing knowledge of traditional buildings, it is therefore possible to contribute to innovation in the construction sector. This renovation is therefore an optimal approach to reduce the impact of buildings in a circular economy perspective. Based on this vision, also oriented towards sustainability, the project proposes new formulations, based on natural air and hydraulic binders, with the addition of pozzolanic, hydraulic materials and salt inhibitors and modifiers, in order to limit the damaging effect that soluble salts have on masonry, particularly in coastal and lagoon environments.

Student signature

[1] The title must be the definitive title, the same as that printed on the cover of the paper delivered.

Estratto per riassunto della tesi di dottorato

L'estratto (max. 1000 battute) deve essere redatto sia in lingua italiana che in lingua inglese e nella lingua straniera eventualmente indicata dal Collegio dei docenti.

L'estratto va firmato e rilegato come ultimo foglio della tesi.

Studente: Destefani Marco _____ matricola: 858827 _____

Dottorato: Scienze Ambientali: SVILUPPO DI NUOVI INTONACI PER LA CONSERVAZIONE DEL PATRIMONIO ARCHITETTONICO _____

Ciclo: PON n°37 ____

Titolo della tesi[1] : Exploring Innovative Formulations for Coastal Heritage Preservation Inspired by Ancient Mortars _____

Abstract:

L'obiettivo principale di questo progetto di dottorato, in collaborazione con Mapei S.p.A., è la progettazione di nuove malte mirata a salvaguardare le murature tradizionali garantendo una maggiore durabilità, soprattutto nelle regioni costiere. La durabilità è da considerarsi un punto fondamentale alla base della sostenibilità e le strutture che hanno superato la prova del tempo nel corso dei secoli offrono preziose informazioni in merito. Approfondendo la conoscenza degli edifici tradizionali è possibile contribuire ad un'innovazione nel settore delle costruzioni e ciò rappresenta un approccio ottimale per ridurre l'impatto degli edifici in una prospettiva di economia circolare. Con questa visione, orientata alla sostenibilità, il progetto propone nuove malte, a base di leganti naturali, con l'aggiunta di materiali pozzolanici, idraulici, inibitori e modificatori salini, per limitare il degrado da sali solubili tipico di ambienti costieri e lagunari come quello Veneziano.

Firma dello studente

[1] Il titolo deve essere quello definitivo, uguale a quello che risulta stampato sulla copertina dell'elaborato consegnato.